Cranfield UNIVERSITY

Investigating the PIO-Susceptibility of the F-4C

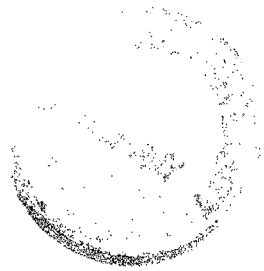

Oliver Brieger

COA Report No. 0004
June 2000

College of Aeronautics
Cranfield University
Cranfield
Bedford MK43 0AL
England

College of Aeronautics Report No.0004
June 2000

INVESTIGATING THE PIO-SUSCEPTIBILITY OF THE F-4C

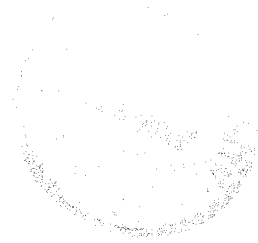

Oliver Brieger
Flight Test and Dynamics Group
College of Aeronautics
Cranfield University,
Cranfield, Bedford MK43 0AL

Supervision

M V Cook
Group Leader and Senior Lecturer
Flight Test and Dynamics Group
and
Prof. Dr. Ing. Dr. Ing. habil. O. Wagner
Lehrstuhl fur Flugmechanik und Flugregelung
Technische Universitat Munchen
Boltzmannstrasse 15
D-85748 Garching GERMANY

June 2000

ISBN 1 86194 051 3

Abstract

Pilot Induced Oscillations are still a serious safety problem in aviation. Especially in regard of the continuous evolution of modern fly-by-wire flight control systems, PIOs seem to occur more frequently. Although test pilots, flight test engineers and handling qualities specialists have dealt with this phenomenon over the past three decades, it still is difficult to apprehend and all too often it catches pilots as well as engineers by surprise. This report gives a brief overview of the mechanisms and the contributing factors in pilot behaviour, in aircraft dynamics and in the environment that lead to a PIO-condition.

A great effort has been made over the years to develop reliable tools, analytically as well as experimentally, which are capable of identifying PIO-prone and PIO-resistant configurations. Five of the most acknowledged, state-of-the-art frequency and time domain criteria for evaluating PIO-susceptibility, based on linear aircraft dynamics, are introduced and compared. These are the Neal and Smith Criterion (original definition), the Bandwidth/Pitch-Rate Overshoot Criterion, the Smith-Geddes Criterion, the Gibson Phase Rate Criterion and the Gibson Dropback Criterion. These Criteria are applied to two selected flight conditions of a linearised, small perturbations model of the F-4C (Phantom II) aircraft, based on the longitudinal equations of motion. The responses of the mathematical aircraft model, which is developed for this purpose using the state space method, are examined and verified with the MATLAB software package and the applicability/suitability of the criteria for this configuration is assessed. Finally, similarities and differences in the application of the criteria, the utilised criterion parameters and the obtained results are discussed. The objective of this exercise is to provide a consolidated review of current criteria for longitudinal PIO-evaluation.

Table of Contents

List of Figures iv
List of Tables vi
Notation vii
1. PIOs, an Introduction 1
1.1 PIO-Development 5
1.2 Classification of PIO 6
2. Criteria for PIO-Assessment 8
2.1 The Neal and Smith Criterion (Original Definition) 8
2.2 Bandwidth/Pitch-Rate Overshoot Criterion 13
2.3 The Smith-Geddes Criterion 16
2.4 The Phase Rate Criterion 18
2.5 The Dropback Criterion 20
3. Objective 23
4. Development of a Small Perurbations Model 24
4.1 F-4C Dimensions, Flight Condition Parameters and Pitch Control System 24
4.2 State Space Model of the Airframe 28
4.3 Airframe State Space Model Augmentation 30
4.4 Actuator Dynamics 33
4.5 Pitch-SAS Dynamics 34
4.6 Gearing, Feel System and Bobweight 36
4.6.1 First Formulation 37
4.6.2 Verification of Aircraft Reponses 42
4.6.2.1 Flight Condition 1 42
4.6.2.2 Flight Condition 3 44
4.6.3 Second Formulation 50
4.6.4 Verification of Aircraft Reponses 52
4.6.4.1 Flight Condition 1 52
4.6.4.2 Flight Condition 3 54
5. Application of PIO-Criteria 57
5.1 The Neal and Smith Criterion 57
5.2 Bandwidth/Pitch-Rate Overshoot Criterion 59
5.3 The Smith-Geddes Criterion 62
5.4 The Phase Rate Criterion 64
5.5 The Dropback Criterion 69
6. Summary of Findings and Conclusions 73
Appendix A 75
Appendix B 76
References 77
Bibliography 79

List of Figures

Figure 2-1	Closed-Loop Pitch Tracking Model (Neal and Smith Criterion)	9
Figure 2-2	Definition of Bandwidth Frequency, Closed-Loop Droop and Closed-Loop Resonance (Neal and Smith Criterion)	10
Figure 2-3	Nichols Chart of Compensated PVS (Neal and Smith Criterion)	12
Figure 2-4	Neal and Smith Criterion Boundaries for the Pitch Tracking Task	12
Figure 2-5	Bandwidth Definition (Bandwidth/Pitch-Rate Overshoot Criterion)	14
Figure 2-6	Pitch-Rate Overshoot Definition (Bandwidth/Pitch-Rate Overshoot Criterion)	15
Figure 2-7	Bandwidth/Pitch-Rate Overshoot Criterion Boundaries	15
Figure 2-8	Average Slope in Bode Plot of Pitch-Attitude-to-Stick-Force-Input Response (Smith-Geddes Criterion)	16
Figure 2-9	Phase of Normal Acceleration-to-Stick-Force-Input Response at Pilot's Position (Smith-Geddes Criterion)	17
Figure 2-10	Phase Rate Definition (Gibson Phase Rate Criterion)	19
Figure 2-11	Gibson Phase Rate Criterion Boundaries	20
Figure 2-12	Definition of Gibson Dropback Criterion Parameters	21
Figure 2-13	Gibson Dropback Criterion Boundaries	22
Figure 4-1	F-4C Flight Envelope	24
Figure 4-2	F-4C General Arrangement	25
Figure 4-3	Coordinate System	26
Figure 4-4	F-4C Pitch Control System	27
Figure 4-5	Basic Airframe Responses, Flight Condition 1	32
Figure 4-6	Basic Airframe Responses, Flight Condition 3	32
Figure 4-7	Pitch Stability Augmentation System	34
Figure 4-8	Feel System and Bobweight Mechanism	37
Figure 4-9	Full Order State Space Model Responses, Flight Condition 1	42
Figure 4-10	Pitch Attitude Responses, Flight Condition 1	43
Figure 4-11	Bode Plot of Pitch Attitude-to-Stick-Force-Input Response, Flight Condition 1	43
Figure 4-12	Full Order State Space Model Responses, Flight Condition 3	44
Figure 4-13	Normal Acceleration Response at Bobweight Position, Flight Condition 3	45
Figure 4-14	Normal Acceleration Response at Pilot's Position, Flight Condition 3	45
Figure 4-15	Pitch Attitude Response for Bobweight Loop Open and Closed, Flight Condition 3	46
Figure 4-16	Pitch Attitude Responses for Bobweight Loop Closed, Flight Condition 3	47
Figure 4-17	Normal Acceleration Responses at Pilot's Position for Bobweight Loop Closed, Flight Condition 3	48

Figure 4-18	Bode Plot of Pitch Attitude-to-Stick-Force-Input Response, Flight Condition 3	49
Figure 4-19	Modified Full Order State Space Model Responses, Flight Condition 1	52
Figure 4-20	Modified Pitch Attitude Response, Flight Condition 1	53
Figure 4-21	Modified Bode Plot of Pitch Attitude-to-Stick-Force-Input Response, Flight Condition 1	53
Figure 4-22	Modified Full Order State Space Model Responses, Flight Condition 3	54
Figure 4-23	Pitch Attitude Responses for Bobweight Loop Closed, Flight Condition 3	55
Figure 4-24	Normal Acceleration at Pilot's Position, Flight Condition 3	55
Figure 4-25	Modified Bode Plot of Pitch Attitude-to-Stick-Force-Input Response, Flight Condition 3	56
Figure 5-1	Neal and Smith Criterion Boundaries for the Pitch Tracking Task	59
Figure 5-2	Bandwidth/Pitch-Rate Overshoot Criterion Boundaries	62
Figure 5-3	Smith-Geddes Criterion Boundaries	64
Figure 5-4	Phase Rate Criterion Boundaries	68
Figure 5-5	Conventional Aircraft Responses	69
Figure 5-6	Pitch Attitude Response to a Rectangular Pulse Input of State Space Model	70
Figure 5-7	Dropback Criterion Boundaries	72

List of Tables

Table 4-1	General Flight Condition Paramters	26
Table 4-2	Longitudinal Aerodynamic Stability and Control Derivatives	28
Table 4-3	F-4C Feel System Metrics	38
Table 4-4	Eigenvalues, Damping and Natural Frequencies, Flight Condition 3	46
Table 5-1	Neal and Smith Criterion Parameters for the Compensated System, Flight Condition 3	58
Table 5-2	Bandwidth/ Pitch-Rate Overshoot Criterion Parameters, Flight Condition 1	61
Table 5-3	Bandwidth/ Pitch-Rate Overshoot Criterion Parameters, Flight Condition 3	61
Table 5-4	Smith-Geddes Criterion Parameters, Flight Condition 1	63
Table 5-5	Smith-Geddes Criterion Parameters, Flight Condition 3	63
Table 5-6	Phase Rate Criterion Parameters for a Stick Force Input, Flight Condition 1	66
Table 5-7	Phase Rate Criterion Parameters for a Stick Deflection Input, Flight Condition 1	66
Table 5-8	Phase Rate Criterion Parameters for a Stick Force Input, Flight Condition 3	67
Table 5-9	Phase Rate Criterion Parameters for a Stick Deflection Input, Flight Condition 3	67
Table 5-10	Dropback Criterion Parameters, Flight Condition 1	71
Table 5-11	Dropback Criterion Parameters, Flight Condition 3	71
Table 6-1	Summary of Results	73

Notation

Abbreviations

AOA	Angle of Attack
APC	Aircraft-Pilot-Coupling
CAT	Clear Air Turbulence
c.g.	Centre of Gravity
FBW	Fly-By-Wire
FC 1	Flight Condition 1
FC 1-1	Flight Condition 1, SAS engaged, bobweight loop closed
FC 1-2	Flight Condition 1, SAS disengaged, bobweight loop closed
FC 1-3	Flight Condition 1, SAS engaged, bobweight loop open
FC 1-4	Flight Condition 1, SAS disengaged, bobweight loop open
FC 1-5*	Flight Condition 1, feel system and bobweight excluded, SAS engaged
FC 1-6*	Flight Condition 1, feel system and bobweight excluded, SAS disengaged
FC 3	Flight Condition 3
FC 3-1	Flight Condition 3, SAS engaged, bobweight loop closed
FC 3-2	Flight Condition 3, SAS disengaged, bobweight loop closed
FC 3-3	Flight Condition 3, SAS engaged, bobweight loop open
FC 3-4	Flight Condition 3, SAS disengaged, bobweight loop open
FC 3-5*	Flight Condition 3, feelsystem and bobweight excluded, SAS engaged
FC 3-6*	Flight Condition 3, feelsystem and bobweight excluded, SAS disengaged
FCC	Flight Control Computer
FCS	Flight Control System
HOS	High Order System
LAHOS	Landing Approach High Order System

* only applicable for Gibson Phase Rate Criterion

N.A.	Not applicable
PA	Power Approach
PIO	Pilot Induced Oscillations, Pilot Involved Oscillations, Pilot In-the-loop Oscillations
PVS	Pilot Vehicle System
SAS	Stability Augmentation System
SL	Sea Level
TF-Function	Transfer Function
VMC	Visual Meteorological Conditions

Standard Symbols

A	State matrix	[-]
$A(\omega_i)$	$=\left\lvert\frac{\theta}{F_{es}}(\omega_i)\right\rvert$, gain of pitch-attitude-to-stick-force-input response	[dB]
a	Aerodynamic matrix	[-]
a_{zBW}	Normal acceleration at bobweight position	[ft/sec^2]
a_{zP}	Normal acceleration at pilot`s position	[ft/sec^2]
a_{zx}	Normal acceleration at distance x from cg	[ft/sec^2]
a_0	Viscous damper, bellows pressure and bellows spring of artificial feel system	[lb/in]
a_1	Lumped viscous damping of artificial feel system	[lb/in/sec]
a_2	Lumped inertia of stick	[lb/in/sec^2]
B	Input matrix	[-]
b	Input matrix	[-]
b	Viscous damper of artificial feel system	[lb/in/sec]
C	Output matrix	[-]
D	Direct matrix	[-]
$D_P(s)$	Pilot time delay transfer function ($D_P(s) = e^{\tau_{Pi}s}$)	[-]
F_{es}	Stick force (positive aft)	[lb]

$F_{P(s)}$	Pilot model transfer function	[-]
F_{BW}	Bobweight force	[lb]
F_{ST}	Stick force (positive aft)	[lb]
F^*_{ST}	Stick force (positive aft), (= F_{ST} - F_{BW})	[lb]
f_{180}	Frequency at -180 deg phase lag	[Hz]
g	Acceleration due to gravity	[ft/sec^2]
g_{1BW}	$= z_u - x_{BW}\ m_u$	
g_{2BW}	$= z_w - x_{BW}\ m_w$	
g_{3BW}	$= z_q - x_{BW}\ m_q - U_0$	
g_{4BW}	$= z_\theta - x_{BW}\ m_\theta$	
g_{5BW}	$= z_{\delta_s} - x_{BW}\ m_{\delta_s}$	
g_{1x}	$= z_u - x\ m_u$	
g_{2x}	$= z_w - x\ m_w$	
g_{3x}	$= z_q - x\ m_q - U_0$	
g_{4x}	$= z_\theta - x\ m_\theta$	
g_{5x}	$= z_{\delta_s} - x\ m_{\delta_s}$	
h	Altitude	[ft]
I	Identity matrix	[-]
i	The complex variable ($\sqrt{-1}$)	[-]
K	gain	[-]
K_{BW}	Bobweight gain ratio	[lb/g]
K_G	Gearing ratio	[-]
K_P	Pilot gain	[-]
K_q	Pitch-SAS feedback gain	[-]
l_{xP}	Distance to pilot`s position along the x-body axis from the *cg* (positive forward)	[ft]
M	Mach Number	[-]

M_q	Normalised longitudinal aerodynamic stability derivative – pitching moment due to pitch rate	[1/sec]
M_u^*	Normalised longitudinal aerodynamic stability derivative – pitching moment due to velocity and thrust	[1/sec-ft]
$M_{\dot{u}}$	Normalised longitudinal aerodynamic stability derivative – pitching moment due to acceleration	[1/sec-ft]
M_w	Normalised longitudinal aerodynamic stability derivative – pitching moment due to 'incidence'	[1/sec-ft]
$M_{\dot{w}}$	Normalised longitudinal aerodynamic stability derivative – pitching moment due to downwash lag	[1/sec-ft]
M_{δ_S}	Normalised longitudinal aerodynamic control derivative – pitching moment due to horizontal stabiliser deflection	[1/sec^2]
m	Mass matrix	[-]
m_q	Normalised longitudinal aerodynamic stability derivative – pitching moment due to pitch rate (state space)	
m_u	Normalised longitudinal aerodynamic stability derivative – pitching moment due to velocity and thrust (state space)	
m_w	Normalised longitudinal aerodynamic stability derivative – pitching moment due to 'incidence' (state space)	
m_{δ_S}	Normalised longitudinal aerodynamic control derivative – pitching moment due to horizontal stabiliser deflection (state space)	
$m_{\delta_{ST}}$	Normalised longitudinal aerodynamic control derivative – pitching moment due to stick deflection (state space)	
m_θ	Normalised longitudinal aerodynamic stability derivative – pitching moment due to pitch attitude angle (state space)	
P_{BF}	Feel system parameter	[ft^2]
$P_P(s)$	Pilot lead/lag compensation transfer function	[-]
PR, PR_{180}	Phase rate around neutral stability point, where ϕ = -180 deg	[deg/Hz]
p	Roll rate	[rad/sec]
q	Pitch rate (positive nose up)	[rad/sec]
$\dot{q}$	Pitch acceleration	[rad/sec^2]
$\bar{q}$	Dynamic pressure	[lb/ft^2]
q_B	Feelsystem parameter	[lb/ft^2]
q_{peak}	Maximum pitch rate	[rad/sec]

q_{SS}	Steady-state pitch rate	[rad/sec]
r	yaw rate	[rad/sec]
S	Average slope in the pitch-attitude-to-stick-force-input gain plot between ω=2.0 rad/sec and ω=6.0 rad/sec (Smith and Geddes Criterion)	[dB/octave]
s	Laplace operator	[-]
TA	Actuator time constant	[sec]
T_{P1}	Time constant for pilot lead/lag compensation	[sec]
T_{P2}	Time constant for pilot lag compensation	[sec]
U	Total axial velocity	[ft/sec]
U_0	Axial component of steady-state velocity	[ft/sec]
u	linear perturbed velocity along the x_b-axis (positive forward)	[ft/sec]
u(t)	Input vector	[-]
$\dot{u}$	linear perturbed acceleration along the x_b-axis (positive forward)	[ft/sec^2]
V_{T0}	Total linear steady-state velocity	[ft/sec]
W	Total normal velocity	[ft/sec]
W_0	Normal component of steady-state velocity	[ft/sec]
w	linear perturbed velocity along the z_b-axis (positive down)	[ft/sec]
$\dot{w}$	linear perturbed acceleration along the z_b-axis (positive down)	[ft/sec^2]
X_q	Normalised longitudinal aerodynamic stability derivative – axial force due to pitch rate	[1/sec]
X_u^*	Normalised longitudinal aerodynamic stability derivative – axial force due to velocity and thrust	[1/sec]
$X_{\dot{u}}$	Normalised longitudinal aerodynamic stability derivative – axial force due to acceleration	[1/sec^2]
X_w	Normalised longitudinal aerodynamic stability derivative – axial force due to 'incidence'	[1/sec]
$X_{\dot{w}}$	Normalised longitudinal aerodynamic stability derivative – axial force due to downwash lag	[1/sec^2]
X_{δ_S}	Normalised longitudinal aerodynamic control derivative – axial force due to horizontal stabiliser deflection	[ft/sec^2 rad]
x	Distance from cg	[ft]

x_{BW}	Distance to bobweight position along the x-body axis from the *cg* (positive forward)	[ft]
x(t)	State vector	[-]
$\dot{x}(t)$	Differentiated state vector	[-]
x_b	Longitudinal coordinate in body axes system	[-]
x_q	Normalised longitudinal aerodynamic stability derivative – axial force due to pitch rate (state space)	
x_u	Normalised longitudinal aerodynamic stability derivative – axial force due to velocity and thrust (state space)	
x_w	Normalised longitudinal aerodynamic stability derivative – axial force due to 'incidence' (state space)	
x_{δ_s}	Normalised longitudinal aerodynamic control derivative – axial force due to horizontal stabiliser deflection (state space)	
x_θ	Normalised longitudinal aerodynamic stability derivative – axial force due to pitch attitude angle (state space)	
y(t)	Output vector	[-]
y_b	Lateral coordinate in body axes system	[1/sec]
Z	Matrix (pitch-SAS)	[-]
Z_q	Normalised longitudinal aerodynamic stability derivative – normal force due to pitch rate	[1/sec]
Z_u^*	Normalised longitudinal aerodynamic stability derivative – normal force due to velocity and thrust	[1/sec]
$Z_{\dot{u}}$	Normalised longitudinal aerodynamic stability derivative – normal force due to acceleration	[1/sec^2]
Z_w	Normalised longitudinal aerodynamic stability derivative – normal force due to 'incidence'	[1/sec^2]
$Z_{\dot{w}}$	Normalised longitudinal aerodynamic stability derivative – normal force due to downwash lag	[1/sec^2]
Z_{δ_s}	Normalised longitudinal aerodynamic control derivative – normal force due to horizontal stabiliser deflection	[ft/sec^2 rad]
z_b	Normal coordinate in body axes system	[-]
z_q	Normalised longitudinal aerodynamic stability derivative – normal force due to pitch rate (state space)	
z_u	Normalised longitudinal aerodynamic stability derivative – normal force due to velocity and thrust (state space)	
z_w	Normalised longitudinal aerodynamic stability derivative – normal force due to 'incidence' (state space)	

z_{δ_S}	Normalised longitudinal aerodynamic control derivative – normal force due to horizontal stabiliser deflection (state space)
$z_{\delta_{ST}}$	Normalised longitudinal aerodynamic control derivative – normal force due to stick deflection (state space)
z_θ	Normalised longitudinal aerodynamic stability derivative – normal force due to pitch attitude angle (state space)

Greek Symbols

α	Angle of attack perturbation	[rad]
α_0	Steady-state (trim) angle of attack relative to fuselage reference line	[rad]
ΔA	Gain margin	[dB]
$\Delta G(q)$	Pitch-rate overshoot	[dB]
$\Delta\phi_{2\omega 180}$	$= \phi_{\omega 180} - \phi_{2\omega 180}$	[deg]
$\Delta\theta$	Attitude dropback	[rad]
δ_{es}	Stick deflection	[in]
δ_S	Horizontal stabiliser deflection from trim (positive for trailing edge down)	[rad]
$\dot{\delta}_S$	Horizontal stabiliser deflection rate	[rad/sec]
δ_S^*	Actuator input ($=\delta_{ST} - \delta_{S_{SAS}}$)	[rad]
$\delta_{S_{SAS}}$	Pitch-SAS output, washed-out pitch rate	[rad]
$\dot{\delta}_{S_{SAS}}$	Washed-out pitch acceleration	[rad/sec^2]
δ_{ST}	Stick deflection after feel system gearing	[rad]
$\dot{\delta}_{ST}$	Stick deflection rate ($= \omega_{ST}$)	[rad/sec]
δ_{ST}^*	Stick deflection	[in]
γ	Flight path angle	[rad]
γ_0	Steady-state flight path angle	[rad]
ϕ	Phase angle	[deg]
ϕ_{azP}	Phase angle of the normal acceleration-to-stick-force-input response at pilot's position	[deg]

$\phi_{c\,azP}$	$= \phi_{azP}(\omega_{cr})$-14.3 ω_{cr}	[deg]
ϕ_{cr}	Phase angle at criterion frequency $\{= \frac{\theta}{F_{es}}(\omega_{cr})\}$	[deg]
ϕ_P	Pilot phase compensation angle	[deg]
$\phi_{\omega 180}$	Phase angle at neutral stability frequency	[deg]
$\phi_{2\omega 180}$	Phase angle of twice the neutral stability frequency	[deg]
ω	Frequency	[rad/sec]
ω_{BW}	Pitch attitude bandwidth frequency (Neal & Smith Criterion)	[rad/sec]
$\omega_{BW\gamma}$	Flight path bandwidth frequency (Bandwidth/Pitch-Rate Overshoot Criterion)	[rad/sec]
$\omega_{BW\theta}$	Aircraft pitch attitude bandwidth frequency (Bandwidth/Pitch-Rate Overshoot Criterion)	[rad/sec]
$\omega_{BW\theta\,gain}$	Frequency, where gain margin is 6 dB (Bandwidth/Pitch-Rate Overshoot Criterion)	[rad/sec]
$\omega_{BW\theta\,phase}$	Frequency, where phase margin is 45 deg (Bandwidth/Pitch-Rate Overshoot Criterion)	[rad/sec]
ω_{cr}	Criterion frequency (Smith-Geddes Criterion)	[rad/sec]
ω_{ST}	Stick deflection rate $(= \dot{\delta}_{ST})$	[rad/sec]
$\dot{\omega}_{ST}$	Stick acceleration	[rad/sec^2]
ω_{135}	Frequency, where phase angle assumes a value of –135 deg (phase margin is 45 deg)	[rad/sec]
ω_{180}	Neutral stability frequency/ frequency, where phase angle is –180 deg	[rad/sec]
τ_{Pi}	Pilot time delay	[sec]
$\tau_{P\theta}$	Aircraft pitch attitude phase delay (Bandwidth/Pitch-Rate Overshoot Criterion)	[sec]
θ	Pitch angle (perturbation)	[rad]
$\dot{\theta}$	Pitch rate	[rad/sec]
θ_{cmd}	Pitch attitude command	[rad]
θ_e	Pitch attitude error	[rad]
θ_0	Steady-state pitch attitude angle	[rad]

1. PIOs, an Introduction

Ref. [5], [7], [10]-[14]

Inadvertent, destabilising pilot-aircraft interactions causing unwanted aircraft attitude and flight path motions are most generally referred to as *Aircraft-Pilot-Coupling* (APC) events. They can be either divergent or oscillatory in nature and occur through a variety of flight conditions. In the latter case these phenomena are called PIOs – *Pilot Induced Oscillations, Pilot Involved Oscillations* or *Pilot In-the-loop Oscillations*. They can happen on any aircraft but have had the most devastating effects when encountered by very agile, high performance aircraft as only recently documented in the accidents of the YF-22 and the JAS-39 "Gripen".

APC events usually occur when the pilot is engaged in a highly demanding, closed loop control task (which means the *Pilot Vehicle System* (PVS) is operated close to its stability margins) and a sudden, abnormal change either in pilot behaviour, in aircraft dynamics or in the environment takes place, creating mismatches between actual and expected aircraft responses, causing the control system to become unstable. The following sinusoidal oscillations or divergences result from the efforts of the pilot to simply maintain control and to impose his will on the aircraft and differ greatly from deliberate oscillations caused by periodic stick motion such as stick pumping, which is open loop in character. It is essential for an APC to occur, that the aircraft and pilot dynamics form a closed loop feedback control system, since the pilot's actions need to depend in part on the motions of the aircraft in response to pilot commands. The pilot is said to be *operating closed loop* or to be *in the loop*.

High gain tasks which are a prerequisite for these rare, unexpected interactions include in-flight refuelling, formation flying, landing on the deck of an aircraft carrier, manual terrain following, target tracking and landing in adverse weather conditions. Severe APC events are most commonly due to deficiencies in the design of an aircraft and although the pilot is an essential element, he cannot be made responsible. Nearly all of the documented APC-events have occurred during flight testing. This may seem very comforting, since it is tempting to say, that this is the perfect environment to track down causes and to eliminate them. Unfortunately, it cannot be ruled out that these phenomena do not also occur when an aircraft has already entered operational service. The reason, why so little is heard about APCs in operational service, is that, according to McRuer in Ref. [13], the reporting mechanisms currently available are insufficient.

APC events can occur in pitch, yaw and roll respectively and in some cases they may involve two or three axes simultaneously. This report focuses on PIOs as the oscillatory variant of APC

events. Depending on the frequency, PIOs may be either attitude or flight path-related. If the frequency is at or near the short period natural frequency, it is almost certainly path-related, whereas, if the frequency is significantly higher, it is more likely to be attitude-related. The severity can range from a harmless *pitch-bobble, roll-ratchet* or *yaw chatter* to a sustained, large amplitude oscillation that may jeopardise the safety of the crew and aircraft. Small amplitude oscillations such as pitch-bobble, roll-ratchet and yaw chatter with a frequency of 2 – 3 Hz are characterised by relatively low control forces and are often encountered by novice pilots getting used to a new configuration. They are sometimes also referred to as *low order* PIOs and consist of continual tracking corrections (e.g. pitch bobble). It can happen on any aircraft and has been experienced by most pilots. The majority of these oscillations may therefore be dismissed as a common learning experience. They may also occur due to coupling of the aircraft motion and the pilot's arm, which can be modelled as a simple spring-mass-damper system and has a resonance frequency between 2 and 3 Hz, depending on the neuromuscular tension (biomechanical PIO). But in general, these oscillations are only temporary, easily corrected and not dangerous. The fully developed, large amplitude PIO at the other end of the spectrum has a frequency of only 0.5 – 1 Hz but can have catastrophic consequences, if the aircraft design limits are exceeded or if encountered within close proximity to the ground or other aircraft. These *high order* PIOs can be associated with inadequate pilot-aircraft closed-loop stability margins due to excessive aircraft gain and phase lag and may cause the pilot's stick inputs to be out of phase with the aircraft responses. In a situation were tight control is demanded, the pilot will tend to "overdrive" unpredictably sluggish aircraft responses. He or she will apply excessive control, induced by lack of immediate response, and will consequently produce an overshoot as the response eventually follows. This is countered with a control reversal, leading to an oscillatory overcontrol situation.

There are numerous elements involved in a PIO, but generally these can be conveniently ascribed to either pilot behaviour, the aircraft dynamics or the triggering events, which are explained below.

Pilot Behaviour

The human pilot is the most unpredictable element in the PVS. Due to his or her uniquely human ability to learn, to adapt to varying circumstances very quickly using a great variety of human sensors and to establish a wide range of PVS organisations, he or she is "modifier*" as well as

* McRuer, Ref. [11]

"operating entity*" within the system. The gross number of available sensing mechanisms to perceive and analyse perturbations in the environment and the strong influence of psychological factors such as stress, motivation or even fear in emergency situations have great impact on pilot behaviour and, depending on the individual mental constitution, may affect pilot actions in various ways. All these characteristics seem to make it extremely difficult to derive an adequate mathematical model of the pilot, suitable for PIO-prediction. But experience has shown, that the spectrum of behavioural patterns needed to successfully control a complex system, which is operated close to its stability margins, is very narrow. Therefore, it is possible to define *behavioural laws*, which a pilot will necessarily have to comply with, if he attempts to cope with such a demanding task. This makes his actions predictable and, more importantly, open to mathematical analysis. The behavioural modes, which can lead to or influence PIO events, are the following:

- In *compensatory behaviour,* as McRuer describes it in Ref. [11], "commands and disturbances are randomly appearing and the pilot's response is primarily conditioned on system errors." By exerting continuous closed-loop control, the pilot will attempt to minimise the error between system input (i.e., desired aircraft attitude) and system output (i.e., perceived aircraft attitude).
- When command inputs and system outputs become distinguishable and the pilot is able to preview system inputs, *pursuit behaviour* is attained. In this behavioural mode the pilot applies open loop control in conjunction with compensatory, closed loop error correction action. This type of pilot behaviour is common in many flight phases in VMC conditions, where sufficient visual cues are available.
- The highest possible level of control is achieved with pure, open-loop, automatic or *precognitive behaviour*. In this case the level of familiarity with the aircraft is so high, that the pilot is able to generate control inputs, which will result almost exactly in the desired aircraft response with nearly no follow-up compensatory action necessary. Just like pursuit behaviour it is also a dual-mode form of control.

Aircraft Dynamics

The aircraft dynamics comprise the dynamics of elements such as the airframe, actuators, Stability Augmentation System (SAS), inceptors (stick, pedals) and the artificial feel system. Since there is a strong correlation between handling qualities and PIO-susceptibility (i.e., in case

of poor handling qualities there is a high degree of PIO-susceptibility), there are a number of design features/deficiencies, which may contribute to a strong PIO-tendency. For instance, if the damping of the short period mode is insufficient, a greater susceptibility to PIOs can be expected. The use of stability augmentation systems, different filters such as notch and anti-aliasing filters in forward and feedback paths, actuators, feel systems, etc. are all sources for additional phase lags. If the lags become excessive, a rapid deterioration of system performance and stability results, possibly leading to a PIO-condition. SAS and other Flight Control System (FCS)-related subsystems share control authority over control surfaces with the pilot. The pilot's control authority can be substantially reduced in situations, where SAS-inputs are given priority over pilot-inputs, causing pilot-commands to be executed with significant delay. Time delays, which stem from the finite processing time of Flight Control Computers (FCC), finite sampling rates, etc. may also contribute to a PIO-tendency in unfavourable circumstances. In large aircraft, control inputs may couple with structural modes of the flexible airframe.

Triggers

Triggers are initiating events, which lead to sudden, as described in Ref. [13], "cliff-like" changes in pilot-vehicle system characteristics, immensely degrading system stability and damping and thus producing a PIO. They may originate in the environment, the aircraft or the pilot. External triggering events include gusts, windshear, Clear Air Turbulence (CAT), icing, vortex encounters or the threat of a mid-air collision.

Aircraft-based triggering events usually involve transitions in the effective vehicle dynamics, causing mismatches between the pilot's control strategy and the predominant vehicle dynamics. These transitions may be caused by system failures, which suddenly compromise control authority or control power (System failures can be a pitch-damper failure, failures in the hydraulic system, actuator failures, etc.) or by modifications of the effective vehicle configuration such as a reheat light-off or an unsymmetrical jettison of outer stores, which abruptly changes the aerodynamic properties and causes the aircraft to be completely out of trim. Or they are due to a shift in control laws, initiated, for example, by a weight-on-wheels switch, changing from "air" to "ground" mode. A critical flight condition may be masked by the engaged autopilot and as soon as manual control is assumed, the pilot is suddenly confronted with an aircraft that is on the verge of a departure. All these incidents have a strong, imminent effect on the pilot, forcing him to shift attention quickly and to perform quick, abrupt control actions, resulting in an increase of stress

and pilot workload. If the aircraft is only marginally stable on its own, it may take only a small increase in pilot gain to destabilise the entire system.

Changes in pilot behaviour are major sources for PIO-triggers as well. These triggers are very often preceded by an environmental or aircraft trigger, causing the pilot to overreact or respond inappropriately. A transition from pursuit to compensatory behaviour or from precognitive to compensatory behaviour may significantly reduce the closed loop system bandwidth. Bandwidth is the frequency range, in which the pilot can operate the aircraft closed-loop, without compromising PVS stability. Such a change in behaviour can be observed extremely well in carrier landings, where close tracking of the carrier deck for an on-spot landing is vital. Similar behaviour may be seen in in-flight-refuelling, where a shift in visual cues takes place. After aligning with the tanker-aircraft, the pilot will focus on the refuelling basket, switching from initially measuring distances in feet or yards to inches. Additionally, task related stress in such manoeuvres impairs the performance of the PVS even further.

1.1. PIO-Development

After the triggering event has occurred and the effective aircraft dynamics have changed, while the pilot is engaged in a full-attention, compensatory task, there follows a period called *post transition retention*. In this stage of a PIO-development the pilot is still responding according to the pre-transition vehicle dynamics. If his control actions are inappropriate to the "new" aircraft dynamics, the closed-loop system stability may suffer, that is, the available closed loop system bandwidth is dramatically reduced and a PIO may develop. Experience has shown that once the PIO is fully developed the pilot progresses through several phases of adaptation and will eventually synchronise his inputs with the ongoing sinusoidal oscillation. At first, he will not recognise the periodic character of the oscillation and will treat it as a series of random disturbances, trying to minimise the error (compensatory behaviour). But after a period of adjustment, the pilot will duplicate the sinusoid without any phase lag up to a frequency of 3 Hz, in which case the pilot can safely be approximated as a pure gain. This special type of behavioural pattern is called *synchronous precognitive behaviour*.

The actual pilot input characteristics depend primarily on the type of inceptor used. Conventional centre-sticks or control columns usually produce sinusoidal inputs, whereas short side-sticks often create rectangular inputs, being fully deflected from backward mechanical stop to forward mechanical stop (*bang-bang-control*).

There are not many possibilities of stopping a fully developed PIO. First, the pilot needs to realise that he is encountering a PIO. This in itself is not very straightforward because very often the pilot will ascribe the oscillation to his or her poor piloting skill or to a malfunction within the FCS. If he eventually does realise the condition, then one way to arrest the oscillation is to open the loop by abandoning the task at hand by either releasing or freezing the stick. With the aircraft left to its own devices, the oscillation will eventually fade away. But in some flight phases such as landing, the pilot just cannot afford to relax control in close proximity to the ground and he becomes locked into a behaviour that will actually sustain the oscillation. This has resulted in many accidents. A further possibility is to counter the oscillation with very sharp, precise control inputs, which is not always feasible, especially in turbulent atmosphere.

1.2. Classification of PIOs

PIOs are divided into three different categories.

Category I

"In Category I PIO phenomena, the effective aircraft dynamics are essentially linear and pilot behaviour is also considered to be *quasi-linear* and time stationary" {McRuer, Ref. [11]}. This means that during the PIO neither the effective aircraft dynamics nor the pilot's dynamics change. There are "no significant frequency-variant non-linearities" {McRuer, Ref. [11]} within the aircraft control system such as non-linear stick sensitivity (break-out forces), command shaping of input signals, hysteresis due to friction in mechanical control systems or the like and no mode shifts in pilot behaviour. Susceptibility to a linear PIO can solely be associated with two factors, one being "the pilot's ability to close the PVS loop on a broad range of pilot generated gains needed to achieve adequate closed loop system performance" {McRuer, Ref. [13]}. If the effective aircraft gain is too high, the added gain of the pilot for the task at hand may drive the system unstable. The other factor is excessive phase or time lag, which limits the possible range of pilot-generated gains and reduces the *neutral stability frequency* (*crossover frequency*), directly affecting closed loop system bandwidth and performance.

Category I PIOs are not always severe and fade away as soon as control is relaxed. They may often be dismissed as a learning experience and are most likely to occur in cases of pilot maladaptation to aircraft dynamics. In cases of major triggering events and disturbances in conjunction with excessive time lags or inadequate available gain margin they do become severe in conditions, where tight aircraft control needs to be sustained.

Category II

Category II PIOs are quasi-linear PVS oscillations with control surface-rate and position-limiting as the only explicitly non-linear factors. Especially rate-limiting, a design feature intended to protect the actuation system from excessive loads, can be a hideous contributor to PIO-development in modern, Fly-By-Wire (FBW) aircraft. The pilot, being engaged in a high gain task, may demand a surface deflection-rate, that is greater than physically possible and overrides the actuation system. Since he or she has no reference about the actual position of the control surface in relation to stick position, the pilot may ask for an opposite deflection-rate, while the control surface is still travelling in the initial direction. This will introduce extra delay in the aircraft response, making the pilot feel more and more "detached" because the aircraft reactions no longer seem to correspond to pilot inputs.

Category II PIOs are always severe due to the fact, that the oscillation amplitudes need to be large enough that rate and position-limiting become effective. Opposed to Category I this adds an amplitude-dependent lag and sets the limit cycle magnitude.

Category III

Category III PIOs comprise essentially non-linear PVS oscillations with transitions. They fundamentally depend on non-linear transitions in either the aircraft dynamics or in the pilot's behavioural dynamics. A transition in aircraft dynamics may result from the large magnitude of pilot commands, internal mode changes in the FCS (change in control laws) or changes in the aerodynamic or propulsion configuration. Transitions in pilot behaviour include shifts in behavioural laws (e.g. compensatory to synchronous precognitive), changing of cues (from pitch-attitude to normal acceleration) and shifting attention and modifying control strategies to comply with demanding, high gain tasks.

2 Criteria for PIO-Assessment

The growing complexity of modern FCSs introduces additional dynamics to the conventional low order response characteristics of an aircraft or alters these completely. Quite often these *High Order Systems* (HOS) produce handling qualities that are not acceptable for human piloted flight, even when short period dynamics are perfectly acceptable. A number of analysis criteria have been developed, which assess handling deficiencies and PIO-tendencies for longitudinal as well as lateral aircraft motions. However, the majority of these criteria address pitch-PIOs, since they are the most spectacular and destructive with the largest excursions in acceleration.

It has to be emphasised that because the number of variables that have to come together for a PIO to occur is so large, these PIO-criteria do not attempt to predict the occurrence of a PIO for a particular aircraft. The intention is to merely predict the susceptibility to PIO with a reasonable degree of confidence. Even if a high level of PIO-potential is diagnosed for a certain configuration, it does not consequently imply that this type will definitely encounter a PIO in its operational life or, vice versa, a design that passed all applied criteria without a flaw may still experience this phenomenon due to very unusual and unique circumstances. Also, all criteria addressed in this report analyse aircraft performance prior to any upset in PVS-characteristics that may cause a PIO. None investigate the *post transition retention phase,* probably the most fundamental phase in the development of a PIO, simply because there are too many unknowns. To ensure that a design is resistant to PIOs, as many different criteria as possible should be applied. This way the probability for an actual PIO to occur can be minimised. Some of the most acknowledged longitudinal PIO-analysis criteria based on linear aircraft dynamics are introduced below.

2.1 The Neal and Smith Criterion (Original Definition)

Ref. [2], [5], [6], [13], [15], [17]

In the attempt to acquire more knowledge about high order effects, a number of flight test programmes were undertaken by the Pentagon in the late 1960's and early 1970's to validate handling qualities of highly augmented fighter aircraft, so called *High Order Systems* (HOS) or aircraft with non-conventional responses, producing enormous amounts of flight test data. In 1970 the *Neal and Smith Criterion* evolved from this effort to assess precision tracking tasks of flight phases of *Category A* (see *Appendix A*). It was later extended to include equivalent tasks of *Flight Phases B* and *C* (using the *Landing Approach High Order System* (LAHOS)-database for verification).

The criterion assumes a simple closed-loop pitch attitude tracking task as shown in *Figure 2-1.*

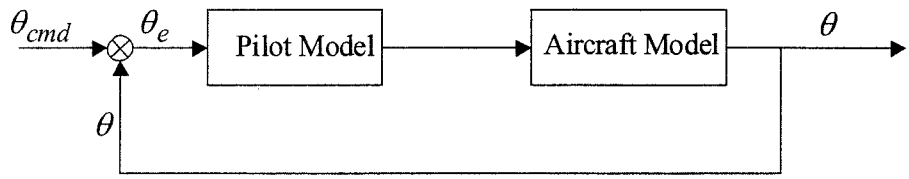

Figure 2-1, Closed-Loop Pitch Tracking Model

It is the only criterion introduced and applied in this project that explicitly includes a pilot model. The pilot can be viewed as a pitch attitude compensator and can be described by the following transfer function.

$$F_P(s) = K_P \cdot e^{-\tau_{Pi} s}\left(\frac{1+sT_{p1}}{1+sT_{p2}}\right) = K_P\, D_P(s)\, P_P(s) \qquad \textit{(Equation 2-1)}$$

The model consists of a variable gain K_P, a pure delay τ_{Pi}, and a first order lead/lag compensation $P_P(s)$. The pilot inherently adjusts K_P, τ_{Pi}, T_{P1} and T_{P2} to establish a PVS-organisation that is adequate for the pursued task. But it was found that the human pilot's ability to vary the time delay τ_{Pi} is confined to a very limited range of only 0.2 – 0.4 sec. Usually a constant time delay of 0.3 sec is assumed.

The criterion, which was primarily developed to analyse handling qualities and applies only indirectly to PIO-prediction, specifies precise performance requirements that have to be fulfilled. These are based on pilot comments addressing the ability to acquire a target quickly and predictably with a minimum of overshoot and oscillation.

- The pilot has to close the loop with a certain degree of aggressiveness. This limit is defined in the frequency domain as the *bandwidth frequency* ω_{BW} at which the phase of the closed-loop system $\angle\, \theta / \theta_{cmd}$ has to be –90 deg. The bandwidth frequency is task-dependent and a measure of how quickly the pilot can move the nose of the aircraft toward the target. According to MIL-STD-1797A, the bandwidth frequency for flight phases of Category A is 3.5 rad/sec. For flight phases of Category B and C it is 1.5 rad/sec except for landing, where a frequency of 2.5 rad/sec is demanded.
- The *low frequency, closed-loop droop*, which describes the maximum excursion of $|\theta / \theta_{cmd}|$ below 0 dB for frequencies less than $\omega = \omega_{BW}$, must not exceed –3 dB. Droop is a measure of how slowly the nose of the aircraft settles on the target.

With the obligation to meet these performance standards, the pilot model parameters (with $\tau_{Pi} = const.$ these comprise K_P, T_{P1}, and T_{P2}) are varied to produce the best overall closed loop performance. The determination of the most suitable pilot model is not trivial and is an iterative optimisation process.

The criterion output parameters are the phase angle of the required pilot compensation ϕ_P (measure of pilot workload) and the maximum value of *closed-loop resonance* $|\theta / \theta_{cmd}|_{max}$. Closed-loop resonance is the magnitude of any resonant peak in the closed loop $|\theta / \theta_{cmd}|$ Bode plot and can be directly related to the damping ratio and the magnitude of pitch attitude oscillations perceived by the pilot when performing a tracking task. Meeting exactly the performance requirements (ω_{BW} = 3.5 rad/sec, droop = -3.0 dB) will result in the smallest achievable closed-loop resonance.

Bandwidth frequency, low frequency closed-loop droop, and closed-loop resonance are depicted in the closed-loop θ / θ_{cmd} Bode plot in *Figure 2-2.*

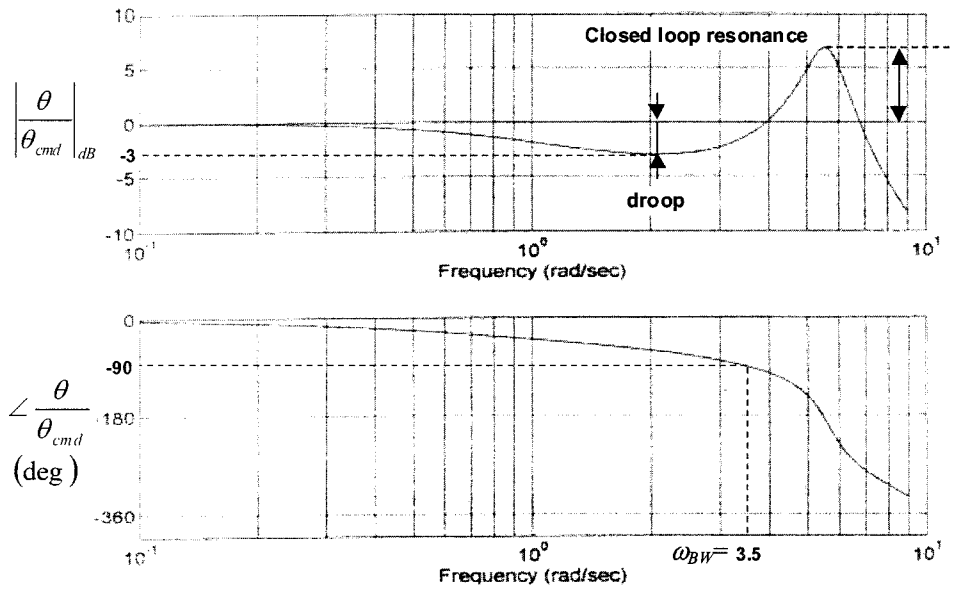

Figure 2-2, Definition of Bandwidth Frequency, Closed-Loop Droop and Closed-Loop Resonance

Bringing the closed-loop gain and phase characteristics into agreement with the performance requirements can be simplified by the use of a Nichols chart, which makes it possible to refer to open and closed-loop gain and phase characteristics simultaneously. The first step is to pre-multiply the transfer function of the aircraft with the pilot time delay $D_P(s) = e^{-\tau_{Pi} s}$ and plotting the resulting open-loop system transfer function, which now only includes fixed parameters ($\tau_{Pi} = const$), on the Nichols chart. The required, pilot-generated phase and gain compensation at a bandwidth frequency of, for instance, 3.5 rad/sec can then be estimated. If a lag compensation is needed, the following transfer function applies

$$P_P(s) = \left(\frac{1 + s T_{P1}}{1 + s T_{P2}} \right) \qquad \textit{(Equation 2-2)}$$

whereas if a lead compensation is required ($T_{P2} = 0$) *Equation 2-2* reduces to

$$P_P(s) = 1 + s T_{P1} \qquad \textit{(Equation 2-3)}$$

The pilot time constants for a lag compensation T_{P1} and T_{P2} have to satisfy the following equations simultaneously

$$\left(\frac{1}{T_{P1} T_{P2}} \right)^{0.5} = \omega_{BW} \qquad \textit{(Equation 2-4)}$$

$$\sin \phi_P = \frac{T_{P1} - T_{P2}}{T_{P1} + T_{P2}} \qquad \textit{(Equation 2-5)}$$

where ϕ_P is the phase angle the pilot needs to generate to fully compensate the system.

Figure 2-3 shows the compensated, closed-loop PVS plotted on a Nichols chart.

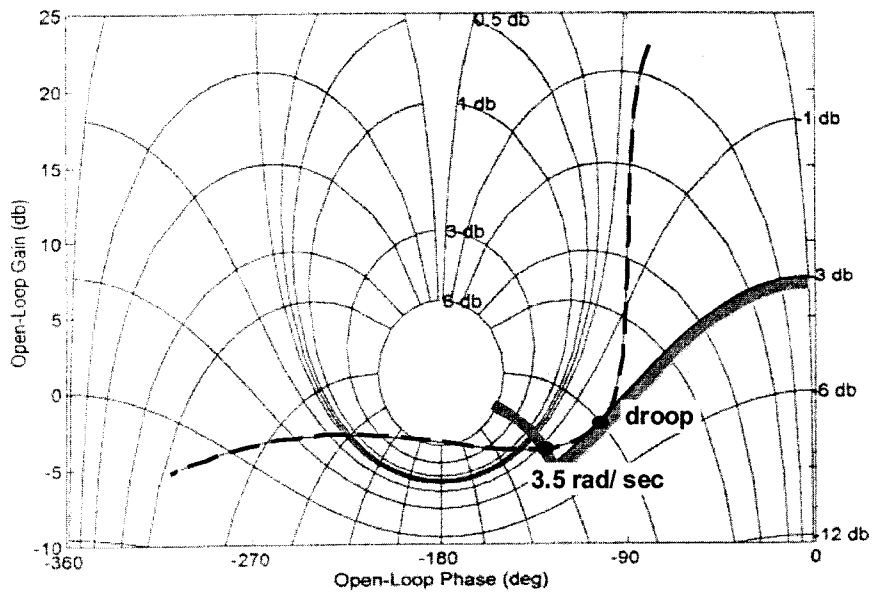

Figure 2-3, Nichols Chart of Compensated PVS

After determining the gain and phase compensation required to meet the criterion limits, the closed-loop resonance and demanded lead/lag phase compensation is then compared against the established criterion boundaries illustrated in *Figure 2-4.* These are based on results obtained from the flight testing campaign mentioned earlier, associating pilot rating with the analysed configurations.

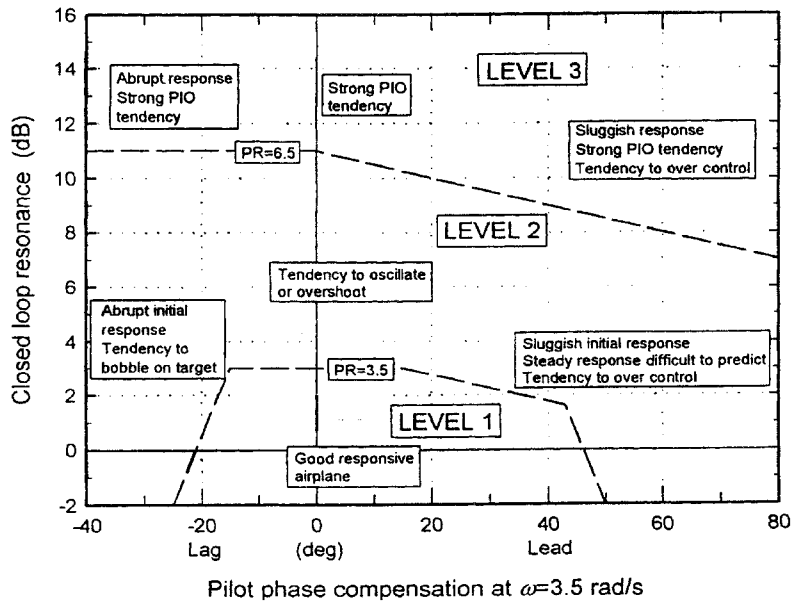

Figure 2-4, Neal and Smith Criterion Boundaries for the Pitch Tracking Task, adapted from Ref. [2]

2.2 Bandwidth/ Pitch-Rate Overshoot Criterion

Ref. [5]-[7], [13], [15], [17]

The original Bandwidth Criterion was developed by Hoh, Mitchell and Hodgkinson in 1982 for the evaluation of handling qualities and PIO-tendencies of highly-augmented aircraft. It relies on the open-loop pitch attitude frequency response characteristics of the aircraft. The two frequency domain metrics originally used for assessment are *aircraft bandwidth* $\omega_{BW\theta}$ and *phase delay* $\tau_{p\theta}$. The aircraft bandwidth is defined as the frequency range in which the pilot–aircraft loop can be closed without threatening stability (i.e., encountering a PIO). Since it is assumed that the pilot can be approximated as a pure gain and can close the loop without having to generate any lead or lag compensation (synchronous behaviour), McRuer describes bandwidth as the frequency range "within which the aircraft dynamics can accommodate changes in pilot gain" {McRuer, Ref. [13]} necessary for a specific task without compromising system stability. The *bandwidth frequency* $\omega_{BW\theta}$ marks the upper end of this range and is defined as the frequency, where the phase margin is either 45 deg or the gain margin is 6 dB, whichever frequency is lower (see *Figure 2-5*). Consequently, a great effort is made to design aircraft with a high bandwidth.

Application of the bandwidth definition to the Neal and Smith database soon revealed that the use of the bandwidth frequency as the sole criterion metric was insufficient for the assessment of handling qualities. It was realised that the rate of phase roll-off beyond the bandwidth frequency (i.e. how fast the phase shift approaches –180 degrees), described by the *pitch attitude phase delay* $\tau_{p\theta}$ has to be considered as well, to account for varying pilot techniques. If the pilot finds it necessary to apply lead compensation due to either a low aircraft bandwidth or high task demands, a low value of phase delay, corresponding to a slow phase roll-off, indicates insensitivity to minor changes in pilot gain. On the other hand, high values of phase delay, corresponding to a more rapid drop of the phase curve, restricts the pilot's ability to operate at frequencies above the bandwidth frequency, if PIO is to be avoided.

$$\tau_{p_\theta} = \frac{\Delta\phi_{2\omega_{180}}}{57.3\,(2\omega_{180})}$$

$$\omega_{BW_\theta} = \min(\omega_{BW_{\theta gain}}, \omega_{BW_{\theta phase}})$$

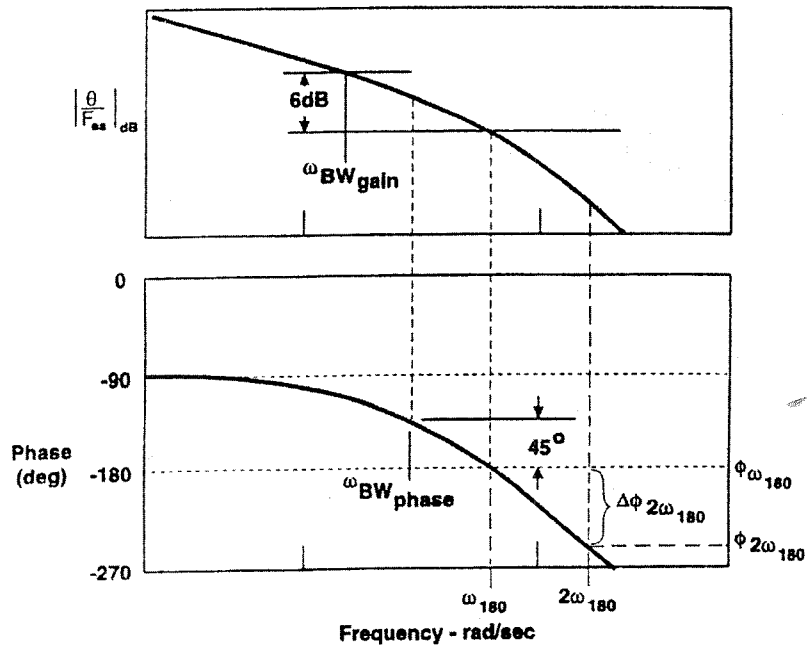

Figure 2-5, Bandwidth Definition, adapted from Ref. [13]

The original Bandwidth Criterion has been adjusted to accommodate *flight path bandwidth* and *pitch-rate overshoot* as additional criterion parameters. The *flight path bandwidth frequency* ω_{BW_γ} is defined as the frequency where the phase margin of the flight-path-to-stick-force response is 45 degrees. A low value of flight path bandwidth, which implies a need for pilot lead compensation to improve aircraft response, in conjunction with a moderate value of phase delay may exhibit PIOs.

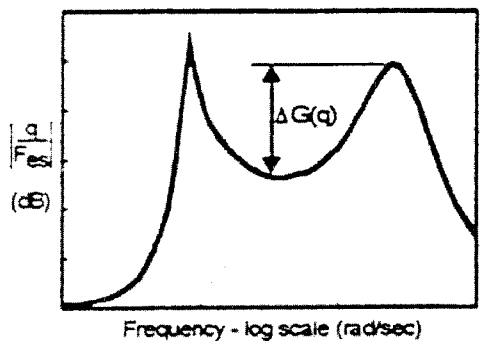

Figure 2-6, Pitch-Rate Overshoot Definition, adapted from Ref. [15]

Pitch-rate overshoot ΔG(q) is a measure of overshoot referenced to the mid-frequency response of the aircraft, where the pilot usually exerts closed loop control. High pitch-rate overshoot is directly linked to bobble-tendencies and abrupt, short-term responses, which are highly undesirable.

The criterion parameters translate into the following graph:

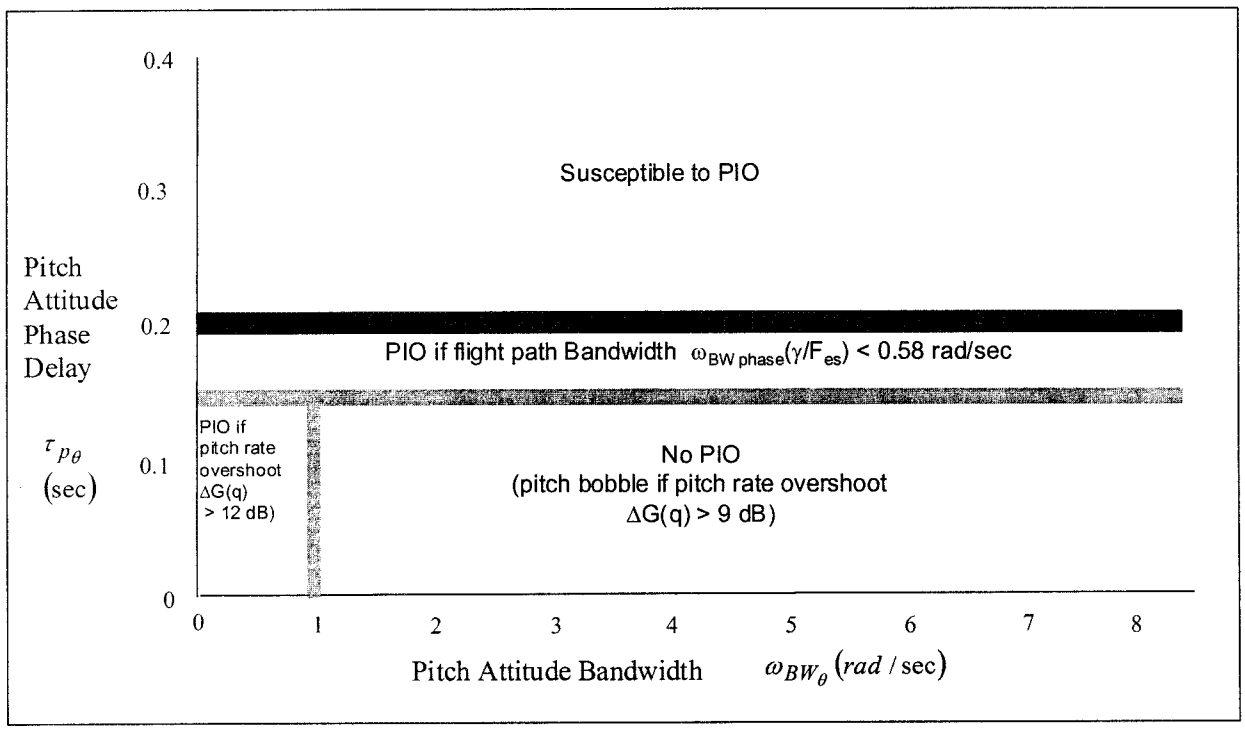

Figure 2-7, Bandwidth/Pitch-Rate Overshoot Criterion Boundaries, adapted from Ref [15]

2.3 The Smith-Geddes Criterion

Ref. [5], [8], [13], [15], [16]

The Smith-Geddes Criterion has evolved out of the Ralph Smith Criterion, developed in 1977. It assumes that for non-PIO closed loop tracking, the pilot/vehicle dynamics are governed by closed-loop pitch attitude characteristics. PIO is considered possible at any closed loop pitch attitude frequency, which promotes loop resonance. These resonant frequencies are referred to as *criterion frequencies* ω_{cr}. It is further assumed that the pilot will change his cues from tracking pitch attitude to tracking normal acceleration at these resonant frequencies. Therefore, the phase characteristics of normal acceleration at the pilot's position must be examined to determine the likelihood of a PIO.

The criterion supplies a formula for ω_{cr}-determination which is based on the calculation of the average slope in *dB/octave* of the gain curve between 2.0 and 6.0 rad/sec in the pitch-attitude-to-stick-force-input frequency response plot shown in the Bode plot in *Figure 2-8.*

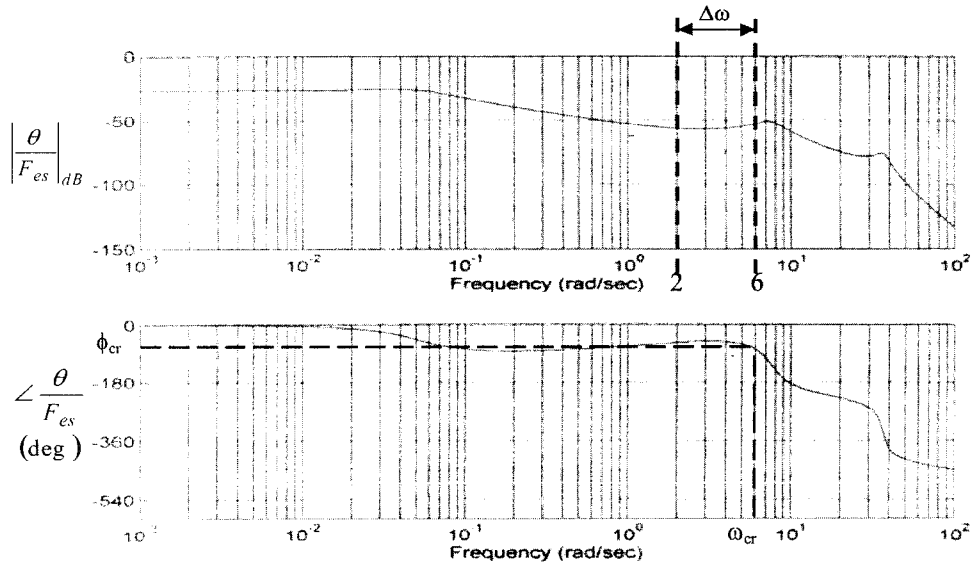

Figure 2-8, Average Slope in Bode Plot of Pitch-Attitude-to-Stick-Force-Input Response

The formula is

$$\omega_{cr} = 6.0 + 0.24\,S \qquad \textit{(Equation 2-6)}$$

where the average slope S is

$$S = \frac{1}{5}\left[A(2) - A(1) + A(3) - A(1.5) + A(4) - A(2) + A(5) - A(2.5) + A(6) - A(3)\right]$$

(Equation 2-7)

$$\text{with } A(\omega_i) = \left|\frac{\theta}{F_{es}}(\omega_i)\right|$$

After calculating the criterion frequency ω_{cr}, the corresponding phase angle of the pitch-attitude-to-stick-force-input response $\phi_{cr} = \angle\frac{\theta}{F_{es}}(\omega_{cr})$ is determined (see *Figure 2-8*). The phase angle can now be used to assess handling qualities based on pilot ratings of the Neal and Smith database (see *Appendix B*) with the following subdivisions:

$$\begin{aligned} &\textit{Level}\,1: && \phi_{cr} \geq -123 \\ &\textit{Level}\,2: && -123 > \phi_{cr} \geq -165 \\ &\textit{Level}\,3: && \phi_{cr} < -165 \end{aligned}$$

For PIO-analysis, as mentioned earlier, the phase characteristics of normal acceleration at the pilot's position has to be considered due to the change in cues. Therefore a second phase angle is calculated for the normal acceleration response.

$$\phi_{c_{azP}} = \phi_{azP}(\omega_{cr}) - 14.3\,\omega_{cr}$$

(Equation 2-8)

$$\text{with } \phi_{azP} = \angle\frac{a_{zP}}{F_{es}}(\omega_i) \text{ (see } \textit{Figure 2-9)}$$

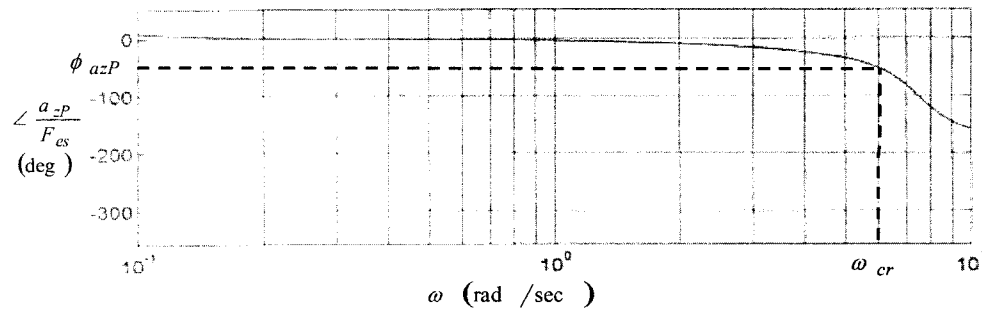

Figure 2-9, Phase of Normal Acceleration to-Stick-Force-Input Response at Pilot's Position

The term $14.3\,\omega_{cr}$ results from an assumed pilot delay of τ_{Pi}=0.25 sec ($180/\pi\,0.25 \approx 14.3$). A PIO-tendency is anticipated, if $\phi_{c_{azP}} \leq -180$ deg.

Although the criterion investigates effective aircraft dynamics, pilot characteristics are taken into account via the definition of the criterion frequency.

2.4 The Phase Rate Criterion

Ref. [3], [5]-[7], [13], [15], [17]

The Phase Rate Criterion was developed by J.C. Gibson to investigate closed-loop handling problems that stem primarily from HOS-effects increasingly encountered on FBW-aircraft. High order system dynamics generally increase the phase lag in the aircraft response characteristics, which constitutes itself as a phase delay in response to control inputs. These handling deficiencies may manifest themselves in the form of *high order* PIOs. They occur due to insufficient gain and phase margins embodied in the aircraft control system. As soon as additional, pilot-generated gain or phase lag is introduced into the system, it may become unstable, promoting a PIO.

The criterion is in the first place a design criterion that ensures acceptable closed-loop system performance without the threat of a PIO. It deals with the open-loop pitch attitude frequency response of the augmented aircraft in the region, where the phase angle first reaches –180 deg. This is the so-called *cross-over* or *neutral stability point.* The two criterion parameters are the *cross-over* or *neutral stability frequency* ω_{180} (where the phase angle is –180 deg) and the *phase rate* PR_{180}, which is a measure for the slope of the attitude phase curve around the neutral stability point. The phase rate is defined as the gradient of phase angle and frequency.

$$PR_{180} = \left| \frac{\Delta\phi(\omega)}{\Delta\omega} \right|_{\phi(\omega)=-180\,\mathrm{deg}} = \left| \frac{\phi_2 - \phi_1}{\omega_1 - \omega_2} \right| \quad \text{in} \quad \left[\frac{\mathrm{deg}}{\mathrm{Hz}} \right] \qquad \textit{(Equation 2-9)}$$

In the original version of the criterion, $\Delta\phi$ was confined to a small area around $\phi(\omega)$= -180 deg. In later versions, it was suggested to calculate $\Delta\phi$ and $\Delta\omega$ between $2\omega_{180}$ and ω_{180}. In this case the phase rate is proportional to the phase delay parameter $\tau_{p\theta}$ used in the Bandwidth/Pitch-Rate Overshoot Criterion. Cross-over frequency ω_{180}, average phase rate PR_{180} and the remaining gain margin ΔA are depicted in *Figure 2-10.*

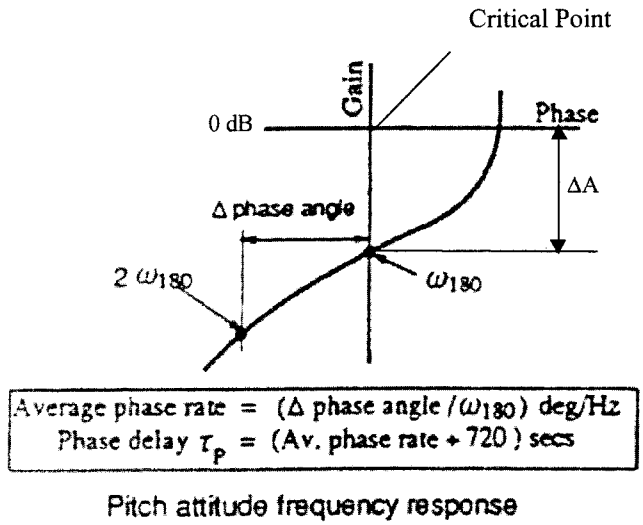

Figure 2-10, Phase Rate Definition, adapted from Ref. [13]

In case the gain margin ΔA (i.e., the distance to the critical point) of the open-loop pitch attitude response is fairly small, the effective aircraft dynamics can only accommodate insignificantly small increases of pilot gain compensation without endangering stability. A small value of cross-over frequency ω_{180} indicates that, if synchronous pilot activity is assumed, the PIO-frequency region can easily be reached. The PIO-frequency region is confined to the region between -180 and –200 deg phase lag, where the response first becomes unstable. A high value of phase rate signifies that a small increase in frequency will result in a rapid drop-off in phase, causing the pitch attitude frequency response curve to quickly approach the *critical point* (0 dB, -180 deg). Consequently, it is endeavoured to combine a low phase rate with a high cross-over frequency. This produces a higher aircraft bandwidth with adequate margins, which can accommodate additional pilot gain and phase compensation necessary to achieve the desired system performance without compromising stability. All these parameters characterise the so-called *high frequency roll-off*, which is known to be a crucial factor in Category I PIOs.

Gibson established criterion boundaries, which assess PIO-potential. These are illustrated in *Figure 2-11*.

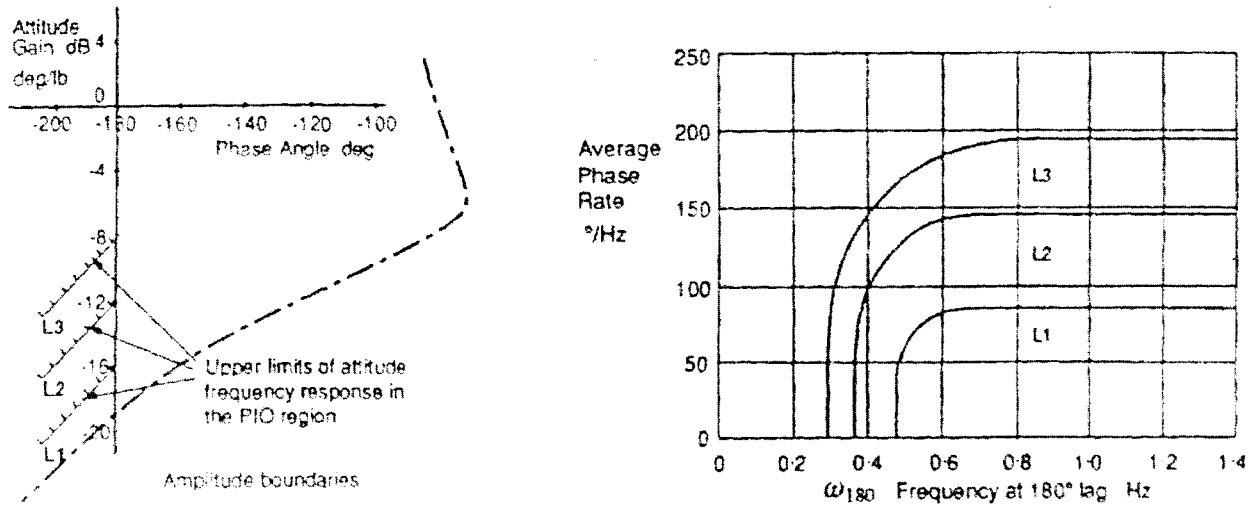

Figure 2-11, Gibson Phase Rate Criterion Boundaries, adapted from Ref. [13]

It can be found that there are significant differences in the interpretation of these boundaries within the handling qualities community. In Ref. [15] the boundaries are characterised as follows: "L1" defines the region where no Category I PIO will occur. If a design falls into the region "L2", a marginal PIO-tendency may be anticipated but is unlikely to be dangerous. A design in "L3" is expected to encounter severe PIOs. In Ref. [13] on the other hand, it is stated that the L2-L3 line is the dividing line used to discriminate between PIO-prone and non-PIO cases.

Also, there are different interpretations as to what system input all requirements are referenced to. According to Ref. [5], analysis is based on the frequency response of θ/F_{es}, i.e. stick force is the relevant input. Ref. [15] states that the feel system dynamics are excluded except for the feel system-gearing. Therefore the analysis utilises the pitch-attitude-to-stick-deflection frequency response θ/δ_{es}.

2.5 The Dropback Criterion

Ref. [3], [4], [6], [7], [13], [17]

The Gibson Dropback Criterion is the only time domain criterion applied in this project. It is rather a criterion for handling qualities than a PIO-criterion and therefore has to be viewed with some reservation. However, in combination with the Phase Rate Criterion it is a useful tool to eliminate complicated cases. The criterion is a good measure of "how well the nose follows the stick". It applies to conventional and highly augmented, FBW-aircraft, which usually use a pitch-rate-command-attitude-hold type control system. In both cases the stick has to be returned to the zero position to arrest the pitch rate. The optimum attitude response in closed loop tracking is

with a pitch rate that is proportional to stick deflection. In this case the attitude appears to precisely follow the stick and remains constant after the input has been removed, characterised by zero *dropback* (pure integral or K/s-like behaviour). In practice this is not exactly achieved, i.e. after a short-term transition the pitch attitude will settle on a value, which is less than the value at the time the input was removed. For good handling in closed loop tracking tasks, dropback has to be minimised. Large dropback is related to the problem of pitch-bobbling, making it difficult to stop the nose on the target. Negative attitude dropback or *overshoot* stems from excessive phase delay and is associated with a very sluggish, unpredictable response. It is to be avoided by all means. The value of dropback is influenced by the *pitch rate overshoot.*

The criterion parameters attitude-dropback-to-steady-state-pitch-rate $\Delta\theta / q_{SS}$ and maximum pitch rate to steady state pitch rate q_{peak} / q_{SS} are obtained from the open loop time domain response to a rectangular pulse input as depicted in *Figure 2-12*

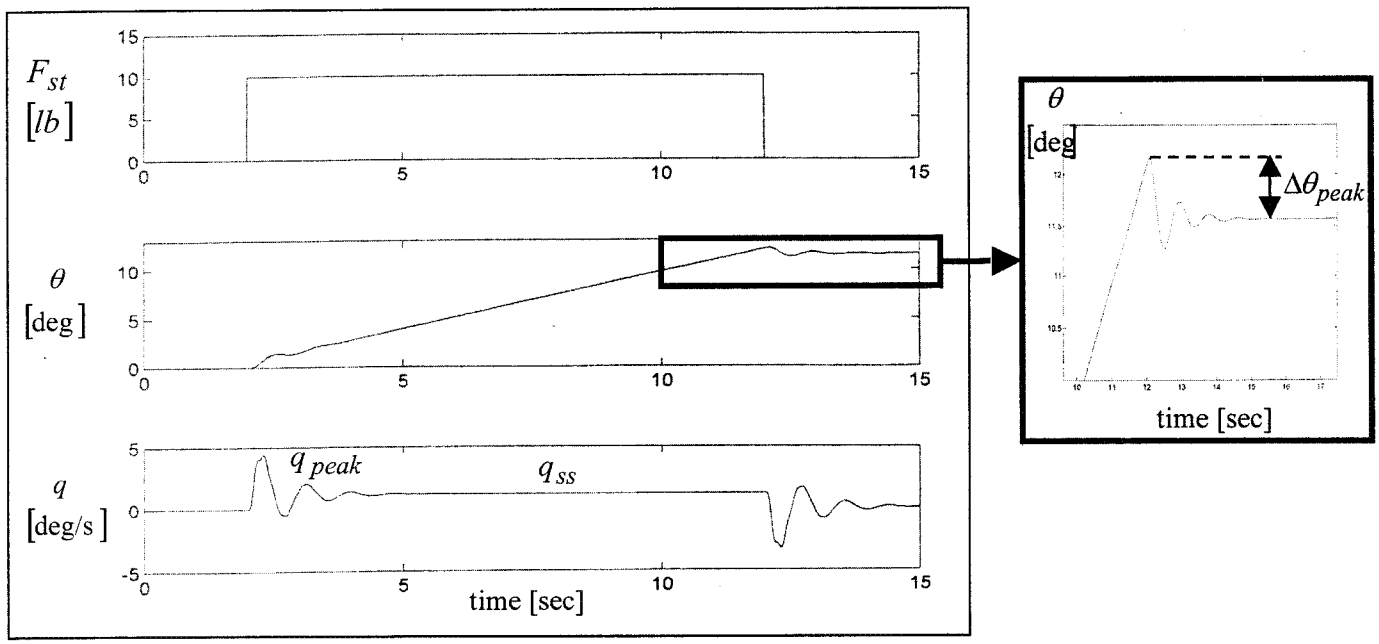

Figure 2-12, Definition of Dropback Criterion Parameters

These are then used in *Figure 2-13* to determine PIO-susceptibility. The boundaries are based on data from fighter aircraft.

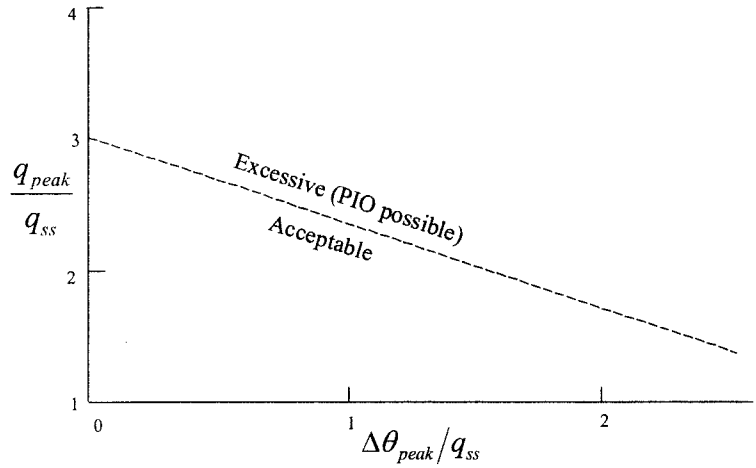

Figure 2-13, Gibson Dropback Criterion Boundaries, adapted from Ref. [13]

3 Objective

On May 18, 1961 an F-4 encountered a destructive pitching-PIO during the attempt to set a new low altitude 800 knot speed record {Ref. [5], Ref. [7], Ref. [11]}. The disturbance was so abrupt and violent, that after only 3 oscillations the g-forces had diverged up to 14 g in just 2 seconds before destruction. The pilot was known to have flown the aircraft in the most forward trim position with the SAS disengaged.

This report analyses linear, Category I PIO-tendencies of a linear, small perturbations model of the F-4C (Phantom II) aircraft based on the longitudinal equations of motion for two different flight conditions, using the analysis criteria introduced in the previous chapter (These include the Neal and Smith Criterion (Original Definition), the Bandwidth/ Pitch-Rate Overshoot Criterion, the Smith-Geddes Criterion, Gibson Phase Rate Criterion and the Gibson Dropback Criterion). Since the aircraft model does not incorporate any non-linearities, PIO-assessment is amenable to frequency domain analysis. The primary aim of the project is to find correlations in the application of the different criteria and to determine whether the results are consistent.

4 Development of a Small Perturbations Model

4.1 F-4C Dimensions, Flight Condition Parameters and Pitch Control System

The two flight conditions shown in the flight envelope of the F-4C in *Figure 4-1* represent a final approach/landing scenario (Flight Condition 1) and the low-level, high-speed terrain following scenario described in *Chapter 3* (Flight Condition 3), each being a demanding, high-gain task with a high level of task-related pilot stress.

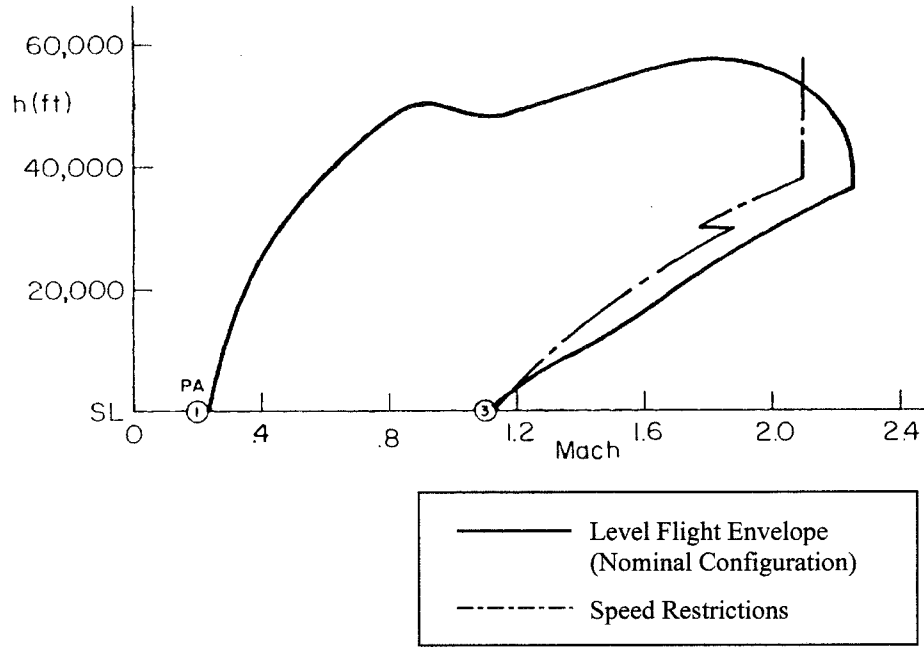

Figure 4-1, F-4C Flight Envelope, Ref. [9]

For primary pitch control, the F-4 uses fully moving horizontal stabilisers.

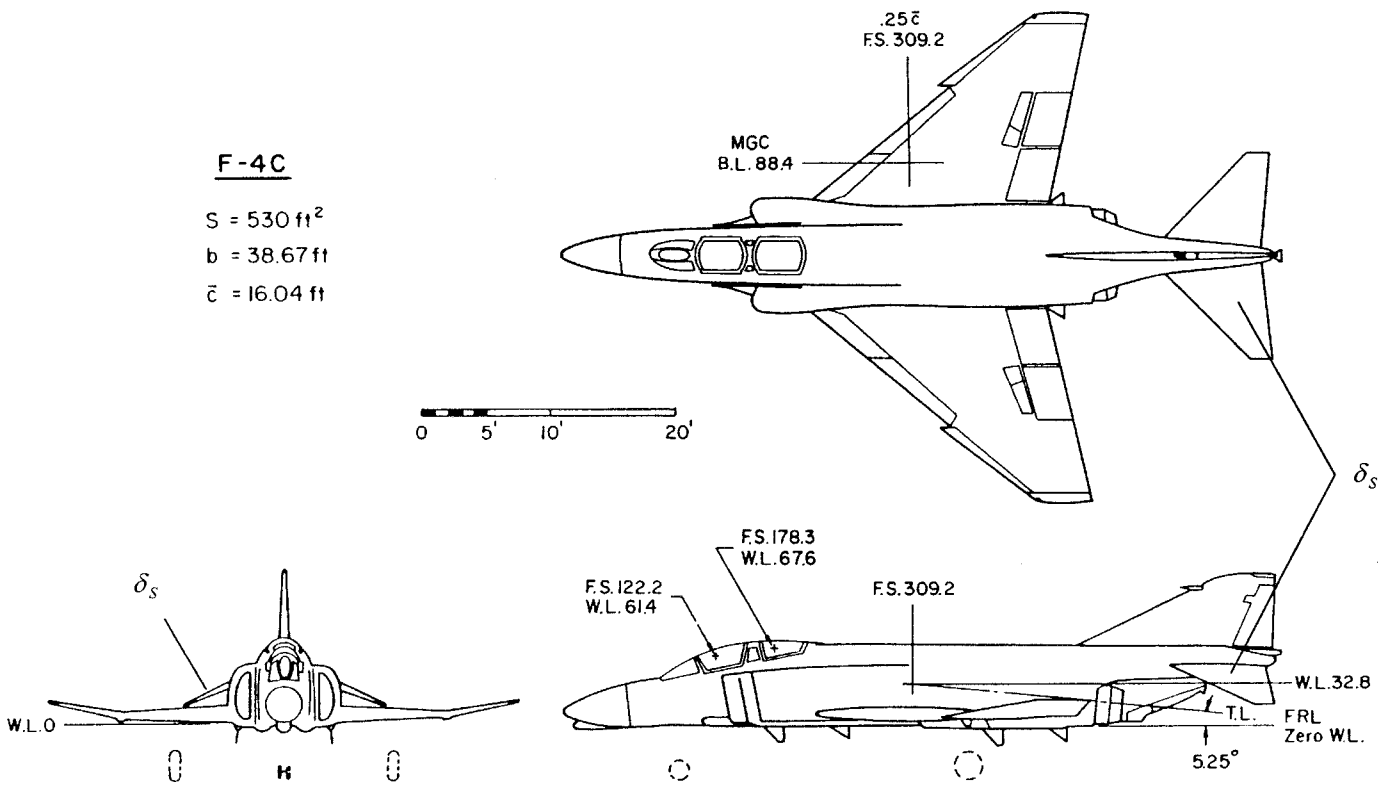

b	Reference wing span
B.L.	Buttock Line
$\bar{c}$	Reference chord
δ_S	Stabilizer surface deflection from trim (positive for trailing edge down)
FRL	Fuselage Reference Line (parallel to x-body axis)
F.S.	Fuselage Station (inches from nose)
MGC	Mean Geometric Chord
S	Reference wing area
T.L.	Thrust Line
W.L.	Water Line

Figure 4-2, F-4C General Arrangement, Ref. [9]

The general parameters for the two analysed flight conditions are listed below in *Table 4-1*.

Flight Condition	**1**	**3**
h [ft]	SL	SL
M [-]	0.206	1.1
V_{T0}[ft/s]	230	1228
c.g. [% MGC]	0.291	0.289
$\bar{q}$ [lb/ft^2]	62.6	1792
α_0 [deg]	11.7	-0.3
γ_0 [deg]	0	0
l_{XP} [ft]	16.3	16.2

Table 4-1,General Parameters, adapted from Ref. [9]

All used measures refer to aircraft body axes. The applied coordinate system is illustrated in *Figure 4-3* below.

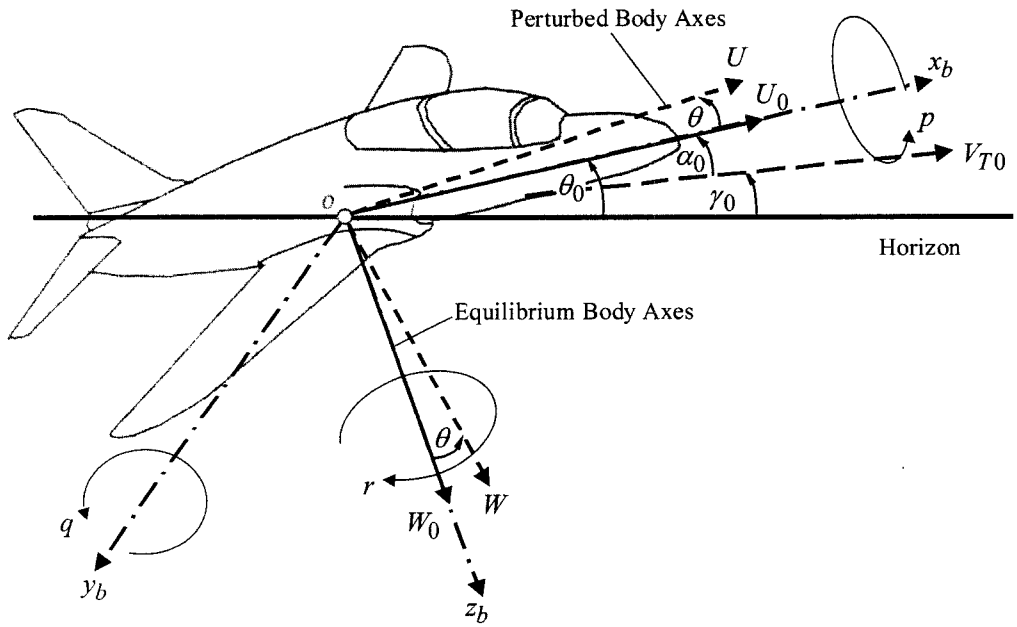

Figure 4-3, Coordinate System, adapted from Ref. [1]

As shown in *Figure 4-4*, the F-4C pitch control system incorporates various control elements in forward and feedback control paths. All components are translated step by step into a mathematical, small perturbation model using the state space method, outlined in Ref. [1]. For computation, the MATLAB software package is used.

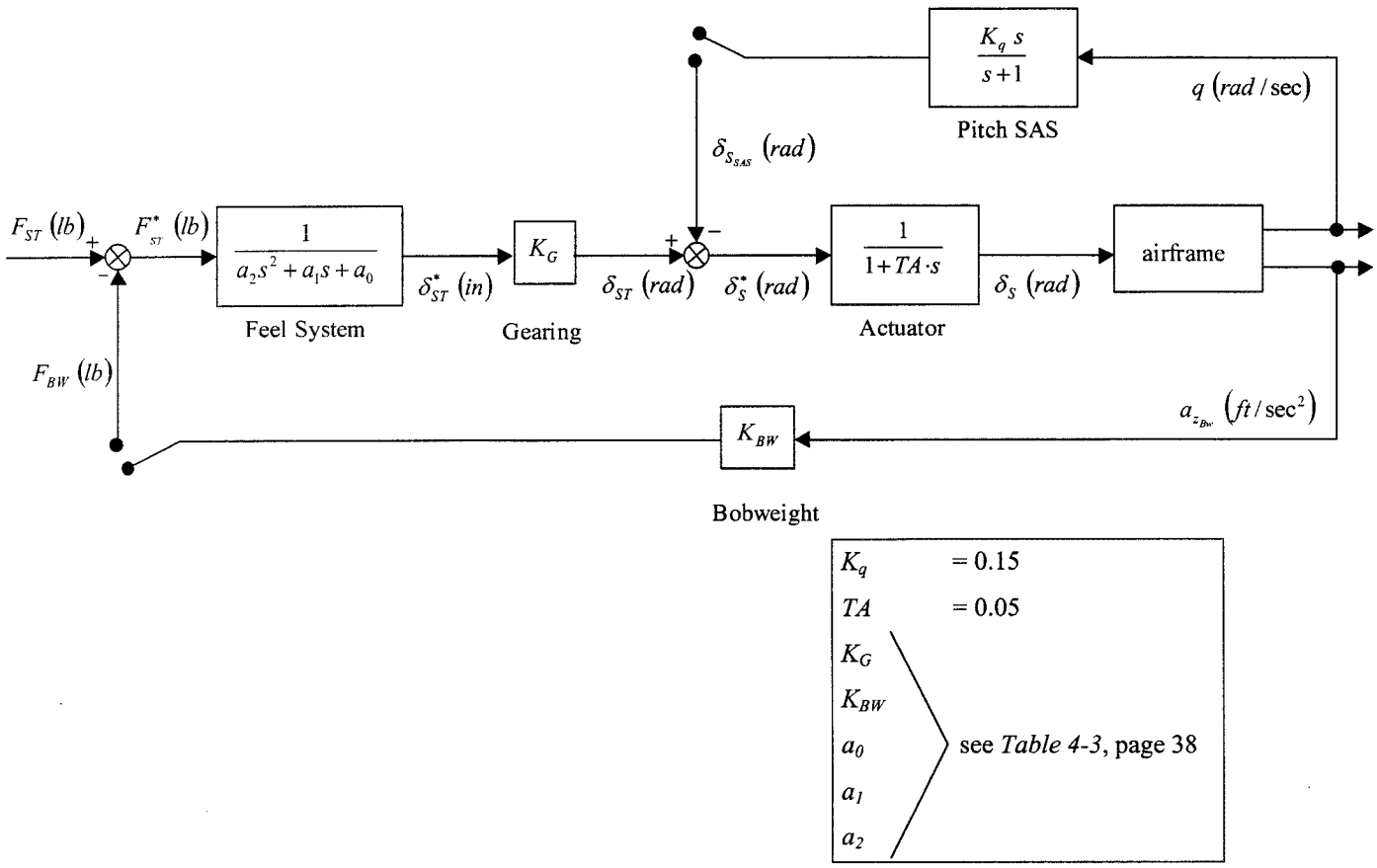

Figure 4-4, F-4C Pitch Control System

4.2 State Space Model of the Airframe

As described in Ref. [9], the decoupled, longitudinal equations of motion referred to aircraft body axes need to be assembled. Given in Laplace transform they are

$$\begin{bmatrix} (1-X_{\dot{u}})s - X_u^* & -(X_{\dot{w}}s + X_w) & (-X_q + W_0)s + g\cdot\cos\theta_0 \\ -Z_{\dot{u}}s - Z_u^* & (1-Z_{\dot{w}})s - Z_w & (-Z_q - U_0)s + g\cdot\sin\theta_0 \\ -M_{\dot{u}}s - M_u^* & -(M_{\dot{w}}s + M_w) & s^2 - M_q s \end{bmatrix} \begin{bmatrix} u \\ w \\ \theta \end{bmatrix} = \begin{bmatrix} X_{\delta_S} \\ Z_{\delta_S} \\ M_{\delta_S} \end{bmatrix} [\delta_S]$$

$$q = s\,\theta$$

(Equation 4-1)

The longitudinal derivatives are listed in *Table 4-2* below

Flight Condition	1	3
X_u^*	-0.0417	-0.0677
Z_u^*	-0.177	0.0226
M_u^*	0.000743	0.00329
X_w	0.13	-0.0107
Z_w	-0.452	-2.11
M_w	-0.00182	-0.0488
Mq	-0.317	-2.2
Xq	0	0
Zq	-2.48	-8.72
$M_{\dot{u}}$	0	0
$X_{\dot{u}}$	0	0
$Z_{\dot{u}}$	0	0
$M_{\dot{w}}$	-0.000642	-0.000729
$X_{\dot{w}}$	0	0
$Z_{\dot{w}}$	-0.00305	-0.00326
X_{δ_S}	5.98	-1.32
Z_{δ_S}	-6.65	-251
M_{δ_S}	-1.46	-61.1

Table 4-2, Longitudinal Aerodynamic Stability and Control Derivatives, adapted from Ref. [9]

Equations 4-1 are converted into the time domain and rearranged, to give

$$\begin{aligned}
&(1 - X_{\dot{u}})\,\dot{u} - X_{\dot{w}}\,\dot{w} = X_u^*\,u + X_w\,w + (X_q - W_0)q - \theta\,g\cos\theta_0 + X_{\delta_S}\,\delta_S \\
&-Z_{\dot{u}}\,\dot{u} + (1 - Z_{\dot{w}})\dot{w} = Z_u^*\,u + Z_w\,w + (Z_q - U_0)q - \theta\,g\sin\theta_0 + Z_{\delta_S}\,\delta_S \\
&-M_{\dot{u}}\,\dot{u} - M_{\dot{w}}\,\dot{w} + \dot{q} = M_u^*\,u + M_w\,w + M_q\,q + M_{\delta_S}\,\delta_S \\
&\dot{\theta} = q
\end{aligned}$$

(Equations 4-2)

Since for level flight it is assumed that

$$\theta_0 = \alpha_0 + \gamma_0 \qquad \textit{(Equation 4-3)}$$

and for all referenced flight conditions γ_0=0 (see *Table 4-1*), *Equation 4-3* simplifies to

$$\theta_0 = \alpha_0 \qquad \textit{(Equation 4-4)}$$

Axial velocity therefore equates to (see *Figure 4-3*)

$$U_0 = V_{T0}\cos\theta_0 \qquad \textit{(Equation 4-5)}$$

and normal velocity becomes

$$W_0 = V_{T0}\sin\theta_0 \qquad \textit{(Equation 4-6)}$$

Equations 4-2 are then written in equivalent matrix form,

$$m\begin{bmatrix}\dot{u}\\ \dot{w}\\ \dot{q}\\ \dot{\theta}\end{bmatrix} = a\begin{bmatrix}u\\ w\\ q\\ \theta\end{bmatrix} + b\left[\delta_S\right] \qquad \textit{(Equation 4-7)}$$

giving,

$$\underset{m}{\begin{bmatrix}(1-X_{\dot{u}}) & -X_{\dot{w}} & 0 & 0\\ -Z_{\dot{u}} & (1-Z_{\dot{w}}) & 0 & 0\\ -M_{\dot{u}} & -M_{\dot{w}} & 1 & 0\\ 0 & 0 & 0 & 1\end{bmatrix}}\underset{\dot{x}(t)}{\begin{bmatrix}\dot{u}\\ \dot{w}\\ \dot{q}\\ \dot{\theta}\end{bmatrix}} = \underset{a}{\begin{bmatrix}X_u^* & X_w & (X_q - W_0) & -g\cos\theta_0\\ Z_u^* & Z_w & (Z_q + U_0) & -g\sin\theta_0\\ M_u^* & M_w & M_q & 0\\ 0 & 0 & 1 & 0\end{bmatrix}}\underset{x(t)}{\begin{bmatrix}u\\ w\\ q\\ \theta\end{bmatrix}} + \underset{b}{\begin{bmatrix}X_{\delta_S}\\ Z_{\delta_S}\\ M_{\delta_S}\\ 0\end{bmatrix}}\underset{u(t)}{\left[\delta_S\right]}$$

(Equation 4-8)

The equations of motion are now transformed into the general state space form, where the state equation is

$$\dot{x}(t) = A\,x(t) + B\,u(t) \qquad \textit{(Equation 4-9)}$$

and the output equation is

$$y(t) = C\,x(t) + D\,u(t) \qquad \textit{(Equation 4-10)}$$

The *state matrix A*, the *input matrix B*, the *output matrix C* and the *direct matrix D* are obtained as follows

$$A = m^{-1}\, a$$
$$B = m^{-1}\, b$$
$$C = I$$
$$D = [0]$$

(Equations 4-11)

This gives the state space form of the airframe as described in *Equations 4-9* and *4-10*

$$\begin{bmatrix} \dot{u} \\ \dot{w} \\ \dot{q} \\ \dot{\theta} \end{bmatrix} = \begin{bmatrix} x_u & x_w & x_q & x_\theta \\ z_u & z_w & z_q & z_\theta \\ m_u & m_w & m_q & m_\theta \\ 0 & 0 & 1 & 0 \end{bmatrix} \begin{bmatrix} u \\ w \\ q \\ \theta \end{bmatrix} + \begin{bmatrix} x_{\delta_S} \\ z_{\delta_S} \\ m_{\delta_S} \\ 0 \end{bmatrix} [\delta_S] \quad \text{and} \quad \begin{bmatrix} u \\ w \\ q \\ \theta \end{bmatrix} = \begin{bmatrix} 1 & 0 & 0 & 0 \\ 0 & 1 & 0 & 0 \\ 0 & 0 & 1 & 0 \\ 0 & 0 & 0 & 1 \end{bmatrix} \begin{bmatrix} u \\ w \\ q \\ \theta \end{bmatrix} + \begin{bmatrix} 0 \\ 0 \\ 0 \\ 0 \end{bmatrix} [\delta_S]$$

$\dot{x}(t)$ A $x(t)$ B $u(t)$ $y(t)$ C $x(t)$ D $u(t)$

(Equation 4-12)

4.3 Airframe State Space Model Augmentation

The state space description of the airframe is now augmented to attain additional response characteristics, which are not included in the equations of motion, but can be expressed in basic aircraft motion variables. These are angle of attack (AOA)(α), flight path angle (γ), and normal acceleration at any given location along the aircraft's longitudinal axis (a_{ZX}).

For small perturbations angle of attack is given by

$$\alpha \cong \tan\alpha = \frac{w}{V_{T0}}$$

(Equation 4-13)

Without changing the state vector $\dot{x}(t)$, angle of attack can be added to the output vector y(t) in *Equation 4-12* as follows

$$\begin{bmatrix} u \\ w \\ q \\ \theta \\ \alpha \end{bmatrix} = \begin{bmatrix} & I & \\ \hline 0 & 1/V_{T0} & 0 & 0 \end{bmatrix} \begin{bmatrix} u \\ w \\ q \\ \theta \end{bmatrix} + \begin{bmatrix} . \\ . \\ 0 \\ . \\ . \end{bmatrix} [\delta_S]$$

y(t) C x(t) D u(t)

(Equation 4-14)

The flight path angle γ is added to the output vector y(t) in the same fashion as angle of attack.

For small perturbations γ equates to

$$\gamma = \theta - \alpha \cong \theta - \frac{w}{V_{T0}} \qquad \textit{(Equation 4-15)}$$

Normal acceleration at any given distance x away from the *cg* along the aircraft's longitudinal axis is

$$a_{zx} = \dot{w} - q\,U_0 - x\,\dot{q} \qquad \textit{(Equation 4-16)}$$

with

$$\dot{w} = z_u\,u + z_w\,w + z_q\,q + z_\theta\,\theta + z_{\delta_S}\,\delta_S \qquad \textit{(Equation 4-17)}$$

and

$$\dot{q} = m_u\,u + m_w\,w + m_q\,q + m_\theta\,\theta + m_{\delta_S}\,\delta_S \qquad \textit{(Equation 4-18)}$$

taken from the state equation in *Equation 4-12*. *Equation 4-16* may now be rewritten as

$$a_{zx} = (z_u - x\,m_u)u + (z_w - x\,m_w)w + (z_q - x\,m_q - U_0)q + (z_\theta - x\,m_\theta)\theta + (z_{\delta_S} - x\,m_{\delta_S})\delta_S \qquad \textit{(Equation 4-19)}$$

For more convenience, let

$$\begin{aligned} g_{1x} &= (z_u - x\,m_u), \quad g_{2x} = (z_w - x\,m_w), \quad g_{3x} = (z_q - x\,m_q - U_0), \\ g_{4x} &= (z_\theta - x\,m_\theta), \quad g_{5x} = (z_{\delta_S} - x\,m_{\delta_S}) \end{aligned} \qquad \textit{(Equation 4-20)}$$

The augmented state space form of the airframe is

$$\begin{bmatrix} \dot{u} \\ \dot{w} \\ \dot{q} \\ \dot{\theta} \end{bmatrix} = \begin{bmatrix} x_u & x_w & x_q & x_\theta \\ z_u & z_w & z_q & z_\theta \\ m_u & m_w & m_q & m_\theta \\ 0 & 0 & 1 & 0 \end{bmatrix} \begin{bmatrix} u \\ w \\ q \\ \theta \end{bmatrix} + \begin{bmatrix} x_{\delta_S} \\ z_{\delta_S} \\ m_{\delta_S} \\ 0 \end{bmatrix} [\delta_S]$$

$\dot{x}(t)$ A $x(t)$ B $u(t)$

$$\begin{bmatrix} u \\ w \\ q \\ \theta \\ \alpha \\ \gamma \\ a_{zx} \end{bmatrix} = \left[\begin{array}{cccc} & & I & \\ \hline 0 & 1/V_{T0} & 0 & 0 \\ 0 & -1/V_{T0} & 0 & 1 \\ g_{1x} & g_{2x} & g_{3x} & g_{4x} \end{array}\right] \left[\begin{array}{c} u \\ w \\ q \\ \theta \\ \hline \\ \\ \end{array}\right] + \left[\begin{array}{c} 0 \\ 0 \\ 0 \\ 0 \\ \hline 0 \\ 0 \\ g_{5x} \end{array}\right] [\delta_S] \qquad \textit{(Equation 4-21)}$$

$y(t)$ C $x(t)$ D $u(t)$

Basic airframe responses to a unit (1 deg) stabiliser pulse input of 4 sec duration for Flight Conditions 1 and 3 respectively are shown in *Figures 4-5* and *4-6.*

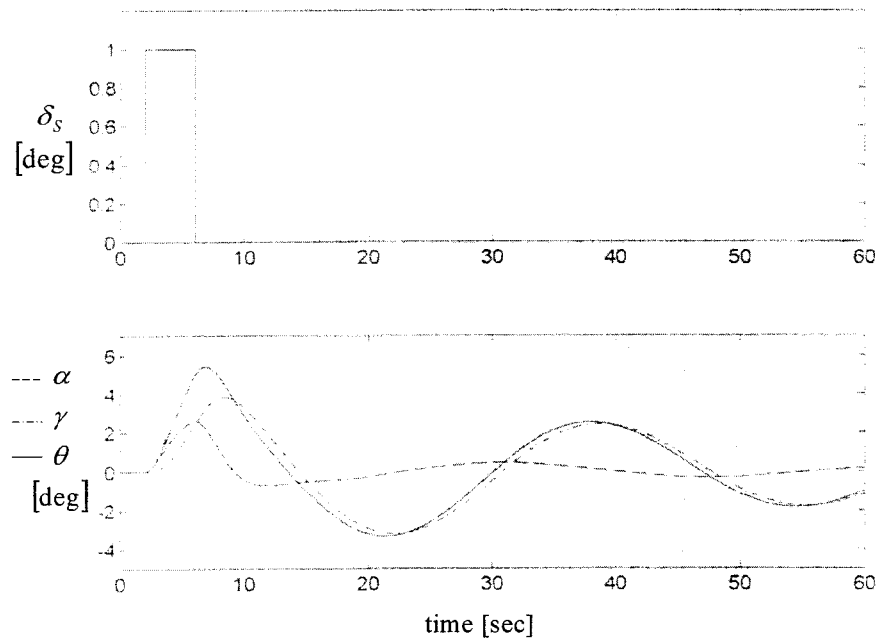

Figure 4-5, Basic Airframe Responses, Flight Condition 1

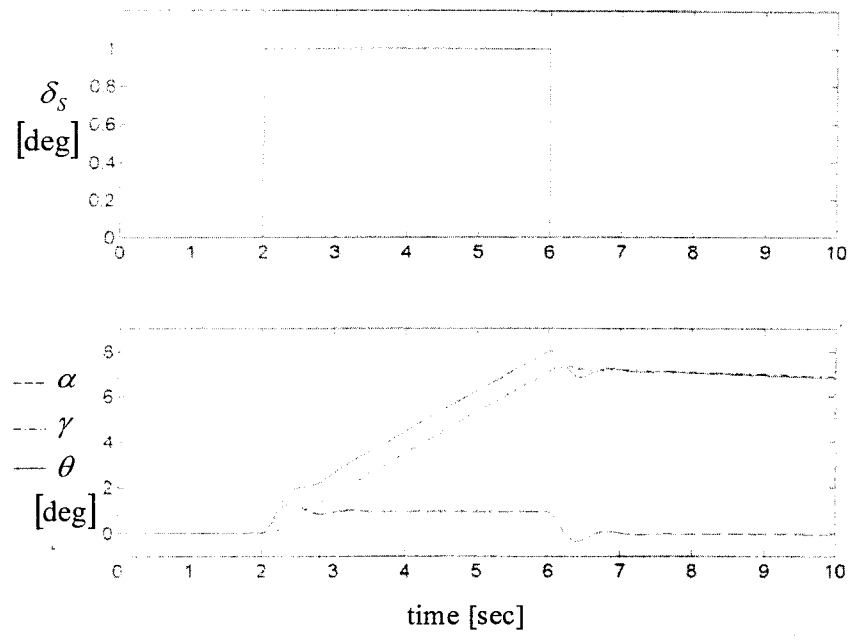

Figure 4-6, Basic Airframe Responses, Flight Condition 3

Note that the time scale is different for each flight condition due to the nature of the responses. It is quite obvious, that in Flight Condition 1 the phugoid mode is excited, with angle of attack α staying nearly constant after the input is removed, whereas Flight Condition 3 exhibits transient, short period pitch responses typical for pitch tracking.

4.4 Actuator Dynamics

As shown in *Figure 4-4*, the actuator dynamics are given by

$$\frac{\delta_S}{\delta_S^*} = \frac{1}{1 + s\,TA} \qquad \textit{(Equation 4-22)}$$

This can be rewritten as

$$\delta_S^* = \delta_S + \delta_S\, s\, TA = \delta_S + \dot{\delta}_S\, TA \qquad \textit{(Equation 4-23)}$$

and equates to

$$\dot{\delta}_S = \frac{\delta_S^* - \delta_S}{TA} \qquad \textit{(Equation 4-24)}$$

δ_S can now be defined as a new state and is included in the state and output equation as follows

$$\begin{bmatrix} \dot{u} \\ \dot{w} \\ \dot{q} \\ \dot{\theta} \\ \dot{\delta}_S \end{bmatrix} = \begin{bmatrix} x_u & x_w & x_q & x_\theta & x_{\delta_S} \\ z_u & z_w & z_q & z_\theta & z_{\delta_S} \\ m_u & m_w & m_q & m_\theta & m_{\delta_S} \\ 0 & 0 & 1 & 0 & 0 \\ 0 & 0 & 0 & 0 & -1/TA \end{bmatrix} \begin{bmatrix} u \\ w \\ q \\ \theta \\ \delta_S \end{bmatrix} + \begin{bmatrix} 0 \\ 0 \\ 0 \\ 0 \\ 1/TA \end{bmatrix} \left[\delta_S^*\right]$$

$$\begin{bmatrix} u \\ w \\ q \\ \theta \\ \delta_S \\ \alpha \\ \gamma \\ a_{zx} \end{bmatrix} = \left[\begin{array}{ccccc} & & I & & \\ & & & & \\ & & & & \\ & & & & \\ & & & & \\ \hline 0 & 1/V_{T0} & 0 & 0 & 0 \\ 0 & -1/V_{T0} & 0 & 1 & 0 \\ g_{1x} & g_{2x} & g_{3x} & g_{4x} & g_{5x} \end{array}\right] \begin{bmatrix} u \\ w \\ q \\ \theta \\ \delta_S \\ \\ \\ \end{bmatrix} + \begin{bmatrix} . \\ . \\ . \\ 0 \\ . \\ . \\ . \\ . \end{bmatrix} \left[\delta_S^*\right] \qquad \textit{(Equation 4-25)}$$

4.5 Pitch-SAS Dynamics

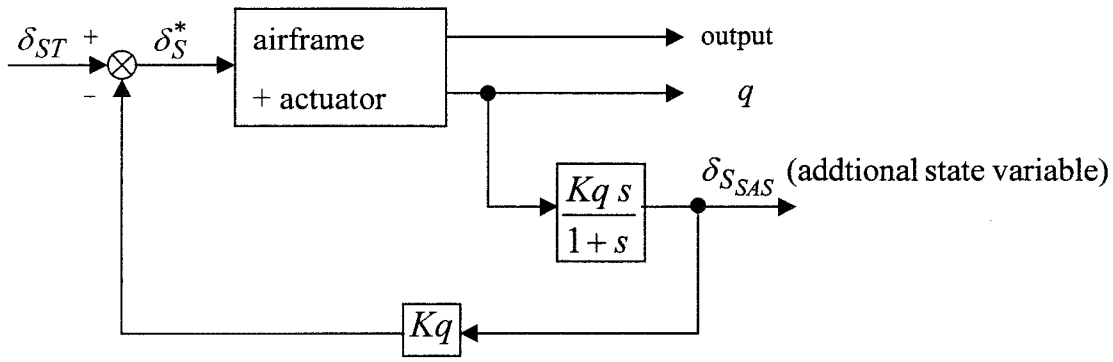

Figure 4-7, Pitch Stability Augmentation System

The pitch-SAS, which comprises a simple washout filter with a gain Kq, is part of a feedback loop that uses pitch rate q, a basic airframe output, as input. The pitch-SAS dynamics are (as described in *Figure 4-7)*

$$\frac{\delta_{S_{SAS}}}{q} = \frac{Kq\ s}{s+1} \qquad \textit{(Equation 4-26)}$$

giving

$$\delta_{S_{SAS}} = Kq\,\dot{q} - \dot{\delta}_{S_{SAS}} \qquad \textit{(Equation 4-27)}$$

$\delta_{S_{SAS}}$ is the washed-out pitch rate q and has to be declared as an additional state in the state space model. The equation that incorporates the feedback loop is

$$\delta_S^* = \delta_{ST} - Kq\,\delta_{S_{SAS}} \qquad \textit{(Equation 4-28)}$$

Equation 4-27 and *Equation 4-28* may now be included in the state space equation as follows. First, *Equation 4-27* is expressed in matrix form, equating to *matrix Z*, and is then added to the state equation of *Equation 4-25*.

$$\begin{bmatrix} & & & & & \cdot \\ & & & & & \cdot \\ & I & & & & 0 \\ & & & & & \cdot \\ & & & & & \cdot \\ \hline 0 & 0 & Kq & 0 & 0 & -1 \end{bmatrix} \begin{bmatrix} \dot{u} \\ \dot{w} \\ \dot{q} \\ \dot{\theta} \\ \dot{\delta}_S \\ \dot{\delta}_{S_{SAS}} \end{bmatrix} = \begin{bmatrix} x_u & x_w & x_q & x_\theta & x_{\delta_S} & \cdot \\ z_u & z_w & z_q & z_\theta & z_{\delta_S} & \cdot \\ m_u & m_w & m_q & m_\theta & m_{\delta_S} & 0 \\ 0 & 0 & 1 & 0 & 0 & \cdot \\ 0 & 0 & 0 & 0 & -1/TA & \cdot \\ \hline \cdot & \cdot & 0 & \cdot & \cdot & 1 \end{bmatrix} \begin{bmatrix} u \\ w \\ q \\ \theta \\ \delta_S \\ \delta_{S_{SAS}} \end{bmatrix} + \begin{bmatrix} 0 \\ 0 \\ 0 \\ 0 \\ 1/TA \\ \hline 0 \end{bmatrix} \left[\delta_S^*\right]$$

Z $\dot{x}(t)$ A $x(t)$ B $u(t)$

(Equation 4-29)

By multiplying both sides of *Equation 4-29* with $Z^{-1} = Z$ and substituting the input vector u(t) with *Equation 4-28*, the new state equation is obtained

$$\begin{bmatrix} \dot{u} \\ \dot{w} \\ \dot{q} \\ \dot{\theta} \\ \dot{\delta}_S \\ \dot{\delta}_{S_{SAS}} \end{bmatrix} = \begin{bmatrix} x_u & x_w & x_q & x_\theta & x_{\delta_S} & \cdot \\ z_u & z_w & z_q & z_\theta & z_{\delta_S} & \cdot \\ m_u & m_w & m_q & m_\theta & m_{\delta_S} & 0 \\ 0 & 0 & 1 & 0 & 0 & \cdot \\ 0 & 0 & 0 & 0 & -1/TA & \cdot \\ \hline Kq\,m_u & Kq\,m_w & Kq\,m_q & Kq\,m_\theta & Kq\,m_{\delta_S} & -1 \end{bmatrix} \begin{bmatrix} u \\ w \\ q \\ \theta \\ \delta_S \\ \delta_{S_{SAS}} \end{bmatrix} + \begin{bmatrix} 0 \\ 0 \\ 0 \\ 0 \\ 1/TA \\ \hline 0 \end{bmatrix} \left[\delta_{ST}\right] - Kq \begin{bmatrix} 0 \\ 0 \\ 0 \\ 0 \\ 1/TA \\ \hline 0 \end{bmatrix} \left[\delta_{S_{SAS}}\right]$$

$\dot{x}(t)$ A $x(t)$ B $u(t)$ B $v(t)$

(Equation 4-30)

Rearranging *Equation 4-30* and augmenting the output equation by including $\delta_{S_{SAS}}$ in the *C-Matrix* finally gives

$$\begin{bmatrix} \dot{u} \\ \dot{w} \\ \dot{q} \\ \dot{\theta} \\ \dot{\delta}_S \\ \dot{\delta}_{S_{SAS}} \end{bmatrix} = \begin{bmatrix} x_u & x_w & x_q & x_\theta & x_{\delta_S} & 0 \\ z_u & z_w & z_q & z_\theta & z_{\delta_S} & 0 \\ m_u & m_w & m_q & m_\theta & m_{\delta_S} & 0 \\ 0 & 0 & 1 & 0 & 0 & 0 \\ 0 & 0 & 0 & 0 & -1/TA & -Kq/TA \\ Kq\,m_u & Kq\,m_w & Kq\,m_q & Kq\,m_\theta & Kq\,m_{\delta_S} & -1 \end{bmatrix} \begin{bmatrix} u \\ w \\ q \\ \theta \\ \delta_S \\ \delta_{S_{SAS}} \end{bmatrix} + \begin{bmatrix} 0 \\ 0 \\ 0 \\ 0 \\ 1/TA \\ 0 \end{bmatrix} \left[\delta_{ST}\right]$$

$$\begin{bmatrix} u \\ w \\ q \\ \theta \\ \delta_S \\ \delta_{S_{SAS}} \\ \alpha \\ \gamma \\ a_{zx} \end{bmatrix} = \begin{bmatrix} & & & & & \\ & & & & & \\ & & & I & & \\ & & & & & \\ & & & & & \\ \hline 0 & 1/V_{T0} & 0 & 0 & 0 & 0 \\ 0 & -1/V_{T0} & 0 & 1 & 0 & 0 \\ g_{1x} & g_{2x} & g_{3x} & g_{4x} & g_{5x} & 0 \end{bmatrix} \begin{bmatrix} u \\ w \\ q \\ \theta \\ \delta_S \\ \delta_{S_{SAS}} \\ \\ \\ \end{bmatrix} + \begin{bmatrix} \cdot \\ \cdot \\ \cdot \\ \cdot \\ 0 \\ \cdot \\ \cdot \\ \cdot \\ \cdot \end{bmatrix} \left[\delta_{ST}\right]$$

(Equation 4-31)

4.6 Gearing, Feel System and Bobweight

The F-4's control system is mainly mechanical, the only exception being the electrical SAS and the actuators, which are powered by hydraulic oil. With increasing speeds in military aviation in the late 1940's and early 1950's, the use of hydraulic powered actuators became essential to move control surfaces that were exposed to large aerodynamic loading. However, this deprived the pilot of the sensation of increasing loads on his stick at high speeds. So an artificial feel system had to be installed to regain this sensation, making the aircraft less responsive to pilot commands with increasing speed. The F-4's artificial feel system is completely mechanical and comprises a variety of springs and dampers, which stiffen with increasing dynamic pressure. The bobweight is an additional mass connected to the stick, intended to improve stationary stick force characteristics by feeding back motion-induced stick forces, usually a combination of normal acceleration and rotary pitch acceleration, to the pilot. The F-4's feel system mechanism is pictured in *Figure 4-8* on the following page.

Bobweights played a considerable part in APC-events related to semi-mechanical flight control systems. Exposed to large stick deflections and stick forces the bobweight couples with the aircraft motion and may significantly reduce the damping of the stick-free short period mode. Also, for small stick forces and normal accelerations the opposing force produced by the bobweight is smaller than the force due to system friction. With increasing stick forces and accelerations this threshold may suddenly be overcome and an abrupt transition in aircraft dynamics occurs, which may consequently lead to a maladaption of the pilot. This is called the "bobweight effect" and was impressively demonstrated in the tragic F-4 PIO mentioned earlier, or in the famous "T-38 PIO", described in Ref. [5] and Ref. [11]. Since the energy the bobweight feeds into this highly coupled system depends on dynamic pressure, bobweight-induced PIOs are usually confined to high airspeed, making even minor oscillations potentially destructive due to the large excursions in normal acceleration.

The incorporation of the feel system dynamics and especially of the bobweight into the state space aircraft model of the F-4C poses some difficulty. Two different approaches are chosen to solve the problem but only one seems to give promising results as will be explained below. The difficulty is to attempt to match aircraft responses attained from the state space model with corresponding, reduced order transfer functions given in Ref .[9], which are not always plausible.

4.6.1 First Formulation

The first formulation is analogous to the addition of actuator dynamics and pitch-SAS. According to *Figure 4-4*, gearing and feel system dynamics may be combined to give

$$\frac{\delta_{ST}}{F^*_{ST}} = \frac{K_G}{a_2 s^2 + a_1 s + a_0} \qquad \textit{(Equation 4-32)}$$

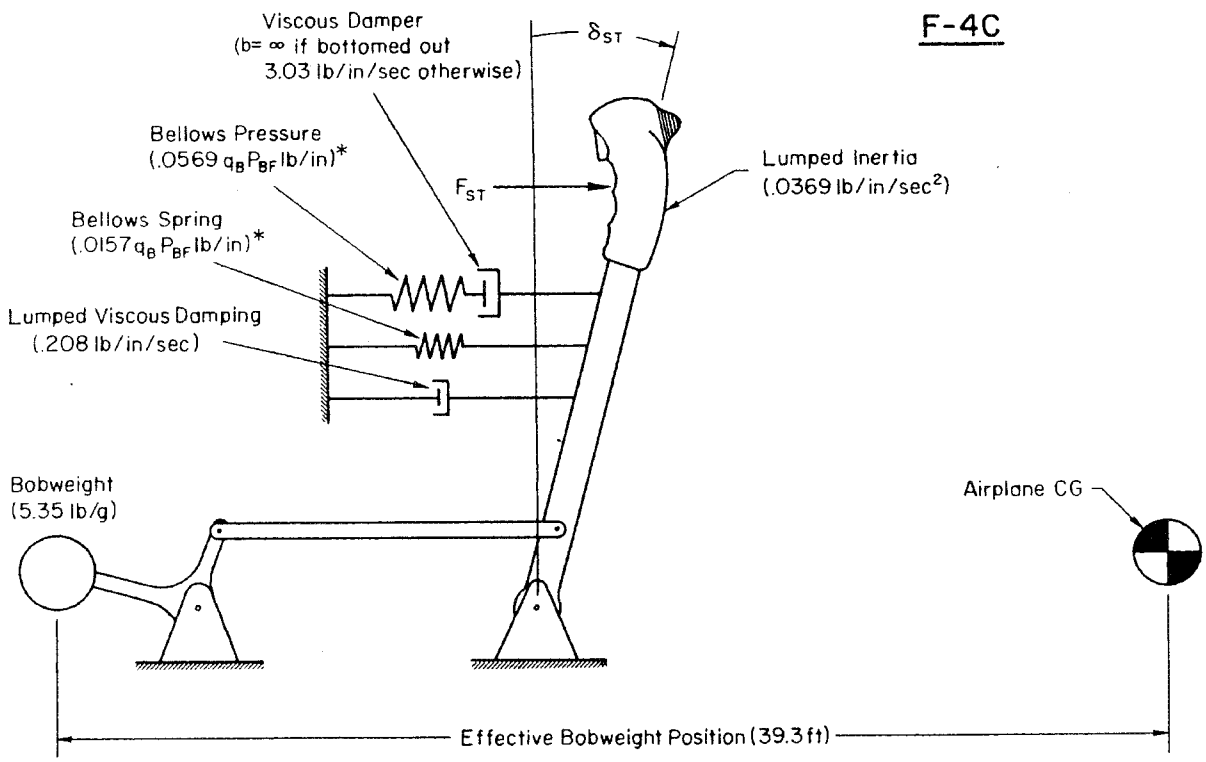

Figure 4-8, Feel System and Bobweight Mechanism, adapted from Ref. [9]

The metrics of the feel system are defined as follows (see also *Figure 4-4* and *4-8)*:

Gearing ratio:	$K_G = \frac{-3.36}{57.3}$
Viscous Damper, Bellows Pressure, Bellows Spring:	$a_0 = 0.0157\, q_B P_{BF} + \frac{0.0569\, q_B P_{BF}}{1 + \frac{0.0569\, q_B P_{BF}}{b\, s}}$ For both referenced flight conditions the viscous damper is bottomed out, i.e., $b = \infty$. Therefore, $a_0 = 0.0157\, q_B P_{BF} + 0.0569\, q_B P_{BF}$
	Flight Condition 1 3 $q_B\ [lb/ft^2]$ $0.2\,\bar{q}$ $0.4\,\bar{q}$ $P_{BF}\ [ft^2]$ 0.93 0.96
Lumped Viscous Damping:	$a_1 = 0.208\ lb/in/\sec$
Lumped Inertia:	$a_2 = 0.0369\ lb/in/\sec^2$
Bobweight Gain Ratio	$K_{BW} = \left(\frac{5.35\ lb}{g}\right) = \left(\frac{5.35\ lb}{32.2\ ft/sec^2}\right)$
Bobweight position referenced to *cg*	$x_{BW} = 39.3\ ft$

Table 4-3, F-4C Feel System Metrics

Equation 4-32 is converted into

$$\frac{\delta_{ST}}{F^*_{ST}} = \frac{\frac{K_G}{a_2}}{s^2 + \frac{a_1}{a_2}s + \frac{a_0}{a_2}} \qquad \textit{(Equation 4-33)}$$

and may now be realised in controllable companion form

$$\begin{bmatrix} \dot{\delta}_{ST} \\ \dot{\omega}_{ST} \end{bmatrix} = \begin{bmatrix} 0 & 1 \\ -a_0/a_2 & -a_1/a_2 \end{bmatrix} \begin{bmatrix} \delta_{ST} \\ \omega_{ST} \end{bmatrix} + \begin{bmatrix} 0 \\ K_G/a_2 \end{bmatrix} \qquad \textit{(Equation 4-34)}$$

with $\omega_{ST} = \dot{\delta}_{ST}$

Equation 4-34 is then added to the aircraft state space model of *Equation 4-31*

$$\begin{bmatrix} \dot{u} \\ \dot{w} \\ \dot{q} \\ \dot{\theta} \\ \dot{\delta}_S \\ \dot{\delta}_{S_{SAS}} \\ \dot{\delta}_{ST} \\ \dot{\omega}_{ST} \end{bmatrix} = \left[\begin{array}{cccccc:cc} x_u & x_w & x_q & x_\theta & x_{\delta_S} & 0 & 0 & 0 \\ z_u & z_w & z_q & z_\theta & z_{\delta_S} & 0 & 0 & 0 \\ m_u & m_w & m_q & m_\theta & m_{\delta_S} & 0 & 0 & 0 \\ 0 & 0 & 1 & 0 & 0 & 0 & 0 & 0 \\ 0 & 0 & 0 & 0 & -1/TA & -Kq/TA & 1/TA & 0 \\ Kq\,m_u & Kq\,m_w & Kq\,m_q & Kq\,m_\theta & Kq\,m_{\delta_S} & -1 & 0 & 0 \\ \hdashline . & . & . & 0 & . & . & 0 & 1 \\ . & . & . & 0 & . & . & -a_0/a_2 & -a_1/a_2 \end{array}\right] \begin{bmatrix} u \\ w \\ q \\ \theta \\ \delta_S \\ \delta_{S_{SAS}} \\ \delta_{ST} \\ \omega_{ST} \end{bmatrix} + \begin{bmatrix} 0 \\ 0 \\ 0 \\ 0 \\ 0 \\ 0 \\ 0 \\ K_G/a_2 \end{bmatrix} \left[F^*_{ST}\right]$$

$$\begin{bmatrix} u \\ w \\ q \\ \theta \\ \delta_S \\ \delta_{S_{SAS}} \\ \delta_{ST} \\ \omega_{ST} \\ \alpha \\ \gamma \\ a_{zx} \end{bmatrix} = \left[\begin{array}{cccccccc} & & & & & & & \\ & & & & I & & & \\ & & & & & & & \\ \hdashline 0 & 1/V_{T0} & 0 & 0 & 0 & 0 & 0 & 0 \\ 0 & -1/V_{T0} & 0 & 1 & 0 & 0 & 0 & 0 \\ g_{1x} & g_{2x} & g_{3x} & g_{4x} & g_{5x} & 0 & 0 & 0 \end{array}\right] \begin{bmatrix} u \\ w \\ q \\ \theta \\ \delta_S \\ \delta_{S_{SAS}} \\ \delta_{ST} \\ \omega_{ST} \\ \\ \\ \\ \end{bmatrix} + \begin{bmatrix} . \\ . \\ . \\ . \\ . \\ 0 \\ . \\ . \\ . \\ . \\ . \end{bmatrix} \left[F^*_{ST}\right]$$

(Equation 4-35)

As described in *Figure 4-4* normal acceleration at the bobweight position is used in the bobweight feedback loop. Normal acceleration at the bobweight position can be calculated in the output equation of *Equation 4-35* by substituting $x_{BW}=39.3\ ft$ into *Equations 4-20*. The output equation then becomes

$$\begin{bmatrix} u \\ w \\ q \\ \theta \\ \delta_S \\ \delta_{S_{SAS}} \\ \delta_{ST} \\ \omega_{ST} \\ \alpha \\ \gamma \\ a_{zBW} \end{bmatrix} = \left[\begin{array}{cccccccc} & & & & & & & \\ & & & & I & & & \\ & & & & & & & \\ \hdashline 0 & 1/V_{T0} & 0 & 0 & 0 & 0 & 0 & 0 \\ 0 & -1/V_{T0} & 0 & 1 & 0 & 0 & 0 & 0 \\ g_{1BW} & g_{2BW} & g_{3BW} & g_{4BW} & g_{5BW} & 0 & 0 & 0 \end{array}\right] \begin{bmatrix} u \\ w \\ q \\ \theta \\ \delta_S \\ \delta_{S_{SAS}} \\ \delta_{ST} \\ \omega_{ST} \\ \\ \\ \\ \end{bmatrix} + \begin{bmatrix} . \\ . \\ . \\ . \\ . \\ 0 \\ . \\ . \\ . \\ . \\ . \end{bmatrix} \left[F^*_{ST}\right]$$

(Equation 4-36)

With the bobweight loop added to the control system, the system input according to *Figure 4-4* becomes

$$F_{ST}^{*} = F_{ST} - F_{BW} \qquad \textit{(Equation 4-37)}$$

The force produced by the bobweight is

$$F_{BW} = K_{BW}\, a_{zBW} \qquad \textit{(Equation 4-38)}$$

This gives

$$F_{ST}^{*} = F_{ST} - K_{BW}\, a_{zBW} \qquad \textit{(Equation 4-39)}$$

which may now be substituted into the state space equation of *Equation 4-35*. Considering *Equation 4-36* with

$$a_{zBW} = g_{1BW}\, u + g_{2BW}\, w + g_{3BW}\, q + g_{4BW}\, \theta + g_{5BW}\, \delta_S \qquad \textit{(Equation 4-40)}$$

the state equation of *Equation 4-35* translates into

$$\begin{bmatrix} \dot{u} \\ \dot{w} \\ \dot{q} \\ \dot{\theta} \\ \dot{\delta}_S \\ \dot{\delta}_{S_{SAS}} \\ \dot{\delta}_{ST} \\ \dot{\omega}_{ST} \end{bmatrix} = \left[\begin{array}{cccccc:cc} x_u & x_w & x_q & x_\theta & x_{\delta_S} & 0 & 0 & 0 \\ z_u & z_w & z_q & z_\theta & z_{\delta_S} & 0 & 0 & 0 \\ m_u & m_w & m_q & m_\theta & m_{\delta_S} & 0 & 0 & 0 \\ 0 & 0 & 1 & 0 & 0 & 0 & 0 & 0 \\ 0 & 0 & 0 & 0 & -1/TA & -Kq/TA & 1/TA & 0 \\ Kq\, m_u & Kq\, m_w & Kq\, m_q & Kq\, m_\theta & Kq\, m_{\delta_S} & -1 & 0 & 0 \\ \hdashline . & . & . & 0 & . & . & 0 & 1 \\ . & . & . & 0 & . & . & -a_0/a_2 & -a_1/a_2 \end{array}\right] \begin{bmatrix} u \\ w \\ q \\ \theta \\ \delta_S \\ \delta_{S_{SAS}} \\ \delta_{ST} \\ \omega_{ST} \end{bmatrix} + \begin{bmatrix} 0 \\ 0 \\ 0 \\ 0 \\ 0 \\ 0 \\ 0 \\ K_G/a_2 \end{bmatrix} [F_{ST}] -$$

$$- \begin{bmatrix} 0 \\ 0 \\ 0 \\ 0 \\ 0 \\ 0 \\ 0 \\ (g_{1BW}\, u + g_{2BW}\, w + g_{3BW}\, q + g_{4BW}\, \theta + g_{5BW}\, \delta_S) K_{BW}\, K_G/a_2 \end{bmatrix}$$

(Equation 4-41)

Further transformation leads to the state and output equations described in *Equation 4-42.*

$$\begin{bmatrix} \dot{u} \\ \dot{w} \\ \dot{q} \\ \dot{\theta} \\ \dot{\delta}_S \\ \dot{\delta}_{S_{SAS}} \\ \dot{\delta}_{ST} \\ \dot{\omega}_{ST} \end{bmatrix} = \left[\begin{array}{ccccc|ccc} x_u & x_w & x_q & x_\theta & x_{\delta_S} & 0 & 0 & 0 \\ z_u & z_w & z_q & z_\theta & z_{\delta_S} & 0 & 0 & 0 \\ m_u & m_w & m_q & m_\theta & m_{\delta_S} & 0 & 0 & 0 \\ 0 & 0 & 1 & 0 & 0 & 0 & 0 & 0 \\ 0 & 0 & 0 & 0 & -1/TA & -Kq/TA & 1/TA & 0 \\ Kqm_u & Kqm_w & Kqm_q & Kqm_\theta & Kqm_{\delta_S} & -1 & 0 & 0 \\ \hdashline 0 & 0 & 0 & 0 & 0 & 0 & 0 & 1 \\ \frac{-g_{1BW} K_G K_{BW}}{a_2} & \frac{-g_{2BW} K_G K_{BW}}{a_2} & \frac{-g_{3BW} K_G K_{BW}}{a_2} & \frac{-g_{4BW} K_G K_{BW}}{a_2} & \frac{-g_{5BW} K_G K_{BW}}{a_2} & 0 & -a_0/a_2 & -a_1/a_2 \end{array}\right] \begin{bmatrix} u \\ w \\ q \\ \theta \\ \delta_S \\ \delta_{S_{SAS}} \\ \delta_{ST} \\ \omega_{ST} \end{bmatrix} + \begin{bmatrix} 0 \\ 0 \\ 0 \\ 0 \\ 0 \\ 0 \\ 0 \\ K_G/a_2 \end{bmatrix} [F_{ST}]$$

$$\begin{bmatrix} u \\ w \\ q \\ \theta \\ \delta_S \\ \delta_{S_{SAS}} \\ \delta_{ST} \\ \omega_{ST} \\ \alpha \\ \gamma \\ a_{zBW} \end{bmatrix} = \left[\begin{array}{cccccccc} & & & & & & & \\ & & & & & & & \\ & & & & & & & \\ & & & & & & & \\ & & & I & & & & \\ & & & & & & & \\ & & & & & & & \\ & & & & & & & \\ \hdashline 0 & 1/V_{T0} & 0 & 0 & 0 & 0 & 0 & 0 \\ 0 & -1/V_{T0} & 0 & 1 & 0 & 0 & 0 & 0 \\ g_{1BW} & g_{2BW} & g_{3BW} & g_{4BW} & g_{5BW} & 0 & 0 & 0 \end{array}\right] \begin{bmatrix} u \\ w \\ q \\ \theta \\ \delta_S \\ \delta_{S_{SAS}} \\ \delta_{ST} \\ \omega_{ST} \\ \\ \\ \\ \end{bmatrix} + \begin{bmatrix} . \\ . \\ . \\ . \\ . \\ 0 \\ . \\ . \\ . \\ . \\ . \end{bmatrix} [F_{ST}]$$

(Equation 4-42)

4.6.2 Verification of Aircraft Responses

4.6.2.1 Flight Condition 1

In *Figure 4-9* aircraft responses in pitch attitude θ, flight path angle γ and angle of attack α to a 4 seconds pulse of 5 lb stick force are depicted.

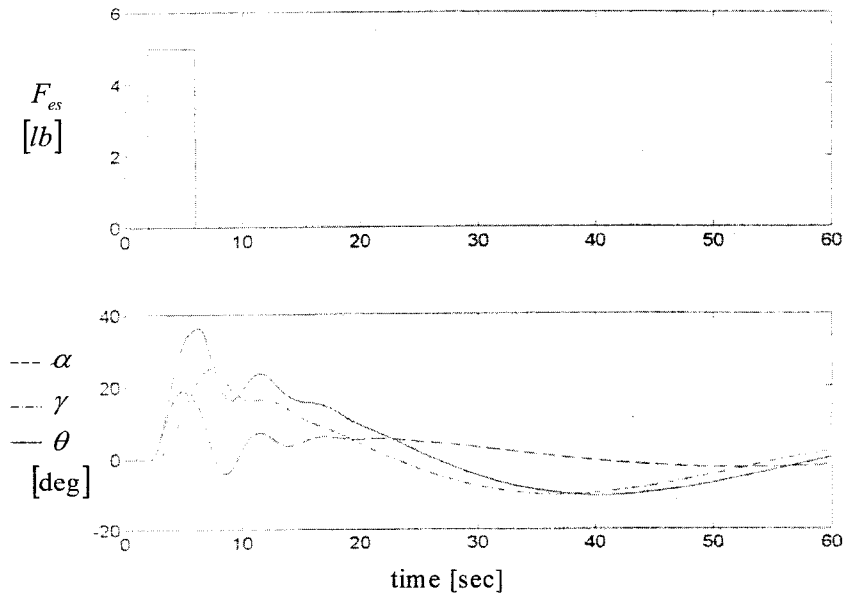

Figure 4-9, Full Order State Space Model Reponses, Flight Condition 1

Responses for flight condition 1 seem to be reasonable. As seen before in *Figure 4-5* the phugoid mode is excited for the given input.

The time domain responses from the mathematical model shown above are now compared with equivalent responses derived from transfer functions given in Ref.[9]. The transfer function for pitch attitude θ to a stick force input F_{ST}, for example, is:

$$\frac{\theta(s)}{F_{ST}(s)} = \frac{46.2(s+0.104)(s+0.379)(s+1)}{(s+1.05)(s+20.6)\left(s^2+2*0.143*0.088\,s+(0.088)^2\right)\left(s^2+2*0.313*1.12\,s+(1.12)^2\right)\left(s^2+2*(0.431)*6.06\,s+(6.06)^2\right)}$$

(Equation 4-43)

Figure 4-10 shows the time domain traces generated from the transfer function stated in *Equation 4-43* and the corresponding response of the mathematical model again for a 5 lb stick force input of 4 seconds

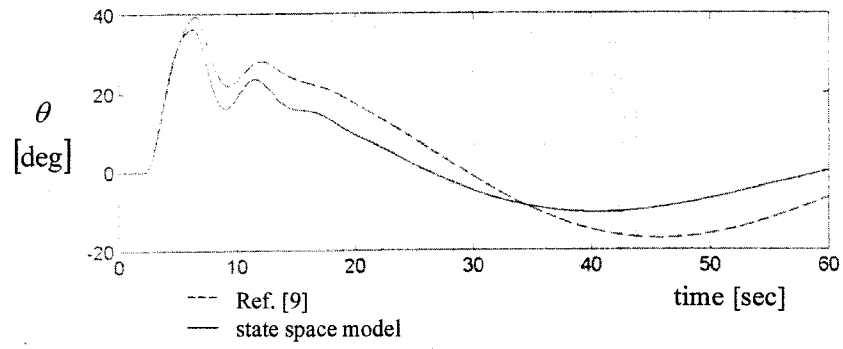

Figure 4-10, Pitch Attitude Responses, Flight Condition 1

Both responses are reasonably similar. Additionally, frequency domain responses, essential for PIO-assessment, need to be analysed as well. *Figure 4-11* shows the open-loop pitch attitude Bode plot for the transfer function obtained from the state space model and from *Equation 4-43*.

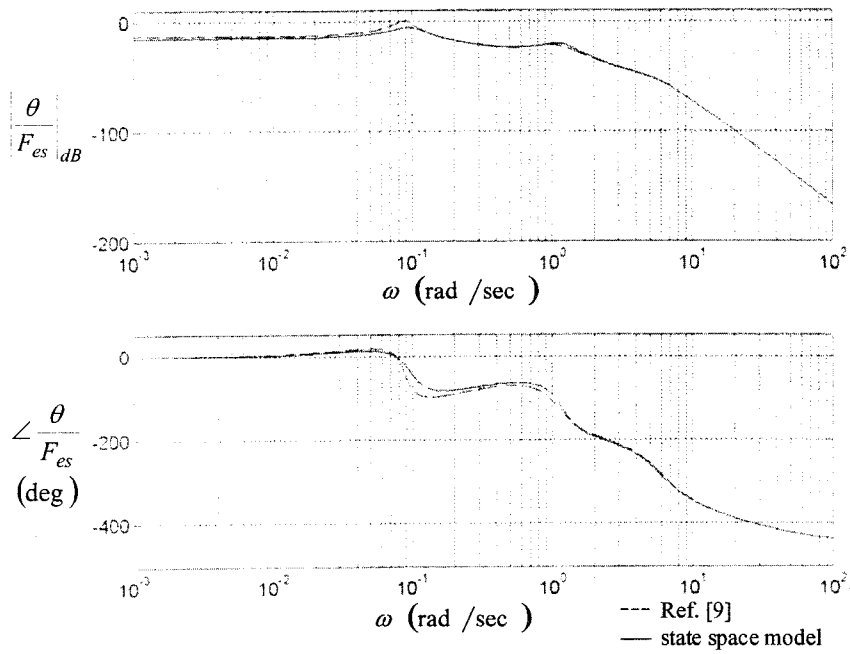

Figure 4-11, Bode Plot of Pitch-Attitude-to-Stick-Force-Input Response, Flight Condition 1

The gain and phase traces also match fairly accurately. The peaks at the phugoid frequency (~ 0.1 rad/sec) and at the short period frequency (~ 1 rad/sec) in the gain plot are clearly visible. Due to the feel system, the aircraft behaves like an attenuator throughout the entire frequency range as illustrated in the gain plot.

4.6.2.2 Flight Condition 3

As for Flight Condition 1, *Figure 4-12* shows the aircraft responses in pitch attitude θ, flight path angle γ and angle of attack α to a 4 seconds pulse of now 40 lb stick force for Flight Conditions 3.

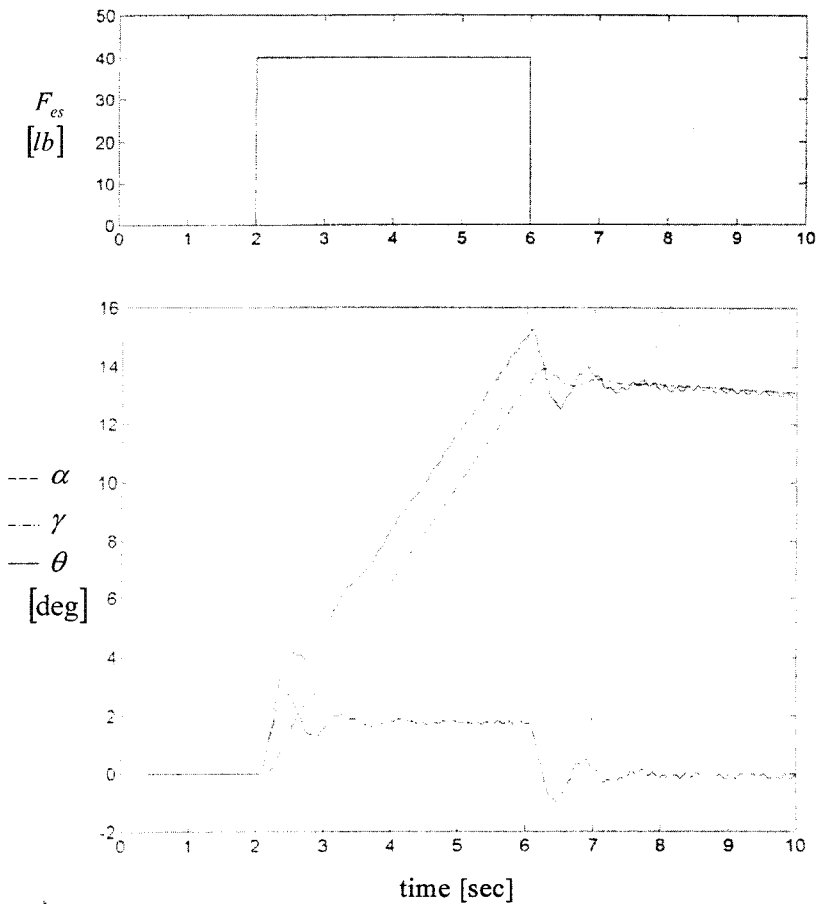

Figure 4-12, Full Order State Space Model Reponses, Flight Condition 3

It has to be noted that the expected responses in pitch attitude θ and angle of attack α are overlain by a high frequency oscillation that does not seem to fade away. This oscillation becomes even more apparent when looking at normal acceleration responses at the bobweight position a_{zBW} or at the pilot's position a_{zP}, shown in *Figures 4-13* and *4-14*. Normal acceleration at the pilot's

position can be obtained by adding a_{zP} to the output equation of *Equation 4-42* in the same manner as a_{zBW} by substituting $x = l_{XP}$ from *Table 4-1* into *Equation 4-20.*

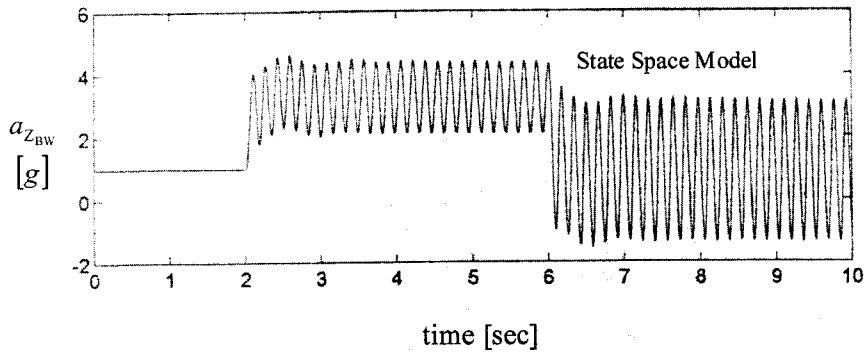

Figure 4-13, Normal Acceleration Response at Bobweight Position, Flight Condition 3

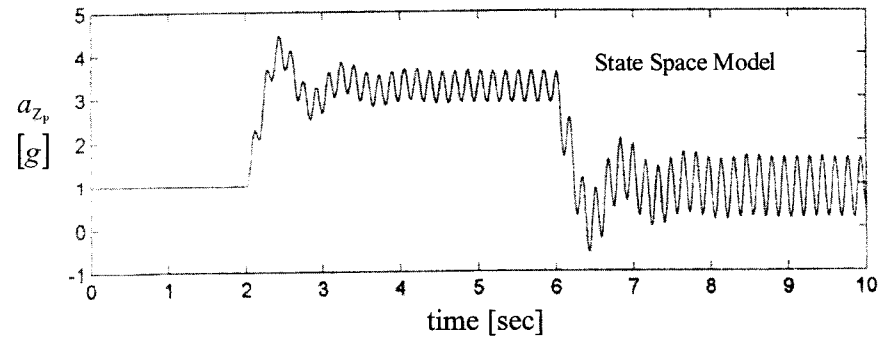

Figure 4-14, Normal Acceleration Response at Pilot's Position, Flight Condition 3

An ongoing oscillation of +1/-1 g amplitude at the pilot's position or of even +3/-1.5 g at the bobweight position after the input signal is removed is highly unlikely. By analysing the root locus plot of the system, it can be found that the addition of the feel system introduces an extra, oscillatory pair of poles with a high natural frequency of ~ 37 rad/sec. Once the bobweight feedback loop is closed, the damping of the oscillation drops dramatically to nearly zero. This is pictured in *Figure 4-15*, which shows the pitch attitude responses θ for the bobweight loop open and closed. As intended, the closure of the bobweight loop decreases the amplitude in the pitch attitude response, but simultaneously the high frequency oscillation becomes apparent. *Table 4-4* lists the eigenvalues, damping, and natural frequencies of the oscillatory poles of the state space model and the transfer function from Ref. [9].

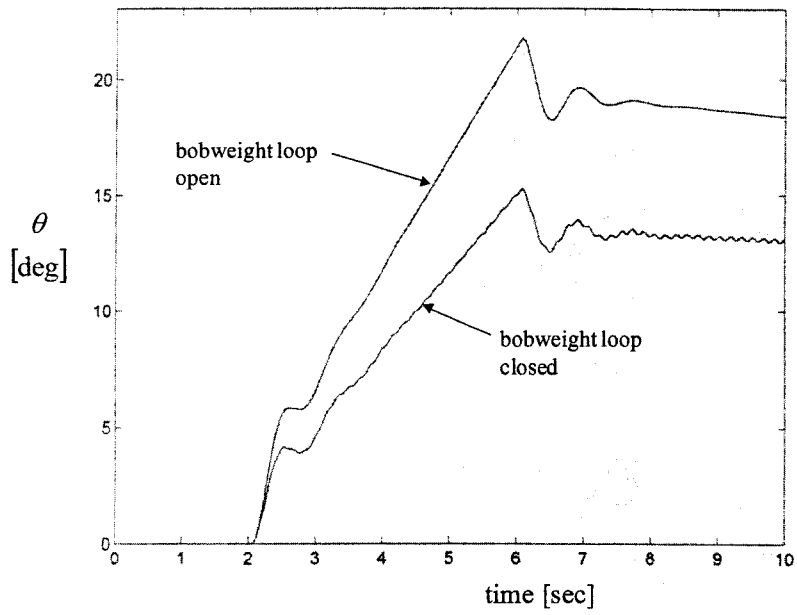

Figure 4-15, Pitch Attitude Response for Bobweight Loop Open and Closed, Flight Condition 3

	Eigenvalue	**Damping**	**Frequency (rad/sec)**	**Comment**
State Space Model *Feel System Excluded*	-0.0347+0.0416 i -0.0347-0.0416 i	0.6406	0.0542	Phugoid
	-1.8996+7.411 i -1.8996-7.411 i	0.2483	7.6506	Short Period
State Space Model *Feel System Included Bobweight Loop Open*	-0.0347+0.0416 i -0.0347-0.0416 i	0.6406	0.0542	Phugoid
	-1.8996+7.411 i -1.8996-7.411 i	0.2483	7.6506	Short Period
	-2.8184+36.687 i -2.8184-36.687 i	0.0766	36.7951	Feel System
State Space Model *Feel System Included Bobweight Loop Closed*	-0.0345+0.0293 i -0.0345-0.0293 i	0.7628	0.0453	Phugoid
	-1.6045+7.5569 i -1.6045-7.5569 i	0.2077	7.7254	Short Period
	-0.0071+38.5619 i -0.0071-38.5619 i	0.0002	38.5619	Feel System
TF-Function, Ref. [9] *Feel System Included Bobweight Loop Closed*	-0.0343+0.0298 i -0.0343-0.0298 i	0.755	0.0454	Phugoid
	-6.6357+7.6143 i -6.6357-7.6143 i	0.657	10.1	Short Period
	-0.0772+39.1999 i -0.0772-39.1999 i	0.002	39.2	Feel System

Table 4-4, Eigenvalues, Damping and Natural Frequencies, Flight Condition 3

The time domain responses from the mathematical model shown in *Figure 4-12* and *4-14* are again compared with equivalent responses derived from transfer functions given in Ref. [9]. The transfer functions for pitch attitude θ and normal acceleration at the pilot's position a_{ZP} to a stick force input F_{ST} for Flight Condition 3, taken from Ref.[9], are:

$$\frac{\theta(s)}{F_{ST}(s)} = \frac{1936(s+0.0678)(s+1)(s+1.9)\left(s^2+2*0.0917*13.9\,s+(13.9)^2\right)}{(s+0.902)(s+17.9)\left(s^2+2*0.755*0.0454\,s+(0.0454)^2\right)\left(s^2+2*0.657*10.1\,s+(10.1)^2\right)\left(s^2+2*(-0.00197)*39.2\,s+(39.2)^2\right.}$$

$$\frac{a_{zP}(s)}{F_{ST}(s)} = \frac{-23430(s+0.000137)(s+0.0679)(s+1)}{(s+0.902)(s+17.9)\left(s^2+2*0.755*0.0454\,s+(0.0454)^2\right)\left(s^2+2*0.657*10.1\,s+(10.1)^2\right)\left(s^2+2*(-0.00197)*39.2\,s+(39.2)^2\right.}$$

(Equation 4-44)

Figures 4-16 and *4-17* show the time domain traces generated from the transfer functions stated above compared with corresponding responses of the mathematical model.

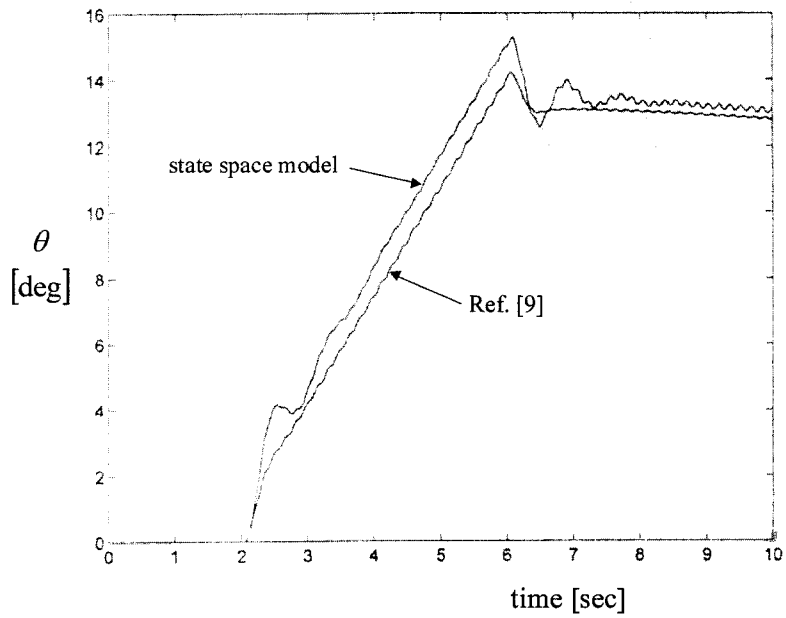

Figure 4-16, Pitch Attitude Responses for Bobweight Loop Closed, Flight Condition 3

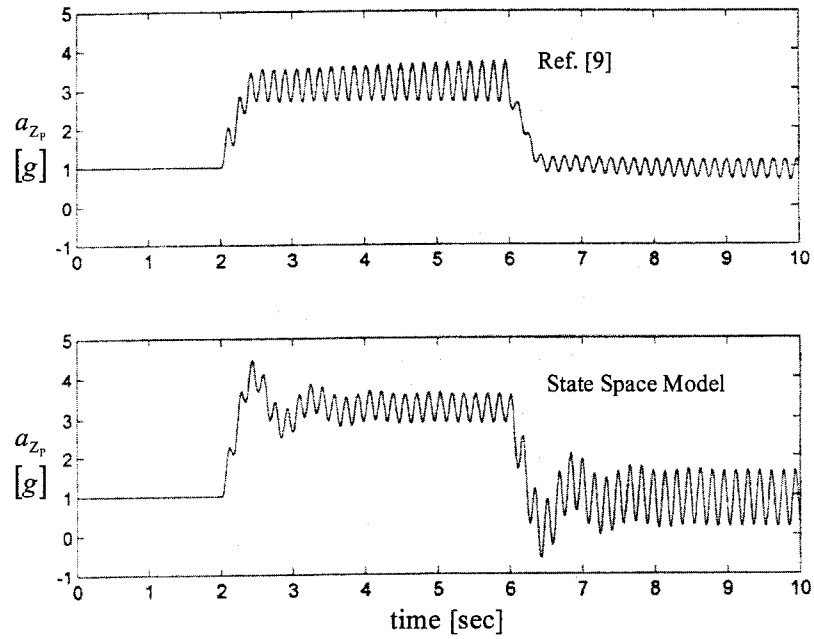

Figure 4-17, Normal Acceleration Responses at Pilot's Position for Bobweight Loop Closed, Flight Condition 3

Surprisingly, they are very similar. Although, the peak value for pitch attitude θ attained by the mathematical model as illustrated in *Figure 4-16,* is slightly higher than that of Ref. [9] and the residual oscillation, present in the pitch attitude response as well as in the normal acceleration response, has larger amplitudes in the traces generated by the state space model, it has to be noted that both sources show a similar behaviour and that neither source exhibits a fading tendency of the residual oscillation.

This similarity can be confirmed by comparing the frequency domain responses. *Figure 4-18* shows the Bode plot of the open-loop pitch-attitude-to-stick-force-input response for both sources.

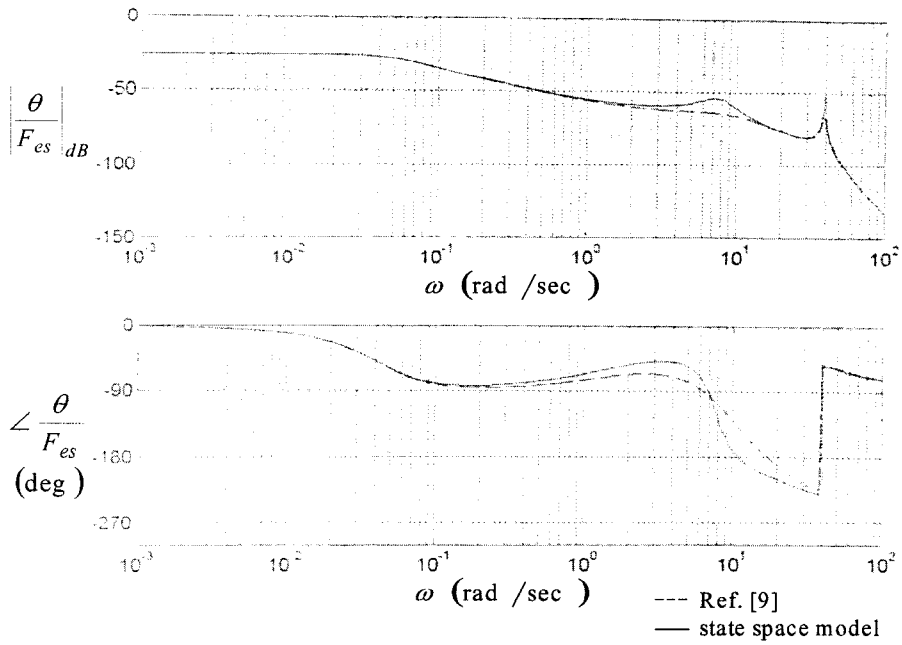

Figure 4-18, Bode Plot of Pitch-Attitude-to-Stick-Force-Input Response, Flight Condition 3

Corresponding to the values in *Table 4-4,* both traces exhibit a very pronounced peak in the gain plot and a non-linearity in the phase plot at the resonance frequency of the feel system. Although this non-linearity occurs at a frequency that is beyond the usual operational frequency range of the aircraft, it is interesting to see, what actually influences it. The only possibility to suppress the residual oscillation is by either increasing the value of the lumped viscous damping in the feel system (a_1 in *Table 4-3*) from 0.208 lb/in/sec to nearly 0.3 lb/in/sec or by moving the bobweight physically closer to the *cg* by reducing the distance x_{BW}.

Ref.[9] does not claim, that the data given is an exact representation of the actual aircraft. But since the data from Ref. [9] is the only data available for this project, a change of control system characteristics such as those mentioned above is not considered to be an option to improve system performance. Instead, a different approach to building the state space model is considered and described in the following chapter.

4.6.3 Second Formulation

In this formulation the stick dynamics are coupled with the airframe straight away. To make the derivation of this formulation less lengthy, the short-period approximation of the airframe is used. *Equation 3-45* already contains the stick dynamics.

$$\begin{bmatrix}\dot{w}\\ \dot{q}\end{bmatrix}=\begin{bmatrix}z_w & z_q\\ m_w & m_q\end{bmatrix}\begin{bmatrix}w\\ q\end{bmatrix}+\begin{bmatrix}0 & z_{\delta_{ST}}\\ 0 & m_{\delta_{ST}}\end{bmatrix}\begin{bmatrix}\omega_{ST}\\ \delta_{ST}\end{bmatrix} \qquad \textit{(Equation 4-45)}$$

$z_{\delta_{ST}}$ and $m_{\delta_{ST}}$ are normal force and pitching moment due to stick deflection. They are calculated as follows

$$z_{\delta_{ST}} = z_{\delta_S}\frac{d\delta_S}{d\delta_{ST}} \quad \text{and} \quad m_{\delta_{ST}} = m_{\delta_S}\frac{d\delta_S}{d\delta_{ST}} \qquad \textit{(Equation 4-46)}$$

with $\frac{d\delta_S}{d\delta_{ST}}$ being the gearing ratio K_G between stick and horizontal stabilisers used for pitch control.

Bobweight dynamics depend primarily on normal acceleration at the bobweight's position a_{zBW}. It may be recalled that according to *Equation 4-16* normal acceleration at the bobweight's position is

$$a_z = \dot{w} - q\,U_0 - x_{BW}\,\dot{q} \qquad \textit{(Equation 4-47)}$$

By including *Equation 4-47,* the equations of motion of the stick, comprising bobweight as well as feel system* dynamics, can be written as

$$\begin{bmatrix}\dot{\omega}_{ST}\\ \dot{\delta}_{ST}\end{bmatrix}=\begin{bmatrix}-a_1/a_2 & -a_0/a_2\\ 1 & 0\end{bmatrix}\begin{bmatrix}\omega_{ST}\\ \delta_{ST}\end{bmatrix}-\begin{bmatrix}K_{BW} & -K_{BW}x_{BW}\\ 0 & 0\end{bmatrix}\begin{bmatrix}\dot{w}\\ \dot{q}\end{bmatrix}-\begin{bmatrix}0 & K_{BW}U_0\\ 0 & 0\end{bmatrix}\begin{bmatrix}w\\ q\end{bmatrix}+\begin{bmatrix}K_G/a_2\\ 0\end{bmatrix} \qquad \textit{(Equation 4-48)}$$

Equation 4-45 is now substituted into *Equation 4-48* to give

$$\begin{bmatrix}\dot{\omega}_{ST}\\ \dot{\delta}_{ST}\end{bmatrix}=\begin{bmatrix}-a_1/a_2 & -a_0/a_2\\ 1 & 0\end{bmatrix}\begin{bmatrix}\omega_{ST}\\ \delta_{ST}\end{bmatrix}-\begin{bmatrix}K_{BW} & -K_{BW}x_{BW}\\ 0 & 0\end{bmatrix}\begin{bmatrix}z_w & z_q\\ m_w & m_q\end{bmatrix}\begin{bmatrix}w\\ q\end{bmatrix}-$$
$$-\begin{bmatrix}K_{BW} & -K_{BW}x_{BW}\\ 0 & 0\end{bmatrix}\begin{bmatrix}0 & z_{\delta_{ST}}\\ 0 & m_{\delta_{ST}}\end{bmatrix}\begin{bmatrix}\omega_{ST}\\ \delta_{ST}\end{bmatrix}-\begin{bmatrix}0 & K_{BW}U_0\\ 0 & 0\end{bmatrix}\begin{bmatrix}w\\ q\end{bmatrix}+\begin{bmatrix}K_G/a_2\\ 0\end{bmatrix} \qquad \textit{(Equation 4-49)}$$

* the feel system includes the gearing ratio K_G as demonstrated in *Equation 4-32*

Equation 4-49 can be rewritten as

$$\begin{bmatrix}\dot{\omega}_{ST}\\ \dot{\delta}_{ST}\end{bmatrix}=\begin{bmatrix}-a_1/a_2 & -a_0/a_2+K_{BW}\left(x_{BW}\,m_{\delta_{ST}}-z_{\delta_{ST}}\right)\\ 1 & 0\end{bmatrix}\begin{bmatrix}\omega_{ST}\\ \delta_{ST}\end{bmatrix}-$$
$$-\begin{bmatrix}K_{BW}\left(z_w-x_{BW}\,m_w\right) & K_{BW}\left(z_q-x_{BW}\,m_q-U_0\right)\\ 0 & 0\end{bmatrix}\begin{bmatrix}w\\ q\end{bmatrix}+\begin{bmatrix}K_G/a2\\ 0\end{bmatrix}$$

(Equation 4-50)

To obtain the required state space form, *Equations 4-45* and *4-50* are combined to give

$$\begin{bmatrix}\dot{\omega}_{ST}\\ \dot{\delta}_{ST}\\ \dot{w}\\ \dot{q}\end{bmatrix}=\begin{bmatrix}-a_1/a_2 & -a_0/a_2+K_{BW}\left(x_{BW}\,m_{\delta_{ST}}-z_{\delta_{ST}}\right) & -K_{BW}\left(z_w-x_{BW}\,m_w\right) & -K_{BW}\left(z_q-x_{BW}\,m_q-U_0\right)\\ 1 & 0 & 0 & 0\\ 0 & z_{\delta_{ST}} & z_w & z_q\\ 0 & m_{\delta_{ST}} & m_w & m_q\end{bmatrix}\begin{bmatrix}\omega_{ST}\\ \delta_{ST}\\ w\\ q\end{bmatrix}+\begin{bmatrix}K_G/a2\\ 0\\ 0\\ 0\end{bmatrix}$$

(Equation 4-51)

By considering *Equation 4-20*, *Equation 4-51* may be rewritten

$$\begin{bmatrix}\dot{\omega}_{ST}\\ \dot{\delta}_{ST}\\ \dot{w}\\ \dot{q}\end{bmatrix}=\begin{bmatrix}-a_1/a_2 & -a_0/a_2+K_{BW}\left(x_{BW}\,m_{\delta_{ST}}-z_{\delta_{ST}}\right) & -K_{BW}\,g_{2_{BW}} & -K_{BW}g_{3_{BW}}\\ 1 & 0 & 0 & 0\\ 0 & z_{\delta_{ST}} & z_w & z_q\\ 0 & m_{\delta_{ST}} & m_w & m_q\end{bmatrix}\begin{bmatrix}\omega_{ST}\\ \delta_{ST}\\ w\\ q\end{bmatrix}+\begin{bmatrix}K_G/a2\\ 0\\ 0\\ 0\end{bmatrix}$$

(Equation 4-52)

These implementations are now applied to the full-order aircraft model described in *Equation 4-31* to give

$$\begin{bmatrix} \dot{u} \\ \dot{w} \\ \dot{q} \\ \dot{\theta} \\ \dot{\delta}_S \\ \dot{\delta}_{S_{SAS}} \\ \dot{\omega}_{ST} \\ \dot{\delta}_{ST} \end{bmatrix} = \begin{bmatrix} x_u & x_w & x_q & x_\theta & x_{\delta_S} & 0 & 0 & 0 \\ z_u & z_w & z_q & z_\theta & z_{\delta_S} & 0 & 0 & z_{\delta_{ST}} \\ m_u & m_w & m_q & m_\theta & m_{\delta_s} & 0 & 0 & m_{\delta_{ST}} \\ 0 & 0 & 1 & 0 & 0 & 0 & 0 & 0 \\ 0 & 0 & 0 & 0 & -1/TA & -Kq/TA & 0 & 1/TA \\ Kq\,m_u & Kq\,m_w & Kq\,m_q & Kq\,m_\theta & Kq\,m_{\delta_S} & -1 & 0 & Kq\,m_{\delta_{ST}} \\ 0 & -K_{BW}\,g_{2_{BW}} & -K_{BW}\,g_{3_{BW}} & 0 & 0 & 0 & -a_1/a_2 & -a_0/a_2 + K_{BW}\left(x_{BW}\,m_{\delta_{ST}} - z_{\delta_{ST}}\right) \\ 0 & 0 & 0 & 0 & 0 & 0 & 1 & 0 \end{bmatrix} \begin{bmatrix} u \\ w \\ q \\ \theta \\ \delta_S \\ \delta_{S_{SAS}} \\ \delta_{ST} \\ \omega_{ST} \end{bmatrix} + \begin{bmatrix} 0 \\ 0 \\ 0 \\ 0 \\ 0 \\ 0 \\ K_G/a_2 \\ 0 \end{bmatrix} [F_{ST}]$$

$$\begin{bmatrix} u \\ w \\ q \\ \theta \\ \delta_S \\ \delta_{S_{SAS}} \\ \delta_{ST} \\ \omega_{ST} \\ \alpha \\ \gamma \\ a_{zBW} \end{bmatrix} = \begin{bmatrix} & & & & & & & \\ & & & & & & & \\ & & & & & & & \\ & & & & & & & \\ & & & I & & & & \\ & & & & & & & \\ & & & & & & & \\ & & & & & & & \\ \hline 0 & 1/V_{T0} & 0 & 0 & 0 & 0 & 0 & 0 \\ 0 & -1/V_{T0} & 0 & 1 & 0 & 0 & 0 & 0 \\ g_{1BW} & g_{2BW} & g_{3BW} & g_{4BW} & g_{5BW} & 0 & 0 & 0 \end{bmatrix} \begin{bmatrix} u \\ w \\ q \\ \theta \\ \delta_S \\ \delta_{S_{SAS}} \\ \delta_{ST} \\ \omega_{ST} \end{bmatrix} + \begin{bmatrix} . \\ . \\ . \\ . \\ . \\ 0 \\ . \\ . \\ . \\ . \\ . \end{bmatrix} [F_{ST}]$$

(Equation 4-53)

4.6.4 Verification of Aircraft Responses

4.6.4.1 Flight Condition 1

In *Figure 4-19* aircraft responses in pitch attitude θ, flight path angle γ and angle of attack α to a 4 seconds pulse of 5 lb stick force for the modified state space model are illustrated.

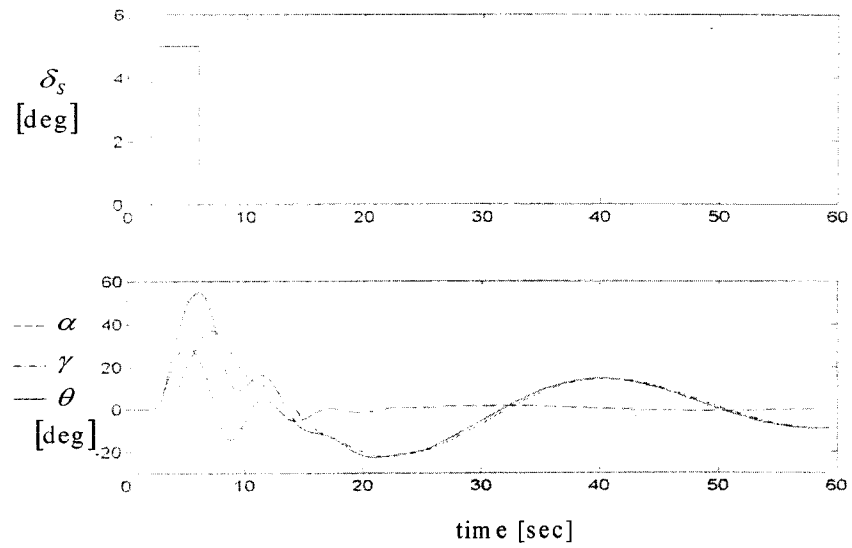

Figure 4-19, Modified Full Order State Space Model Responses, Flight Condition 1

Responses for Flight Condition 1 are conclusive. Again the phugoid mode is clearly visible. But compared to the original responses shown in *Figure 4-9*, it has to be remarked that amplitudes for α, γ and θ are slightly larger. Also the frequency of the phugoid mode has increased which becomes apparent when plotting the response of the modified state space model side by side with the response derived from the transfer function (*Equation 4-43*) from Ref. [9] as pictured in *Figure 4-20.*

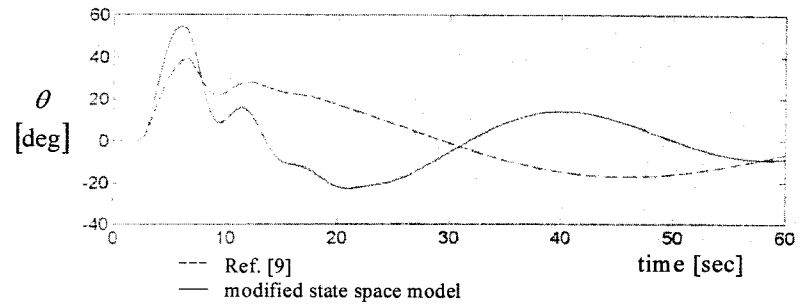

Figure 4-20, Modified Pitch Attitude Response, Flight Condition 1

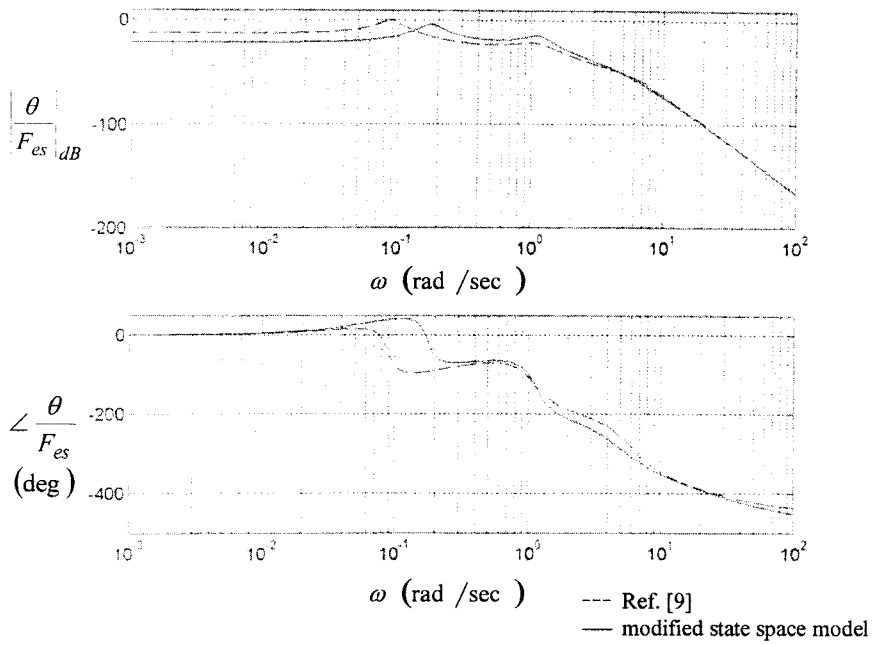

Figure 4-21, Modified Bode Plot of Pitch-Attitude-to-Stick-Force-Input Response, Flight Condition 1

The increase in the phugoid-frequency is confirmed by a shift in gain ratio and phase angle at the specified frequency as depicted in the Bode plot of the open-loop pitch-attitude-to-stick-force-input response in *Figure 4-21.*

4.6.4.2 Flight Condition 3

Again aircraft responses in pitch attitude θ, flight path angle γ and angle of attack α of the modified state space model to a 4 seconds pulse of 40 lb stick force are investigated.

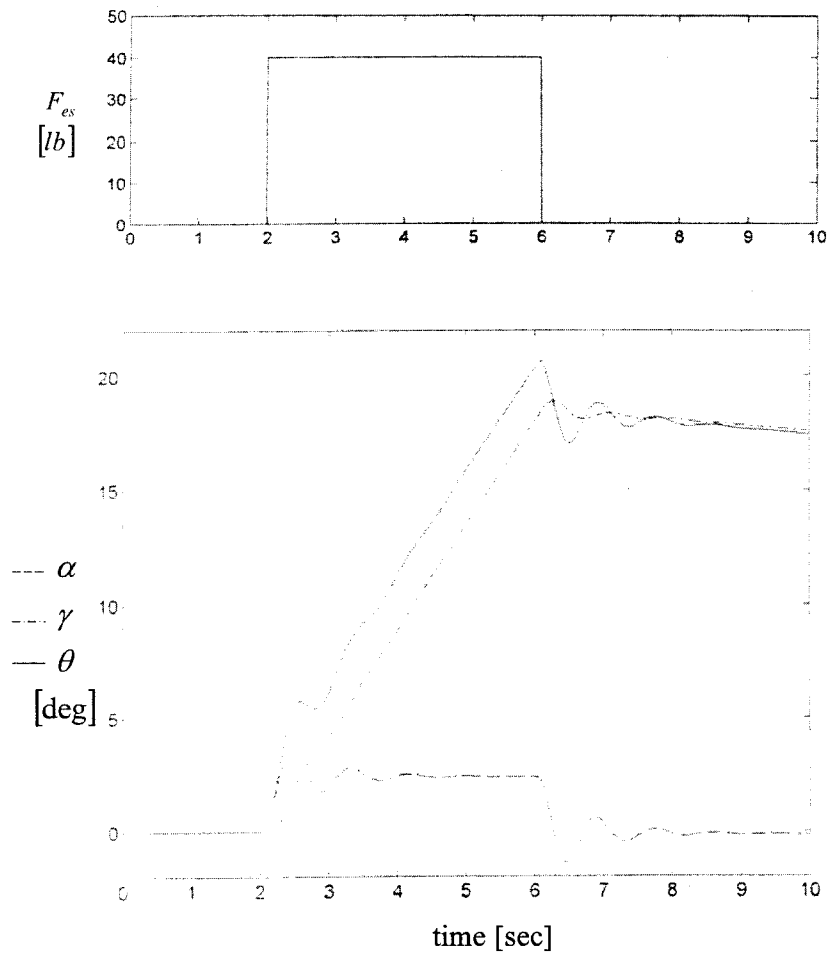

Figure 4-22, Modified, Full Order State Space Model Reponses, Flight Condition 3

It is evident in *Figure 4-22* that the responses in pitch attitude θ, flight path γ and normal acceleration a_{zP} (*Figure 4-24*) are no longer disturbed by the residual, high frequency oscillation. Also, similar to Flight Condition 1, amplitudes are larger than in the responses generated by the initial full order model decribed in *Figure 4-12* or when compared to transfer function responses from Ref. [9] as illustrated in *Figures 4-23* and *4-24*.

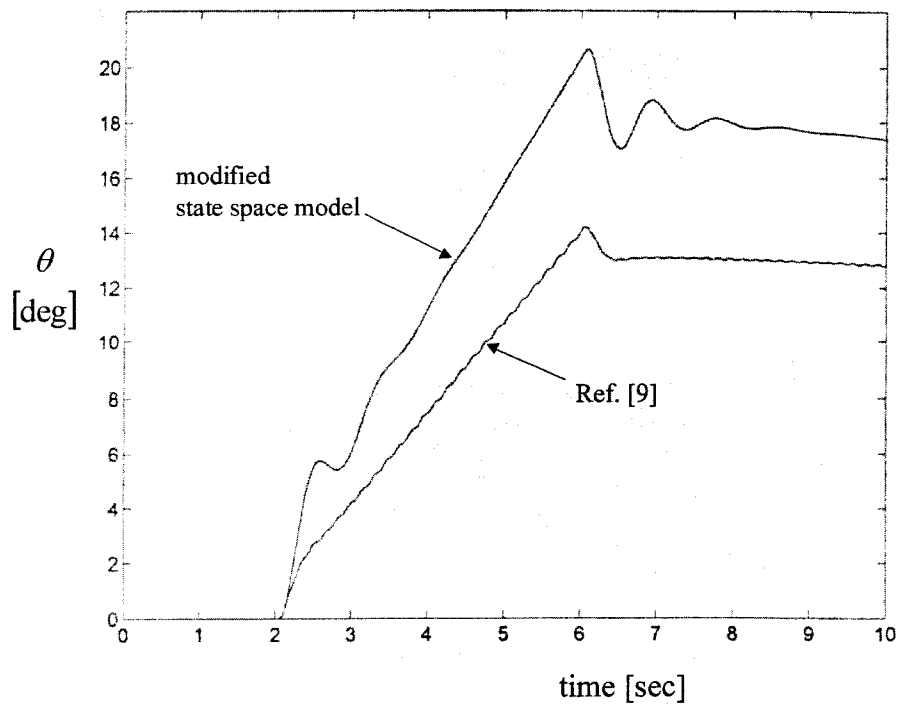

Figure 4-23, Pitch Attitude Responses for Bobweight Loop Closed, Flight Condition 3

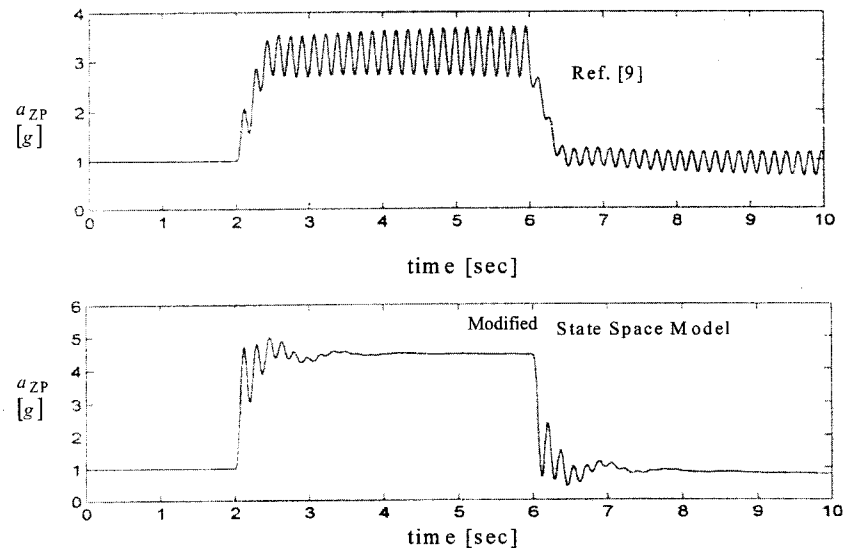

Figure 4-24, Normal Acceleration at Pilot's Position, Flight Condition 3

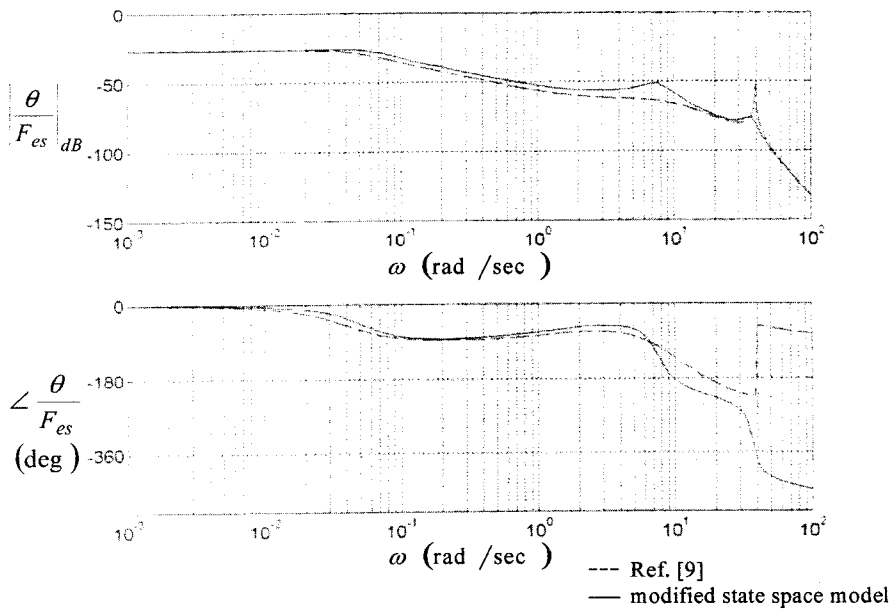

Figure 4-25, Modified Bode Plot of Pitch-Attitude-to-Stick-Force-Input Response, Flight Conditon 3

By analysing the frequency domain response of the modified state space model and the response derived from the transfer function obtained from Ref. [9] in *Figure 4-25*, it becomes apparent that the non-linearity is no longer present.

Although the study of the initial state space model described by *Equation 4-42* reveals that only time and frequency domain responses of Flight Condition 3 are affected by the residual, high frequency oscillation, it is decided to use the modified state space model, derived in the second formulation in *Chapter 4.6.3*, for PIO-assessment of both flight conditions. Even though responses match less accurately the results given in Ref. [9], they appear to be more realistic and the development of the mathematical model is equally comprehensible.

5 Application of PIO-Criteria

The PIO-criteria introduced in *Chapter 2* are now applied to the mathematical model of the F-4C. For each of the two flight conditions selected for analysis, four different operational conditions of the pitch control system are investigated. These are for *Flight Condition 1* (FC 1) and *Flight Condition 3* (FC 3) respectively (see also *Figure 4-4*):

- FC 1-1/ FC 3-1 SAS engaged, bobweight loop closed
- FC 1-2/ FC 3-2 SAS disengaged, bobweight loop closed
- FC 1-3/ FC 3-3 SAS engaged, bobweight loop open
- FC 1-4/ FC 3-4 SAS disengaged, bobweight loop open
- (FC 1-5/ FC 3-5) (feel system and bobweight excluded, SAS engaged)*
- (FC 1-6/ FC 3-6) (feel system and bobweight excluded, SAS disengaged)*

5.1 The Neal and Smith Criterion

Flight Condition 1

For the landing case, according to *Chapter 2.1,* the Neal and Smith Criterion demands a value of –90 deg phase lag at a bandwidth frequency of $\omega_{BW} = 2.5$ rad/sec for the closed-loop pitch attitude frequency response. After multiplying the open-loop aircraft transfer function $\theta(s)/F_{ST}(s)$ with the pilot time delay $D_P(s) = e^{-\tau_{Pi}s}$, which is estimated by a 3rd order Pade-approximation with $\tau_{Pi} = 0.3$ sec, the resulting response is plotted on a Nichols chart (see also *Figure 2-3*). For case FC 1-1, at 2.5 rad/sec, the open-loop phase angle has already dropped to a value of -267 deg. This would imply that the pilot would need to generate a phase lead of more than 90 deg to hit the –90 deg closed-loop phase curve with the 2.5 rad/sec bandwidth frequency point. This is a value beyond any practical application, considering that phase compensation is a measure of pilot workload, and exceeds the limit of 80 deg phase lead, a criterion boundary in *Figure 2-4.* Unfortunately, this applies for cases FC 1-2 through FC 1-4 as well. Therefore, it has to be concluded that it is not possible to apply the Neal and Smith Criterion to Flight Condition 1 in the version described in this report.

* only applicable for Gibson Phase Rate Criterion

Flight Condition 3

Flight Condition 3, identified as a low-level terrain-following task, can be ascribed to flight phases of Category A (see *Appendix A*). Therefore the bandwidth frequency, where a phase angle of –90 deg needs to be attained, is ω_{BW} = 3.5 rad/sec. Again a 3rd order Pade-approximation is used for the pilot time delay $D_P(s) = e^{-\tau_{Pi} s}$ with τ_{Pi} = 0.3 sec. At 3.5 rad/sec the phase angle of the open-loop pitch attitude frequency response of the aircraft transfer function for case FC 3-1 multiplied with the pilot time delay $D_P(s)$ is –112 deg. By employing a Nichols chart it becomes apparent that the pilot has to generate lag compensation in order to hit the –90 deg closed-loop phase curve and fulfil the criterion requirements. This applies for all FC 3-cases. A closed-loop droop of –3.0 dB is achieved for all cases. *Table 5-1* lists the values of the necessary pilot gain compensation K_P, the time constants for the lag compensation T_{P1} and T_{P2}, the phase compensation angle ϕ_P and the value of the closed-loop resonance.

	K_P [dB]	T_{P1} [sec]	T_{P2} [sec]	ϕ_P [deg]	Closed-loop [dB] resonance
FC 3-1	55.15	0.209	0.390	-17.60	11.06
FC 3-2	55.09	0.225	0.363	-13.57	7.73
FC 3-3	55.09	0.219	0.373	-15.08	8.95
FC 3-4	55.07	0.235	0.347	-11.10	6.73

Table 5-1, Neal and Smith Criterion Parameters for the Compensated System, Flight Condition 3

The criterion output parameters ϕ_P and the maximum value of closed-loop resonance are now plotted on the criterion graph as pictured in *Figure 5-1*.

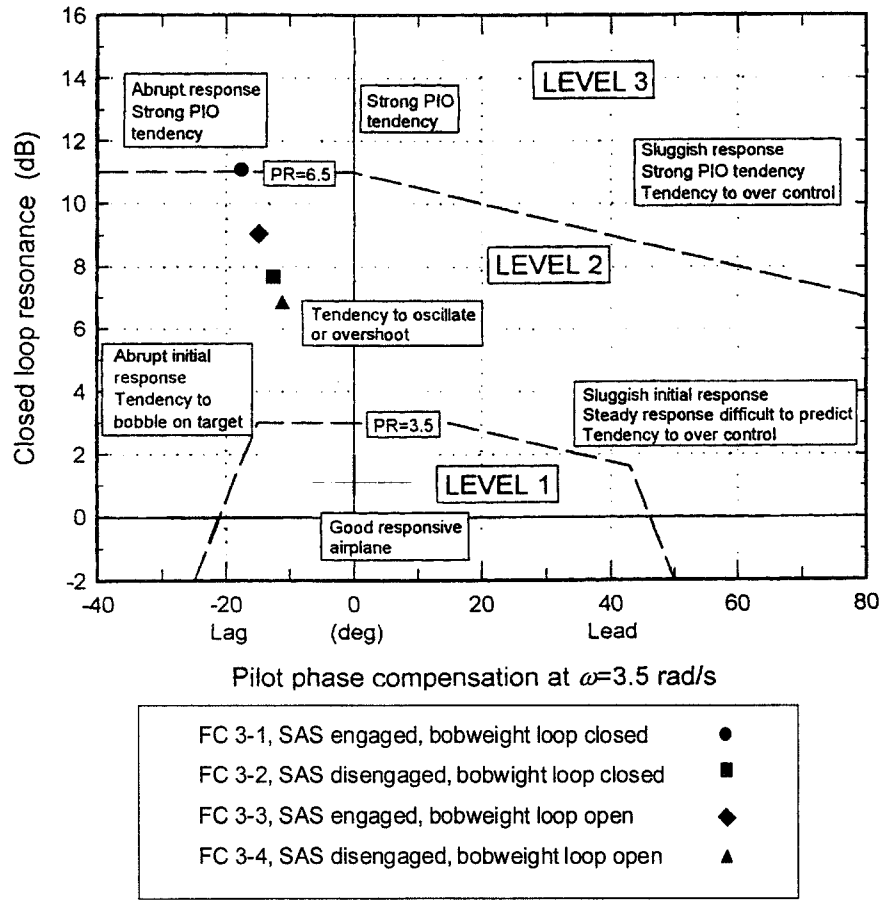

Figure 5-1, Neal and Smith Criterion Boundaries for the Pitch Tracking Task, adapted from Ref. [2]

Except for case FC 3-1 all cases fall into the Level 2 handling qualities region, exhibiting a tendency to oscillate and bobble on the target. Case FC 3-1 falls directly onto the Level 2/ Level 3-dividing line, separating strong PIO-tendency from minor bobbling tendency.

5.2 Bandwidth/ Pitch-Rate Overshoot Criterion

Flight Condition 1

The application of the Bandwidth/ Pitch-Rate Overshoot criterion comprises the following steps to obtain the criterion parameters (see also *Figure 2-5*).

First, the pitch attitude bandwidth $\omega_{BW\theta}$ is calculated, where the phase margin is 45 deg or the gain margin is 6 dB. The phase plot of the open-loop pitch-attitude-to-stick-force-input frequency response is examined and the neutral stability frequency ω_{180}, where the phase angle ϕ assumes a value of –180 deg, is determined.

For case FC 1-1 it is

$\omega_{180} = 1.419$ rad/sec

Next, the gain plot of the open-loop pitch attitude frequency response is studied and the gain at $\omega_{180} = 1.419$ rad/sec is read. Here it is

$$\left|\frac{\theta}{F_{ST}}\right|_{dB_{\phi=-180}} = -19.917 \text{ dB}$$

Next a gain margin of 6 dB is added to this value, giving

$$\left|\frac{\theta}{F_{ST}}\right|_{dB_{BW\theta gain}} = -13.917 \text{ dB}$$

In the gain plot of the pitch attitude frequency response, the corresponding frequency can now be determined. For FC 1–1 it is

$\omega_{BW_{\theta gain}} = 0.285$ rad/sec

The next step is to obtain the frequency, where the phase margin is 45 deg. Therefore, the frequency at $\phi_{135} = \angle\frac{\theta}{F_{ST}} = -135$ deg has to be determined. In this case it is

$\omega_{135} = \omega_{BW_{\theta phase}} = 1.158$ rad/sec

Since the bandwidth frequency $\omega_{BW\theta}$ is defined as being either $\omega_{BW_{\theta gain}}$ or $\omega_{BW_{\theta phase}}$, whichever has the lower value, the final value of $\omega_{BW\theta}$ is

$\omega_{BW\theta} = 0.285$ rad/sec

For the calculation of the pitch attitude phase delay $\tau_{p\theta}$ the phase angle at $2\omega_{180}$ has to be determined.

$2\omega_{180} = 2.838$ rad/sec

$\phi_{2\omega_{180}} = -233.438$ deg

According to *Figure 2-5* the pitch attitude phase delay $\tau_{p\theta}$ equates to

$$\tau_{p_\theta} = \frac{\Delta\phi_{2\omega_{180}}}{57.3(2\omega_{180})} = \frac{\phi_{2\omega_{180}} - \phi_{\omega_{180}}}{57.3(2\omega_{180})} = 0.329 \text{ sec}$$

The values of all required parameters are listed in *Table 5-2* for cases FC 1-1 through FC 1-4

		FC 1-1	FC 1-2	FC 1-3	FC 1-4
ω_{180}	[rad/sec]	1.419	1.431	1.386	1.401
$\left\|\frac{\theta}{F_{ST}}\right\|_{dB_{\phi=-180}}$	[dB]	-19.917	-20.454	-24.955	-25.303
$\left\|\frac{\theta}{F_{ST}}\right\|_{dB_{BW\theta gain}}$	[dB]	-13.917	-14.454	-18.955	-19.303
$\omega_{BW_{\theta gain}}$	[rad/sec]	0.285	0.296	0.982	0.989
$\omega_{135} = \omega_{BW_{\theta phase}}$	[rad/sec]	1.158	1.156	0.767	0.762
$\omega_{BW\theta}$	[rad/sec]	0.285	0.296	0.767	0.762
$2\omega_{180}$	[rad/sec]	2.838	2.862	2.772	2.802
$\phi_{2\omega 180}$	[rad/sec]	-233.438	-233.415	-224.235	-224.480
τ_{p_θ}	[rad/sec]	0.329	0.326	0.279	0.277

Table 5-2, Bandwidth/ Pitch-Rate Overshoot Criterion Parameters, Flight Condition 1

For Flight Condition 1 no further parameters are required for PIO-evaluation.

Flight Condition 3

The procedure for acquiring the criterion parameters for Flight Condition 3 is equivalent to Flight Condition 1. Additionally, a value of pitch rate overshoot $\Delta G(q)$ is required (see also *Figure 2-6*). It is obtained from the gain plot of the open-loop pitch rate frequency response $\left|\frac{q}{F_{ST}}\right|_{dB}$.

Table 5-3 lists the values of all required parameters for cases FC 3-1 to FC 3-4.

		FC 3-1	FC 3-2	FC 3-3	FC 3-4
ω_{180}	[rad/sec]	9.618	10.584	10.200	11.15
$\left\|\frac{\theta}{F_{ST}}\right\|_{dB_{\phi=-180}}$	[dB]	-57.443	-60.453	-59.596	-62.106
$\left\|\frac{\theta}{F_{ST}}\right\|_{dB_{BW\theta gain}}$	[dB]	-51.443	-54.453	-53.596	-56.106
$\omega_{BW_{\theta gain}}$	[rad/sec]	7.720	8.052	-7.934	8.241
$\omega_{135} = \omega_{BW_{\theta phase}}$	[rad/sec]	7.765	8.112	7.918	8.271
$\omega_{BW\theta}$	[rad/sec]	7.720	8.052	7.918	8.241
$2\omega_{180}$	[rad/sec]	19.236	21.168	20.400	22.300
$\phi_{2\omega 180}$	[rad/sec]	-225.698	-229.071	-227.354	-230.380
τ_{p_θ}	[rad/sec]	0.0415	0.04046	0.0405	0.0394
$\Delta G(q)$	[dB]	19.911	17.265	18.0692	15,8642

Table 5-3, Bandwidth/ Pitch-Rate Overshoot Criterion Parameters, Flight Condition 3

The criterion output parameters are compared against the established criterion boundaries in *Figure 5-2.*

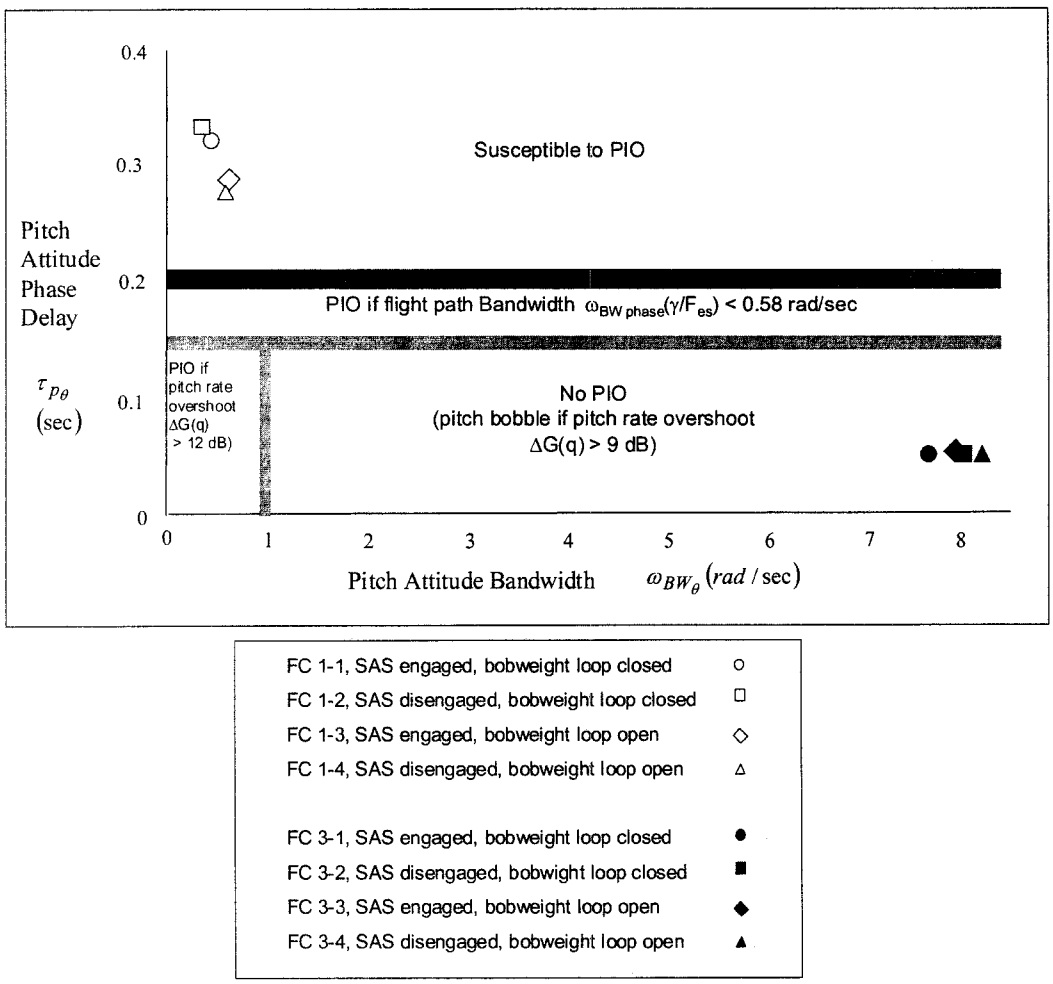

Figure 5-2,Bandwidth/ Pitch-Rate Overshoot Criterion Boundaries, adapted from Ref. [15]

The results are very clear. All cases in Flight Condition 1 fall into the region, where PIO-susceptibility is expected. All cases in Flight Condition 3 show no PIO-potential but a strong bobble tendency.

5.3 The Smith-Geddes Criterion

Flight Condition 1

The criterion is applied according to the procedure given in *Chapter 2.3. Table 5-4* contains the values of the necessary criterion parameters, which are the average slope *S*, the criterion frequency ω_{cr}, the phase angle of the pitch attitude frequency response (at ω_{cr}) ϕ_{cr}, and the phase

angle of the normal acceleration frequency response (at ω_{cr}) ϕ_{azP}. As explained earlier, it is assumed that the pilot changes cues from controlling pitch attitude to controlling normal acceleration at the criterion frequency. The normal-acceleration-to-stick-force-input frequency response at the pilot's position depends on the distance between pilot seat and *cg*. For Flight Condition 1, according to *Table 4-1,* it is l_{xP}=16.3 ft.

		FC 1-1	FC 1-2	FC 1-3	FC 1-4
S	[dB/octave]	-16.105	-16.008	-13.957	-13.878
ω_{cr}	[rad/sec]	2.135	2.158	2.65	2.67
ϕ_{cr}	[deg]	-214.82	-214.604	-220.83	-220.77
ϕ_{azP}	[deg]	-180.6	-179.7	-149	-146.9
ϕ_{CazP}	[deg]	-211.126	-210.56	-186.9	-185.086

Level 1: $\phi_{cr} \geq -123$

Level 2: $-123 > \phi_{cr} \geq -165$ PIO if $\phi_{c_{az\,P}} \leq -180$ deg

Level 3: $\phi_{cr} < -165$

Table 5-4, Smith-Geddes Criterion Parameters, Flight Condition 1

Flight Condition 3

For Flight Condition 3, according to *Table 4-1,* the distance between the pilot seat and the *cg* is l_{xP}=16.2 ft. The values of the average slope S, the criterion frequency ω_{cr}, the phase angle of the pitch attitude frequency response (at ω_{cr}) ϕ_{cr}, and the phase angle of the normal acceleration frequency response (at ω_c) ϕ_{azP} are listed in *Table 5-5.*

		FC 1-1	FC 1-2	FC 1-3	FC 1-4
S	[dB/octave]	0.122	-0.497	-0.233	-0.825
ω_{cr}	[rad/sec]	6.03	5.88	5.94	5.80
ϕ_{cr}	[deg]	-76.8	-79.31	-79.87	-81.70
ϕ_{azP}	[deg]	-52.9	-55.1	-55.93	-57.37
ϕ_{CazP}	[deg]	-139.1	-139.18	-140.93	-140.34

Level 1: $\phi_{cr} \geq -123$

Level 2: $-123 > \phi_{cr} \geq -165$ PIO if $\phi_{c_{az\,P}} \leq -180$ deg

Level 3: $\phi_{cr} < -165$

Table 5-5, Smith-Geddes Criterion Parameters, Flight Condition 3

The values of the criterion parameters can now be plotted in the graph depicted in *Figure 5-3* below.

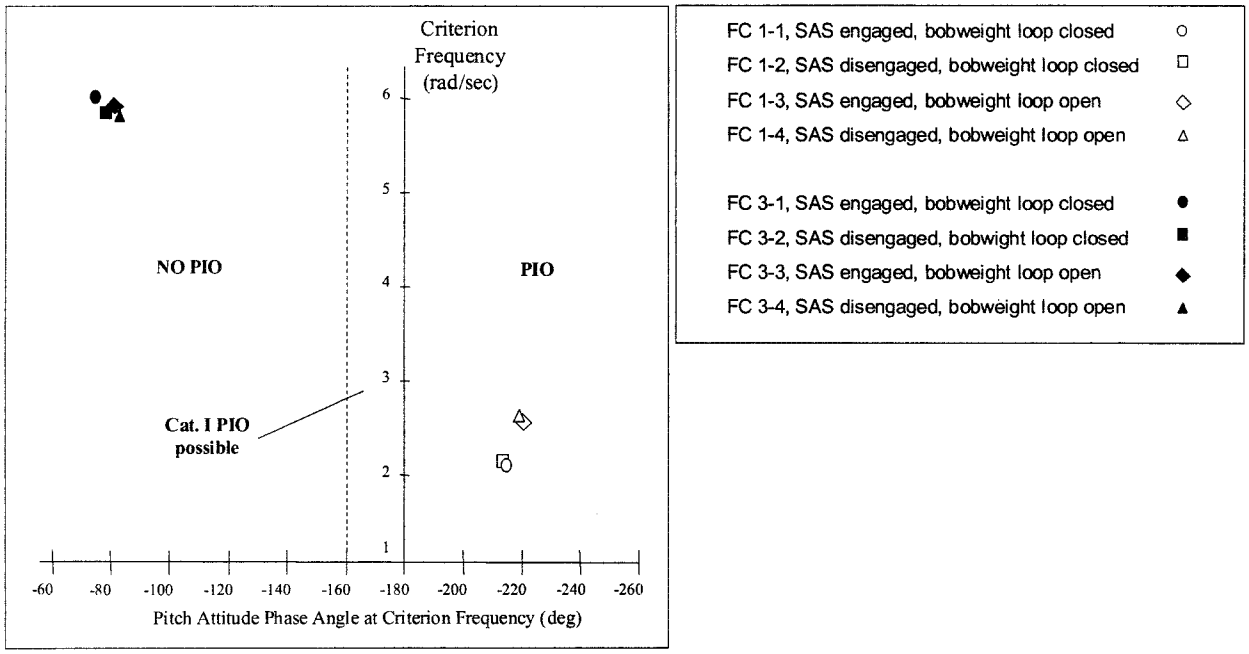

Figure 5-3, Smith-Geddes Criterion Boundaries, adapted from Ref. [15]

The results are again unambiguous. All cases of Flight Condition 1 are susceptible to PIO. All cases of Flight Condition 3 are resistant to PIOs.

5.4 The Phase Rate Criterion

The application of the Gibson Phase Rate Criterion has to be viewed with reservation. As discussed in *Chapter 2.4*, the criterion was primarily developed to assess FBW-aircraft and the influence of HOS-effects in the design-phase of a new aircraft, as successfully demonstrated in development of the control laws for the *Eurofighter/Typhoon*. The F-4C is a conventional aircraft that uses a purely mechanical artificial feel system with mechanical gearing and a bobweight. Also, the mathematical model described in this report is limited and of rather low order compared to control systems of 2nd and 3rd generation fighter aircraft. The motivation for applying this criterion to the F-4C model is to see, if the results differ from those obtained with the previous criteria.

As mentioned earlier, Ref. [5] and Ref. [15] give two different interpretations as to what system inputs are required for PIO-evaluation. According to Ref. [15], analysis is based on the frequency

response of θ/δ_{ST}. Ref. [5] utilises the frequency response of θ/F_{ST} like the Bandwidth/Pitch-Rate Overshoot Criterion. Both versions of the criterion are used in this project.

If stick deflection is the referenced system input, then feel system and bobweight dynamics need to be excluded. The feel system-gearing remains part of mathematical model. According to *Figure 4-4*, the required transfer function has to be $\theta(s)/\delta^*_{ST}(s)$. In this case, the two control system conditions, bobweight-loop open/bobweight-loop closed, are omitted. The modified mathematical model of the aircraft is

$$\begin{bmatrix} \dot{u} \\ \dot{w} \\ \dot{q} \\ \dot{\theta} \\ \dot{\delta}_S \\ \dot{\delta}_{S_{SAS}} \end{bmatrix} = \begin{bmatrix} x_u & x_w & x_q & x_\theta & x_{\delta_S} & 0 \\ z_u & z_w & z_q & z_\theta & z_{\delta_S} & 0 \\ m_u & m_w & m_q & m_\theta & m_{\delta_S} & 0 \\ 0 & 0 & 1 & 0 & 0 & 0 \\ 0 & 0 & 0 & 0 & -1/TA & -Kq/TA \\ Kq\,m_u & Kq\,m_w & Kq\,m_q & Kq\,m_\theta & Kq\,m_{\delta_S} & -1 \end{bmatrix} \begin{bmatrix} u \\ w \\ q \\ \theta \\ \delta_S \\ \delta_{S_{SAS}} \end{bmatrix} + \begin{bmatrix} 0 \\ 0 \\ 0 \\ 0 \\ K_G/TA \\ 0 \end{bmatrix} \left[\delta^*_{ST}\right]$$

$$\begin{bmatrix} u \\ w \\ q \\ \theta \\ \delta_S \\ \delta_{S_{SAS}} \\ \alpha \\ \gamma \\ a_{zx} \end{bmatrix} = \begin{bmatrix} & & & & & \\ & & & & & \\ & & & I & & \\ & & & & & \\ & & & & & \\ & & & & & \\ \hline 0 & 1/V_{T0} & 0 & 0 & 0 & 0 \\ 0 & -1/V_{T0} & 0 & 1 & 0 & 0 \\ g_{1x} & g_{2x} & g_{3x} & g_{4x} & g_{5x} & 0 \end{bmatrix} \begin{bmatrix} u \\ w \\ q \\ \theta \\ \delta_S \\ \delta_{S_{SAS}} \\ \\ \\ \end{bmatrix} + \begin{bmatrix} . \\ . \\ . \\ . \\ 0 \\ . \\ . \\ . \\ . \end{bmatrix} \left[\delta^*_{ST}\right]$$

(Equation 5-1)

The values of the criterion parameter *average phase rate* PR_{180} and *cross-over frequency* ω_{cr} for stick-force inputs F_{ST} and stick-deflection inputs δ^*_{ST} are listed for Flight Condition 1 and Flight Condition 3 respectively in the following tables.

Flight Condition 1

a) *Stick-Force Input*

		FC 1-1	FC 1-2	FC 1-3	FC 1-4
ω_{180}	[rad/sec]	1.419	1.431	1.3859	1.401
f_{180}	[Hz]	0.226	0.228	0.221	0.223
$2\omega_{180}$	[rad/sec]	2.838	2.862	2.7718	2.802
$2f_{180}$	[Hz]	0.452	0.456	0.442	0.446
$\phi_{2\omega_{180}}$	[deg]	-233.438	-233.415	-224.235	-224.48
PR_{180}	[deg/Hz]	236.65	234.533	200.55	199.48

Table 5-6, Phase Rate Criterion Parameters for a Stick Force Input, Flight Condition 1

b) *Stick-Deflection Input (Feel System and Bobweight Dynamics excluded)*

		FC 1-5	FC 1-6
ω_{180}	[rad/sec]	3.079	3.17
f_{180}	[Hz]	0.49	0.505
$2\omega_{180}$	[rad/sec]	6.158	6.34
$2f_{180}$	[Hz]	0.98	1.01
$\phi_{2\omega_{180}}$	[deg]	-192.93	-193.3
PR_{180}	[deg/Hz]	26.4	26.3

Table 5-7, Phase Rate Criterion Parameters for a Stick Deflection Input, Flight Condition 1

Flight Condition 3

a) *Stick-Force Input*

		FC 3-1	FC 3-2	FC 3-3	FC 3-4
ω_{180}	[rad/sec]	9.618	10.584	10.2	11.15
f_{180}	[Hz]	1.531	1.685	1.623	1.775
$2\omega_{180}$	[rad/sec]	19.236	21.168	20.4	22.3
$2f_{180}$	[Hz]	3.062	3.37	3.246	3.55
$\phi_{2\omega_{180}}$	[deg]	-225.698	-229.071	-227.354	-230.38
PR_{180}	[deg/Hz]	29.849	29.131	29.17	28.39

Table 5-8, Phase Rate Criterion Parameters for a Stick Force Input, Flight Condition 3

b) *Stick-Deflection Input (Feel System and Bobweight Dynamics excluded)*

		FC 1-5	FC 1-6
ω_{180}	[rad/sec]	10.636	11.72
f_{180}	[Hz]	1.693	1.865
$2\omega_{180}$	[rad/sec]	21.727	23.44
$2f_{180}$	[Hz]	33.386	3.73
$\phi_{2\omega_{180}}$	[deg]	-218.345	-220.12
PR_{180}	[deg/Hz]	22.656	21.52

Table 5-9, Phase Rate Criterion Parameters for a Stick Deflection Input, Flight Condition 3

The values are then plotted on a graph with the established criterion boundaries illustrated in *Figure 5-4.*

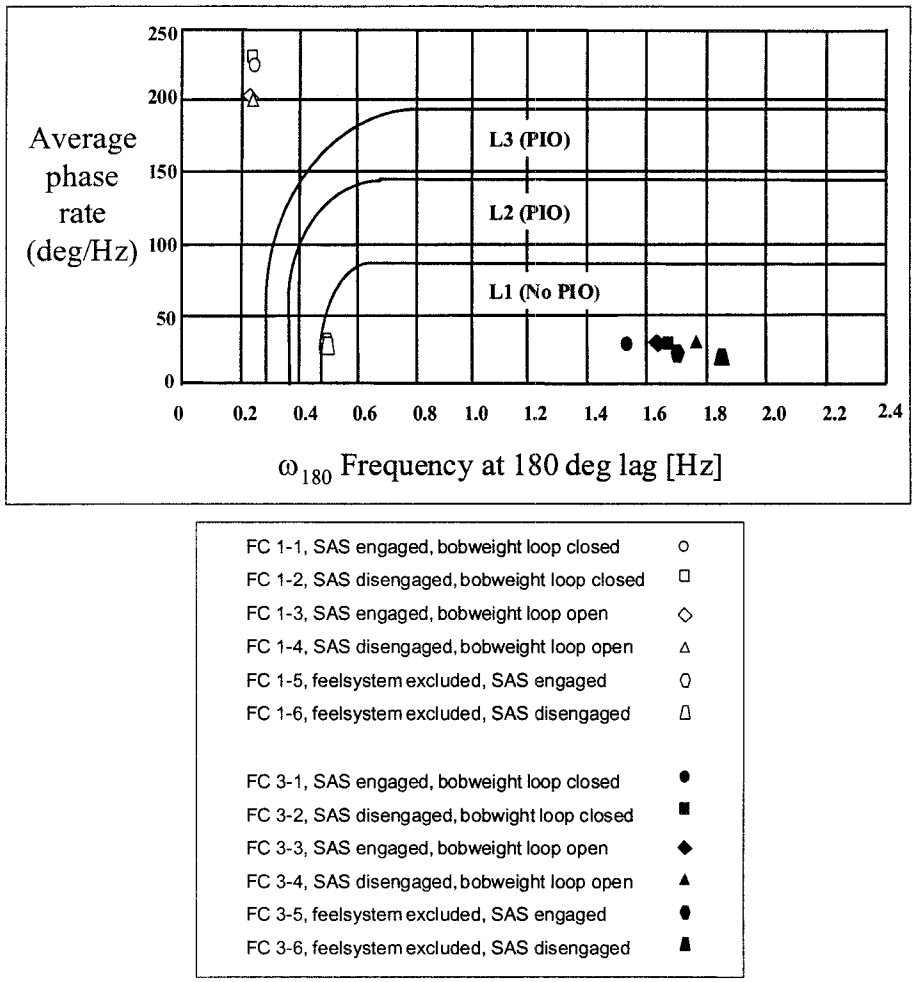

Figure 5-4, Phase Rate Criterion Boundaries, adapted from Ref. [13]

Looking at *Figure 5-4*, it has to be pointed out that for Flight Condition 1 it does make a tremendous difference, whether feel system and bobweight dynamics are included or excluded in the mathematical model. With the feel system and bobweight included, all cases of Flight Condition 1 display a strong PIO-tendency, whereas if the feel system and bobweight are excluded, two cases (SAS engaged and SAS disengaged only) are close to the L1-L2 line, but still within the L1 region (no Cat. I PIO).

All cases for Flight Condition 3 fall into the L1-region and therefore no PIO-tendency is anticipated.

5.5 The Dropback Criterion

It has been mentioned, that the Gibson Dropback Criterion is rather a handling qualities criterion than a tool to evaluate PIO-potential. Therefore, it also has to be regarded with prudence. The criterion parameters are attitude dropback to steady state pitch rate $\Delta\theta / q_{SS}$ and maximum pitch rate to steady state pitch rate q_{peak} / q_{SS} as illustrated in *Figure 2-13*. Since the F-4 is a conventional aircraft, it displays typical time domain responses to a pulse-input, as pictured in *Figure 5-5*.

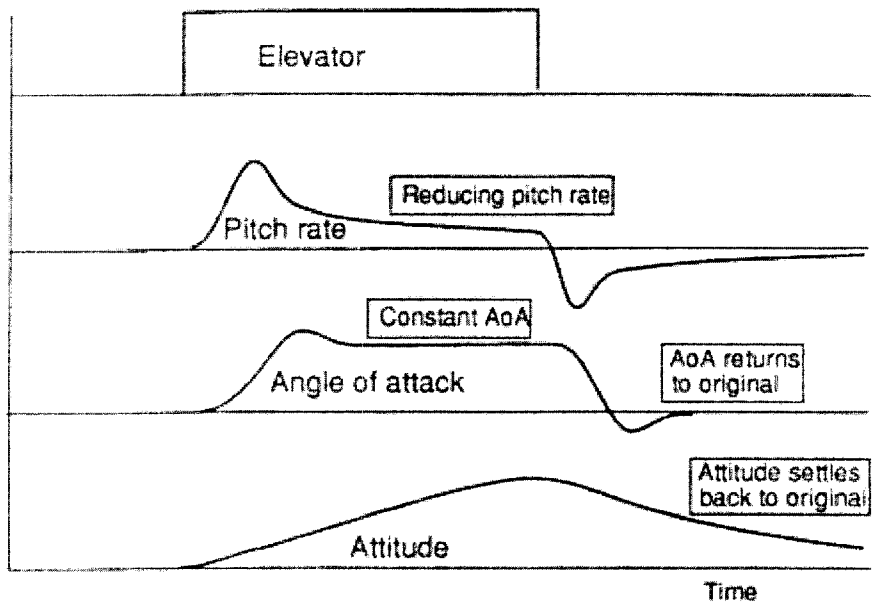

Figure 5-5, Conventional Aircraft Responses, adapted from Ref. [7]

The pitch rate decreases while exposed to the pulse input and the pitch attitude settles back to the original value, when the input is removed. For the devised mathematical model the decrease in pitch rate is marginal but perceivable. The drop in pitch attitude is far more apparent and illustrated in *Figure 5-6*.

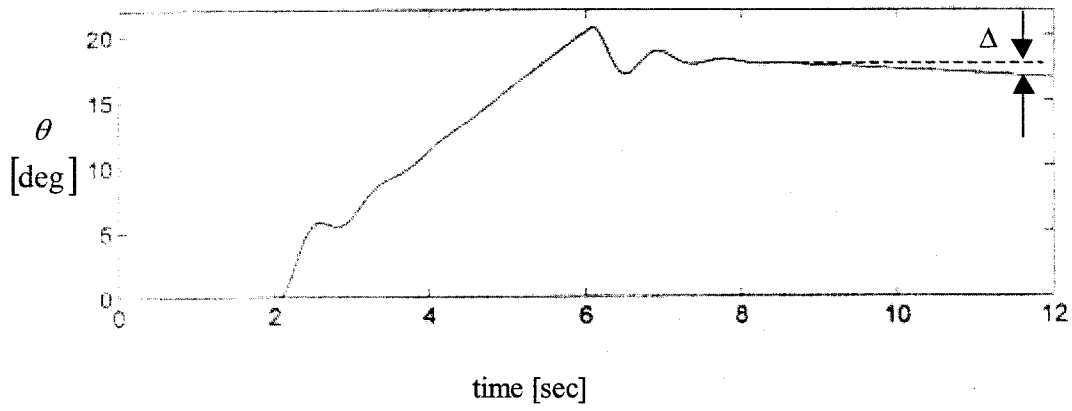

Figure 5-6. Pitch Attitude Response to a Rectangular Pulse Input of State Space Model

To acquire a response that resembles the response depicted in *Figure 2-12,* which is characterised by steady state value in pitch rate and pitch attitude, the phugoid mode has to be omitted. This is accomplished by using the short period approximation of the aircraft as described in *Equation 5-2.*

$$\begin{bmatrix} \dot{w} \\ \dot{q} \end{bmatrix} = \begin{bmatrix} z_w & z_q \\ m_w & m_q \end{bmatrix} \begin{bmatrix} w \\ q \end{bmatrix} + \begin{bmatrix} z_{\delta_S} \\ m_{\delta_S} \end{bmatrix} [\delta_S]$$

(Equation 5-2)

$$\begin{bmatrix} w \\ q \end{bmatrix} = \begin{bmatrix} 1 & 0 \\ 0 & 1 \end{bmatrix} \begin{bmatrix} w \\ q \end{bmatrix} + \begin{bmatrix} 0 \\ 0 \end{bmatrix} [\delta_S]$$

Applied to the full-order aircraft model, this gives

$$\begin{bmatrix} \dot{w} \\ \dot{q} \\ \dot{\delta}_S \\ \dot{\delta}_{S_{SAS}} \\ \dot{\omega}_{ST} \\ \dot{\delta}_{ST} \end{bmatrix} = \begin{bmatrix} z_w & z_q & z_{\delta_S} & 0 & 0 & z_{\delta_{ST}} \\ m_w & m_q & m_{\delta_S} & 0 & 0 & m_{\delta_{ST}} \\ 0 & 0 & -1/TA & -Kq/TA & 0 & 1/TA \\ Kq\, m_w & Kq\, m_q & Kq\, m_{\delta_S} & -1 & 0 & Kq\, m_{\delta_{ST}} \\ -K_{BW}\, g_{2BW} & -K_{BW}\, g_{3BW} & 0 & 0 & -a_1/a_2 & -a_1/a_2 + K_{BW}\left(x_{BW}\, m_{\delta_{ST}} - z_{\delta_{ST}}\right) \\ 0 & 0 & 0 & 0 & 1 & 0 \end{bmatrix} \begin{bmatrix} w \\ q \\ \delta_S \\ \delta_{S_{SAS}} \\ \omega_{ST} \\ \delta_{ST} \end{bmatrix} + \begin{bmatrix} 0 \\ 0 \\ 0 \\ 0 \\ K_G/a_2 \\ 0 \end{bmatrix} [F_{ST}]$$

$$\begin{bmatrix} w \\ q \\ \delta_S \\ \delta_{S_{SAS}} \\ \omega_{ST} \\ \delta_{ST} \end{bmatrix} = \begin{bmatrix} & & I & & & \end{bmatrix} \begin{bmatrix} w \\ q \\ \delta_S \\ \delta_{S_{SAS}} \\ \omega_{ST} \\ \delta_{ST} \end{bmatrix} + \begin{bmatrix} . \\ . \\ 0 \\ . \\ . \\ . \end{bmatrix} [F_{ST}]$$

(Equation 5-3)

Although pitch attitude θ is no longer a defined state in the state space model, it can be obtained by integrating pitch rate q, since $q = \dot{\theta}$. In terms of Laplace transforms, this is accomplished by raising the order of the denominator of the $q(s)/F_{ST}(s)$ transfer function by one.

The criterion is now applied to the modified aircraft model. It is necessary to generate a pulse input of sufficient duration and to continue the recording of the response for some time after the input has been removed, so the short period mode transition phase in pitch attitude is completed and a steady state value is attained. The values of the criterion parameters are listed in the tables below.

Flight Condition 1

For Flight Condition 1 a stick force input of 10 lb is applied for 10 sec.

	FC 1-1	FC 1-2	FC 1-3	FC 1-4
$\frac{\Delta\theta}{q_{ss}}$	2.06	2.05	1.11	1.09
$\frac{q_{peak}}{q_{ss}}$	2.77	2.74	1.4	1.39

Table 5-10, Dropback Criterion Parameters, Flight Condition 1

Flight Condition 3

For Flight Condition 1 a stick force input of 1 lb is applied for 43 sec.

	FC 3-1	FC 3-2	FC 3-3	FC 3-4
$\frac{\Delta\theta}{q_{ss}}$	0.51	0.47	0.5	0.46
$\frac{q_{peak}}{q_{ss}}$	3.8	3.41	3.58	3.21

Table 5-11, Dropback Criterion Parameters, Flight Condition 3

The values are then compared against the established criterion boundaries as illustrated in *Figure 5-7.*

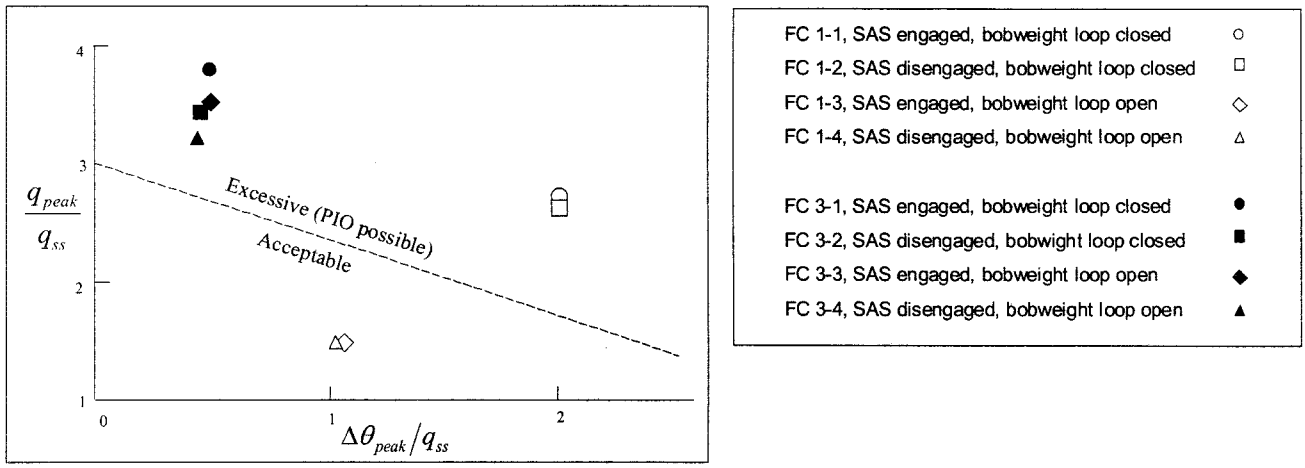

Figure 5-7, Dropback Criterion Boundaries, adapted from Ref. [13]

According to the Dropback Criterion, all cases of Flight Condition 3 are prone to PIO. The two cases of Flight Condition 1, where the bobweight loop is open, are the only cases with an acceptable response.

6. Summary of Findings and Conclusions

A summary of all results is given in *Table 6-1.*

Criteria	Flight Condition	Result
Neal and Smith	1	N.A.
	3	Bobble-tendency
Bandwidth/ Phase-Rate Overshoot	1	Susceptible to PIO
	3	Bobble-tendency
Smith-Geddes	1	Susceptible to PIO
	3	No PIO-tendency
Gibson Phase-Rate	1	Susceptible to PIO
	1*	No PIO-tendency
	3	No PIO-tendency
	3*	No PIO-tendency
Gibson Dropback	$1^{\oplus}$	No PIO-tendency
	$1^{\varnothing}$	Susceptible to PIO
	3	Susceptible to PIO

* feelsystem excluded
$^{\oplus}$ SAS engaged/ disengaged bobweight loop open
$^{\varnothing}$ SAS engaged/ disengaged bobweight loop closed

Table 6-1, Summary of Results

As documented in *Table 6-1*, the majority of the applied criteria ascertain a strong PIO-tendency for Flight Condition 1, the low speed case, and a minor bobble-tendency or no PIO-tendency at all for Flight Condition 3, the high speed case. The only exception is the Gibson Dropback Criterion, which finds that all cases of Flight Condition 3 are PIO-prone and two cases of Flight Condition 1 are acceptable. It has to be noted that the results provided by the various criteria differ in their valence. The Smith-Geddes Criterion and the Gibson Dropback Criterion simply discriminate between PIO-prone and non-PIO cases. The Neal and Smith Criterion and the Bandwidth/Pitch-Rate Overshoot Criterion additionally investigate pitch-bobbling and other harmless, but undesirable, oscillatory tendencies. The Gibson Phase Rate Criterion can be ascribed to either group, depending on the interpretation of the criterion boundaries, as described in *Chapter 2.4.* In this context, the results may be interpreted in the following fashion.

The Neal and Smith Criterion predicts a tendency to bobble on the target and to oscillate or overshoot, equivalent to Level 2 handling qualities, for three cases of Flight Condition 3. Case

FC 3-1 falls directly onto the border line, separating minor bobble-tendency and strong PIO-susceptibility. Again, it is not possible to apply the Neal and Smith Criterion to any cases of Flight Condition 1. With the Bandwidth/Pitch-Rate Overshoot Criterion it is found that all cases of Flight Condition 1 are susceptible to PIO, whereas all cases of Flight Condition 3 display a tendency to bobble. This corresponds to the findings of the Neal and Smith Criterion. The Smith-Geddes Criterion predicts that all cases, belonging to Flight Condition 1, are PIO-prone and all cases of Flight Condition 3 exhibit no PIO-potential. This is confirmed by the results obtained with the Gibson Phase Rate Criterion, but only in case stick force is used as system input. If the feel system and bobweight dynamics are excluded and stick deflection becomes the relevant system input, all cases of Flight Condition 1 and 3 fall into the No-PIO region.

These results are all fairly consistent. The results supplied by the Gibson Dropback Criterion on the other hand do not correspond at all. All cases of Flight Condition 3 are PIO-prone and only two cases of Flight Condition 1 are found to be acceptable. McRuer claims in Ref. [13] that the Dropback Criterion is only applicable to rate-type control elements and will not directly apply to attitude command-type control systems, valid for the effective F-4C dynamics. By using the short-period approximation of the full-order aircraft model, it is attempted to give the initially conventional aircraft response a rate command-type characteristic. But this action may have altered dominant aircraft properties, possibly falsifying the results. Furthermore, it is mentioned earlier that the Gibson Dropback Criterion is principally a criterion intended to assess handling qualities. It may therefore be concluded that it is not suitable for evaluating PIO-susceptibility in this given case.

In summary, it has to be pointed out that it was not possible to find any indications that would explain the PIO-incident during the attempted low altitude high speed run, described in *Chapter 3*. Also, neither in interviews with former F-4 pilots nor through the extensive study of contemporary literature on this topic could the PIO-tendency, discovered for the landing/approach scenario, be verified. This is most probably due to deficiencies in the aircraft modelling. As mentioned earlier, the accessible information from Ref. [9] is very limited and does not claim to be an exact representation of the actual aircraft.

Conclusively, it can be said that this report does satisfy the intention of providing a consolidated review of current PIO-criteria, identifying shortcomings and serious misconceptions about applicability and validity of the criteria. This only shows that more research is necessary on the way to a unified approach to predict PIO, so that at some point it will be feasible to completely rule out the possibility of a PIO, preferably early in the design phase of an aircraft.

Appendix A

Operational Flight Envelopes (adapted from Ref. [1])

Flight phase category	Flight phase
A	Air-to-air-combat Ground attack Weapon delivery/launch Reconnaissance In-flight refuelling (receiver) Terrain following Maritime search Aerobatics Close formation flying
B	Climb Cruise Loiter In-flight refuelling (tanker) Descent Aerial delivery
C	Take-off Approach Overshoot Landing

Appendix B

Levels of Flying Qualities (adapted from Ref. [1])

Level 1 Flying qualities clearly adequate for the mission flight phase

Level 2 Flying qualities clearly adequate to accomplish the mission flight phase, but with an increase in pilot workload and/or degradation in mission effectiveness

Level 3 Degraded flying qualities, but such that aeroplane can be controlled, inadequate mission effectiveness and high, or limiting, pilot workload.

References

[1] Cook, M. V. (1997). *Flight Dynamics Principles.* Arnold, London

[2] Cook, M. V. (August 1998). The Neal and Smith Criterion. Lecture Notes, Issue 2, Cranfield University, College of Aeronautics

[3] Cook, M. V. (September 1998). The Gibson Criteria. Lecture Notes, Issue 3, Cranfield University, College of Aeronautics

[4] Cook, M. V. (March 1999). Analysis of the Gibson Dropback Criterion. Lecture Notes, Issue 2, Cranfield University, College of Aeronautics

[5] Duda, H. (1997). Flying Qualities Criteria Considering Rate Limiting. Institut für Flugmechanik der DLR, Braunschweig, DLR-Forschungsbericht 97-15

[6] French, M. A. (August 1995). Comparative Analysis of Modern Longitudinal Handling Qualities Criteria. MSc Thesis, Cranfield University, College of Aeronautics

[7] Gibson, J. C. (February 1995). The definition, understanding and design of aircraft handling qualities. Delft University of Technology, Faculty of Aerospace Engineering, Report LR-756

[8] Givens, M. L. (March 1994). Evaluation of B-2 Susceptibility to Pilot-Induced Oscillations. Northrop Grumman, B-2 Division, White Paper

[9] Heffley, R. K. and Jewell, W. F. (1972). Aircraft Handling Qualities Data. NASA Contractor Report, Washington D.C., NASA CR-2144

[10] McRuer, D. T. (December 1992). Human Dynamics and Pilot Induced Oscillations. Massachusetts Institute of Technology, Department of Aeronautics and Astronautics, Cambridge Massachusetts, Twenty Second Minta Martin Lecture

[11] McRuer, D. T. (December 1995). Human Dynamics and Pilot Induced Oscillations. NASA Contractor Report, Washington D.C., NASA CR-4683

[12] McRuer, D. T. et. al. (1996). Development of a Comprehensive PIO Theory. AIAA-96-3433-CP

[13] McRuer, D. T. et. al. (1997). *Aviation Safety and Pilot Control – Understanding and Preventing Unfavourable Pilot-Vehicle Interactions.* National Academy Press, Washington

[14] Mitchell, D. G. and Hoh, R. H. (1996). Development of a Unified Method to Predict PIO. AIAA-96-3435-CP

[15] Mitchell, D. G. and Klyde, D. H. (1998). A Critical Examination of PIO Prediction Criteria. AIAA-98-4335

[16] Smith, R. H. and Geddes, N. D. (August 1978). Handling Quality Requirements for Advanced Aircraft Design: Longitudinal Mode. Technical Report AFFDL-TR-78-154

[17] Wünnenberg, H. et. al. (1991). Handling Qualities of Unstable, Highly Augmented Aircraft. AGARD Advisory Report 279, Neuilly-sur-Seine, AGARD-AR-279

Bibliography

[18] Adams, J. J. (1980). Simulator Study of of Conventional General Aviation Instrument Displays in Path-Following Tasks with Emphasis on Pilot-Induced Oscillations. NASA Technical Paper, Washington D.C., NASA TP-1776

[19] Banks, S. P. (1986). *Control Systems Engineering, Modelling and Simulation – Control Theory and Microprocessor Implementation.* Prentice-Hall International, Englewood Cliffs

[20] Brockhaus, R. (1994). *Flugregelung.* Springer Verlag, Berlin

[21] Day, R. E. (1997). Coupling Dynamics in Aircraft, a Historical Perspective. NASA Special Publication, Washington D.C., NASA/SP-532

[22] Foringer, L. A. and Leggett, D. B. (1998). An Analysis of the Time-domain Neal-Smith Criterion. AIAA-98-4250

[23] Gibson, J. C. and Hess, R. A.(1997). Stick and Feel System Design. AGARD Report, Neuilly-sur-Seine, AGARD/AR-332

[24] Hoh, R. H. (1982). Proposed MIL-Standard and Handbook for Flying Qualities of Air Vehicles. Ohio, Wright-Patterson AFB, AFWAL/TR-82/3081

[25] Kempel, R. W. (1971). Analysis of a Coupled Roll-Spiral-Mode, Pilot-Induced Oscillation Experienced with the M2-F2 Lifting Body. NASA Technical Note, Washington D.C., NASA TN D-6496

[26] Kish, B. A., et. al. (1996). Concepts for Detecting Pilot-Induced Oscillations Using Manned Simulation. AIAA-96-3431-CP

[27] Klyde, D. H., McRuer, D. T. and Myers, T. T. (1996). PIO Analysis with Actuator Rate Limiting. AIAA-96-3432-CP

[28] Lamendola, J. E. and Anderson, M. R. (1998). Limit Cycle PIO Analysis with Asymmetric Saturation. AIAA-98-4332

[29] Lin, G., Lan, C. E. and Brandon, J. M. (1998). Simulation of Aircraft-Pilot Coupling as Limit-Cycle Oscillations. AIAA-98-4147

[30] Mehra, R. K. and Prasanth, R. K. (1998). Bifurcation and Limit Cycle Analysis of Nonlinear Pilot Induced Oscillations. AIAA-98-4249

[31] Nise, N. S. (1995). *Control Systems Engineering.* 2nd ed. Addison-Wesley Publishing Company, Menlo Park, California

[32] Riley, D. R. and Miller, G. Kimball Jr. (1980). Simulator Study of the Effect of Control-System Time Delays on the Occurrence of Pilot-Induced Oscillations and on Pilot Tracking Performance with a Space-Shuttle-Orbiter Configuration. NASA Technical Memorandum, Washington D.C., NASA/TM-83267

[33] Riley, D. R. and Miller, G. Kimball Jr. (1982). Comparison of Analytical Predictions of Longitudinal Short Period Pilot Induced Oscillations with Results from a Simulation Study of the Space Shuttle Orbiter. NASA Technical Paper, Washington D.C., NASA TP-1588

[34] Sarma, G. R. and Adams, J. J. (1981). Simulator Evaluation of Separation of Display Parameters in Path-following Tasks. NASA Technical Paper, Washington D.C., NASA TP-1915

[35] Smith, J. W. and Berry D. T. (1975). Analysis of Pilot-Induced Oscillation Tendencies of YF-12 Aircraft. NASA Technical Note, Washington D.C., NASA TN D-7900

[36] Smith, J. W. and Montgomery, T. (1996). Biomechanically Induced and Controller Coupled Oscillations Experienced on the F-16XL Aircraft During Rolling Manoeuvres, NASA Technical Memorandum, Washington D.C., NASA/TM-4752

[37] Tischler, M. B. (1996). *Advances in Aircraft Flight Control.* Taylor and Francis, London

[38] Waller, M. C., et. al. (1981). Influence of Display and Control Compatibility on Pilot-Induced Oscillations. NASA Technical Paper, Washington D.C., NASA TP-1936

[39] Westphal, L. C. (1995). *Sourcebook of Control Systems Engineering.* 1st ed. Chapman & Hall, London